

May 2018

Use of Sodium Bismuthate Chromatography for Separation of Americium from Curium and Other Elements in Spent Nuclear Fuel

Jason Michael Richards
jason.richards241@gmail.com

Follow this and additional works at: <https://digitalscholarship.unlv.edu/thesesdissertations>

 Part of the [Radiochemistry Commons](#)

Repository Citation

Richards, Jason Michael, "Use of Sodium Bismuthate Chromatography for Separation of Americium from Curium and Other Elements in Spent Nuclear Fuel" (2018). *UNLV Theses, Dissertations, Professional Papers, and Capstones*. 3319.

<https://digitalscholarship.unlv.edu/thesesdissertations/3319>

This Dissertation is protected by copyright and/or related rights. It has been brought to you by Digital Scholarship@UNLV with permission from the rights-holder(s). You are free to use this Dissertation in any way that is permitted by the copyright and related rights legislation that applies to your use. For other uses you need to obtain permission from the rights-holder(s) directly, unless additional rights are indicated by a Creative Commons license in the record and/or on the work itself.

This Dissertation has been accepted for inclusion in UNLV Theses, Dissertations, Professional Papers, and Capstones by an authorized administrator of Digital Scholarship@UNLV. For more information, please contact digitalscholarship@unlv.edu.

USE OF SODIUM BISMUTHATE CHROMATOGRAPHY FOR SEPARATION OF
AMERICIUM FROM CURIUM AND OTHER ELEMENTS IN
SPENT NUCLEAR FUEL

By

Jason Michael Richards

Bachelor of Science – Chemistry
Utah State University
2014

A dissertation submitted in partial fulfillment
of the requirements for the

Doctor of Philosophy – Radiochemistry

Department of Chemistry and Biochemistry
College of Sciences
The Graduate College

University of Nevada, Las Vegas
May 2018

Copyright 2018 by Jason Michael Richards

All Rights Reserved

Dissertation Approval

The Graduate College
The University of Nevada, Las Vegas

March 16, 2018

This dissertation prepared by

Jason Michael Richards

entitled

Use of Sodium Bismuthate Chromatography for Separation of Americium from Curium
and Other Elements in Spent Nuclear Fuel

is approved in partial fulfillment of the requirements for the degree of

Doctor of Philosophy – Radiochemistry
Department of Biochemistry and Chemistry

Ralf Sudowe, Ph.D.
Examination Committee Chair

Kathryn Hausbeck Korgan, Ph.D.
Graduate College Interim Dean

Frederic Poineau, Ph.D.
Examination Committee Member

Samundeeswari Mariappan Balasekaran, Ph.D.
Examination Committee Member

Alexander Barzilov, Ph.D.
Graduate College Faculty Representative

ABSTRACT

A novel method for partitioning americium from curium has been developed using sodium bismuthate as both an oxidant and a separation medium. The presence of americium and curium in nuclear waste increases the heat load in geological repositories and leads to larger waste volumes. These elements are also the source of most of the long-term radiotoxicity of the waste. However, the heat load and long-term radiotoxicity contribution from americium is much greater than that from curium. The contribution of curium to the heat load and radiotoxicity of the waste is significant on the same time scale as longer-lived fission products (^{137}Cs , ^{90}Sr , etc.). The currently envisioned advanced fuel cycle includes recycling of americium into fast reactor fuel, thus reducing the long-term radiotoxicity of the waste. The presence of curium in fuel would greatly complicate fuel fabrication and handling, making curium recycling undesirable. Efficient minor actinide separations are therefore an imperative capability for the development of advanced nuclear fuel cycles.

Methods for the partitioning of americium from curium are often complicated and time-consuming due to the similar chemical properties of these elements. A simple method for the isolation of americium from mixtures containing curium, as well as lanthanides and other fission product elements, could allow for the development of an efficient and economically feasible nuclear fuel-reprocessing scheme that would reduce the volume and hazardous lifetime of nuclear waste and increase fuel resource sustainability. This work demonstrates that sodium bismuthate chromatography is a promising method to address the challenge of isolating americium from curium, lanthanides, and fission product elements in a simple and cost-effective manner.

ACKNOWLEDGEMENTS

I would like to acknowledge and thank those who made this work possible. I would first like to thank my advisor, Dr. Ralf Sudowe, for his kind support, encouragement, and understanding during the course of this degree. This work would not have been possible without his constant support. I am grateful for the freedom that he gave me to pursue my research interests. I would also like to acknowledge the other members of my dissertation committee, Dr. Gary Cerefice and Dr. Frederic Poineau, and thank them for all that they have taught me. I owe much of my knowledge in nuclear science to their instruction. I would like to thank Dr. Bruce Mincher for advising me during my internship at Idaho National Laboratory. The experience that I gained there was invaluable. I would also like to acknowledge the great help and support provided by Wendee Johns, Julie Bertoia, and Trevor Low. They made all the work performed in the Radiochemistry program possible. I would like to express my gratitude to all the students in the Radiochemistry program for their help and friendship and for providing a great environment to work in. I would like to thank my parents, Jay and Carri Richards, for encouraging me to pursue what I love. I would not have made it to this point without their support and love. I would like to extend a special thank you to my two daughters, Lucy and Ally, for letting Daddy work in the lab and making it all worth it. Finally, my greatest debt of gratitude goes to my sweet wife and eternal lab partner, Amber, for being with me and supporting me through this degree.

TABLE OF CONTENTS

ABSTRACT	iii
ACKNOWLEDGEMENTS	iv
LIST OF TABLES	xi
LIST OF FIGURES	xiii
CHAPTER 1: INTRODUCTION	1
1.1 Motivation	1
1.2 Solution Chemistry of Americium and Curium	5
1.2.1 Americium	5
1.2.2 Curium	6
1.3 Separation of Americium from Curium	6
1.3.1 Separation of Trivalent Americium from Curium	6
1.3.2 Separation of Americium in High Oxidation States from Curium	7
1.4 Project Goals	10
1.5 Dissertation Overview	10
CHAPTER 2: MATERIALS, METHODS, AND INSTRUMENTATION	12
2.1 Materials	12
2.1.1 Sodium Bismuthate	12
2.1.2 DGA Resin	12
2.1.3 UTEVA Resin	13
2.2 Methods	14
2.2.1 Solvent Extraction	14
2.2.2 Ion Exchange Chromatography	14

2.2.3 Extraction Chromatography.....	15
2.2.4 Batch Contact Studies.....	16
2.2.5 CeF ₃ Microprecipitation	16
2.3 Instrumentation.....	17
2.3.1 Alpha Spectrometry	17
2.3.2 Liquid Scintillation Counting	18
2.3.3 Atomic Emission Spectroscopy	20
2.3.4 Mass Spectrometry	21
 CHAPTER 3: ADSORPTION BEHAVIOR OF AMERICIUM AND CURIUM ON EXTRACTION CHROMATOGRAPHY RESINS IN THE PRESENCE OF SODIUM BISMUTHATE.....	
3.1 Abstract	22
3.2 Motivation and Objectives	22
3.3 Adsorption Behavior on DGA.....	24
3.3.1 Experimental.....	24
3.3.2 Results and Discussion	25
3.3.2.1 Americium and Curium on DGA.....	25
3.3.2.2 Americium and Curium on DGA in the presence of NaBiO ₃	25
3.3.2.3 Bi(III) Interference	27
3.4 Adsorption Behavior on UTEVA.....	29
3.4.1 Experimental.....	29
3.4.2 Results and Discussion	29
3.4.2.1 Americium and Curium on UTEVA.....	29

3.4.2.2 Americium and Curium on UTEVA in the presence of NaBiO ₃	30
3.5 DBBP Solvent Extraction of Bismuthate-Oxidized Am	31
3.5.1 Experimental.....	31
3.5.2 Results and Discussion	32
3.6 Conclusions	33
CHAPTER 4: ADSORPTION OF AMERICIUM AND CURIUM TO SODIUM BISMUTHATE	
SOLID.....	35
4.1 Abstract	35
4.2 Motivation and Objectives	35
4.3 Nitric Acid Dependency of Adsorption	35
4.3.1 Experimental.....	35
4.3.1.1 Americium and Curium on NaBiO ₃	35
4.3.1.2 Americium and Curium on Preconditioned NaBiO ₃	36
4.3.2 Results and Discussion	36
4.4 Time Dependence of Adsorption	38
4.4.1 Experimental.....	38
4.4.2 Results and Discussion	39
4.5 Nitric Acid Dependency of Sorption with Short Contact Time	40
4.5.1 Experimental.....	40
4.5.2 Results and Discussion	40
4.6 Nitrate Dependence of Sorption	42
4.6.1 Experimental.....	42
4.6.2 Results and Discussion	42

4.7 Conclusions	43
CHAPTER 5: SEPARATION OF AMERICIUM FROM CURIUM UTILIZING SODIUM BISMUTHATE.....	
5.1 Abstract	45
5.2 Motivation and Objectives	45
5.3 Batch Solid-Liquid Separation Method.....	45
5.3.1 Experimental.....	45
5.3.2 Results and Discussion	46
5.4 Sodium Bismuthate Chromatography Separation Method.....	47
5.4.1 Experimental.....	47
5.4.2 Results and Discussion	49
5.5 Conclusions	50
CHAPTER 6: PROPERTIES OF SODIUM BISMUTHATE AS A SEPARATION MEDIUM 52	
6.1 Abstract	52
6.2 Motivation and Objectives	52
6.3 Adsorption Capacity.....	53
6.3.1 Experimental.....	53
6.3.2 Results and Discussion	53
6.4 Surface Area and Particle Size	56
6.4.1 Experimental.....	56
6.4.2 Results and Discussion	56
6.5 Dissolution of Sodium Bismuthate in Nitric Acid	57
6.5.1 Experimental.....	57

6.5.2 Results and Discussion	57
6.6 Comparison of High Purity and Reagent Grade NaBiO ₃	60
6.6.1 Experimental.....	60
6.6.2 Results and Discussion	60
6.7 Conclusions	62
CHAPTER 7: APPLICATION OF SODIUM BISMUTHATE CHROMATOGRAPHY TO CHALLENGES IN ADVANCED PARTITIONING OF USED NUCLEAR FUEL	64
7.1 Abstract	64
7.2 Motivation and Objectives	64
7.3 Sorption of Lanthanides on Sodium Bismuthate Solid	65
7.3.1 Experimental.....	65
7.3.2 Results and Discussion	65
7.4 Sorption of Uranium, Plutonium, and Technetium on Sodium Bismuthate Solid.....	68
7.4.1 Experimental.....	69
7.4.2 Results and Discussion	69
7.5 Post-TRUEX Application	70
7.5.1 Experimental.....	70
7.5.2 Results and Discussion	70
7.6 Post-PUREX Application.....	71
7.6.1 Experimental.....	71
7.6.2 Results and Discussion	72
7.7 Conclusions	79
CHAPTER 8: CONCLUSIONS AND IMPLICATIONS	82

8.1 Extraction Chromatography	82
8.2 Sorption of Am and Cm on NaBiO ₃	82
8.3 Separation of Am and Cm with NaBiO ₃	83
8.4 Properties of Sodium Bismuthate.....	83
8.5 Application of Sodium Bismuthate Chromatography	85
8.6 Proposed Future Work	86
APPENDIX: RAW DATA FOR FIGURES.....	89
REFERENCES	98
CURRICULUM VITAE.....	103

LIST OF TABLES

Table 1: Comparison of americium D-values at different concentrations extracted by DBBP	33
Table 2: TRUEX strip solution simulant composition and D_w at 0.1 and 2.0 M HNO_3	71
Table 3: PUREX raffinate simulant composition and D_w at 0.1 M HNO_3	73
Table 4: Raw Data for Figure 7	89
Table 5: Raw Data for Figure 8	89
Table 6: Raw Data for Figure 9	89
Table 7: Raw Data for Figure 11	90
Table 8: Raw Data for Figure 12	90
Table 9: Raw Data for Figure 14	90
Table 10: Raw Data for Figure 15	91
Table 11: Raw Data for Figure 16	91
Table 12: Raw Data for Figure 17	91
Table 13: Raw Data for Figure 18	92
Table 14: Raw Data for Figure 21	92
Table 15: Raw Data for Figure 22	92
Table 16: Raw Data for Figure 23	92
Table 17: Raw Data for Figure 24	93
Table 18: Raw Data for Figure 25	93
Table 19: Raw Data for Figure 26	93
Table 20: Raw Data for Figure 27	94
Table 21: Raw Data for Figure 28	94
Table 22: Raw Data for Figure 29	95

Table 23: Raw Data for Figure 30	95
Table 24: Raw Data for Figure 31	96
Table 25: Raw Data for Figure 33	96
Table 25 (cont.): Raw Data for Figure 33.....	97

LIST OF FIGURES

Figure 1: Radiotoxicity (volume of water required to dilute material to within drinking water standards in units of meters cubed per metric ton of initial heavy metal or $m^3/MTIHM$) of high-level waste as a function of time after discharge compared with natural uranium (dotted line) ¹³ . 2	2
Figure 2: Radiotoxicity of high-level waste over time with americium and neptunium removed ¹³³	133
Figure 3: Radiotoxicity of high-level waste over time with neptunium, americium and curium removed ¹³	4
Figure 4: Standard reduction potentials for Am in acidic and basic media ¹⁷	8
Figure 5: N,N,N',N'-tetra-n-octyldiglycolamide.....	13
Figure 6: Diamyl amyolphosphonate.....	13
Figure 7: Nitric acid dependency of k' for Am and Cm on DGA resin.....	25
Figure 8: Nitric acid dependency of k' for Am and Cm on DGA in the presence of $NaBiO_3$	26
Figure 9: Effect of different preconditioning times and resin masses on k' for Cm on DGA.....	27
Figure 10: k' for selected transition and post transition elements on DGA resin ⁴⁴	28
Figure 11: Nitric acid dependency of k' for Am and Cm on UTEVA resin.....	30
Figure 12: Nitric acid dependency of k' for Am and Cm on UTEVA in the presence of $NaBiO_3$	31
Figure 13: D_{Am} plotted against Am concentration.....	33
Figure 14: Nitric acid dependency of D_w for Am and Cm on $NaBiO_3$ powder.....	37
Figure 15: Nitric acid dependency of D_w for Am and Cm on preconditioned $NaBiO_3$ solid.....	37
Figure 16: Time dependence of D_w of Am and Cm in 0.1 M HNO_3 on $NaBiO_3$	39
Figure 17: Nitric acid dependency of D_w for Am and Cm on preconditioned $NaBiO_3$ solid with a contact time of 10 minutes	41

Figure 18: Nitrate dependency of D_w for Cm on preconditioned NaBiO_3 solid compared with nitric acid dependency	43
Figure 19: Sodium bismuthate chromatography column setup	48
Figure 20: Alpha spectrum of the pre-separation mixture (green), the 0.1 M fraction (red) and the 2.0 M fraction (blue)	50
Figure 21: Mass of lanthanum adsorbed versus lanthanum concentration in solution	54
Figure 22: C_e/q_e versus C_e for lanthanum on sodium bismuthate in 0.1 M nitric acid with a 10-minute contact time.....	55
Figure 23: Bismuth concentration in nitrate media in contact with sodium bismuthate over the course of four hours	58
Figure 24: Dissolved bismuth in 0.1 M nitric acid in contact with preconditioned sodium bismuthate over the course of four hours.....	59
Figure 25: Dissolved bismuth in 0.1 M nitric acid/2.0 M NaNO_3 in contact with preconditioned sodium bismuthate over the course of four hours.....	60
Figure 26: Comparison of D_w values for americium and curium on reagent grade (RG) and high purity (HP) sodium bismuthate.....	61
Figure 27: D_w of lanthanides on NaBiO_3 solid in 0.1 M HNO_3 (individually tested)	66
Figure 28: D_w of lanthanides on NaBiO_3 solid in 0.1 M HNO_3 (interference study).....	67
Figure 29: Nitric acid dependency of D_w (0.05, 0.1, 0.5, 1.0, 2.0 M) of lanthanides on sodium bismuthate with a 10-minute contact time compared with americium and curium.....	68
Figure 30: Nitric acid dependency of D_w of uranium and plutonium on sodium bismuthate with a 10-minute contact time compared with americium and curium	69

Figure 31: Measured D_w values for PR-50 elements with significant D_w at 2.0 M HNO_3 over time in 2.0 M HNO_3 after adsorption in 0.1 M HNO_3 74

Figure 32: D_w of PUREX-relevant elements on sodium bismuthate in 0.1 M nitric acid 75

Figure 33: Elution profile of PUREX raffinate elements in a sodium bismuthate chromatography separation 76

Figure 34: Proposed process scheme for isolation of americium from PUREX raffinate using sodium bismuthate chromatography 79

CHAPTER 1: INTRODUCTION

1.1 Motivation

Novel partitioning technologies are imperative to enabling advanced nuclear fuel cycles. In the document “Nuclear Fuel Cycle Evaluation and Screening – Final Report” published by the Department of Energy, forty different fuel cycle options were evaluated¹. Two of the three fuel cycles considered the most promising included the continuous recycle of uranium and transuranic (TRU) elements. The TRU elements that can be found in significant quantities in spent nuclear fuel are neptunium, plutonium, americium, and curium. Processes for the separation of neptunium and plutonium from fission product elements have been well established and have been implemented on an industrial scale². The separation of americium and curium from fission product elements is complicated by the similarities in chemical behavior between lanthanide and other rare earth elements and trivalent actinides³.

Americium, curium, lanthanides, and other rare earth elements are predominantly trivalent in the acidic solutions used for fuel pellet dissolution, and all have similar ionic radii³. Extensive research has been done to create a process to separate americium and curium from the lanthanides⁴⁻¹¹. This has led to the development of partitioning technologies such as TALSPEAK (Trivalent Actinide Lanthanide Separation by Phosphorous Extractants and Aqueous Komplexants). This process utilizes a solvent extraction system in which ligands are present in the aqueous and organic phases and actinides are preferentially extracted into the organic phase. These processes, while effective, have been difficult to apply on an industrial scale since very strict control of the pH of the system must be maintained and large amounts of buffer must be used. While these systems separate the trivalent actinides (Am, Cm) from the lanthanides, they do not separate americium and curium from each other.

Many of the benefits of recycling americium and curium come from removal of americium from high-level waste. The Nuclear Regulatory Commission (NRC) defines high-level radioactive waste or HLW as irradiated reactor fuel, liquid wastes resulting from the operation of the first cycle solvent extraction system, or equivalent, and the concentrated wastes from subsequent extraction cycles, or equivalent, in a facility for reprocessing irradiated reactor fuel, and solids into which such liquid wastes have been converted.¹² It typically has a greater radiotoxicity than natural uranium for over ten thousand years (Figure 1)¹³.

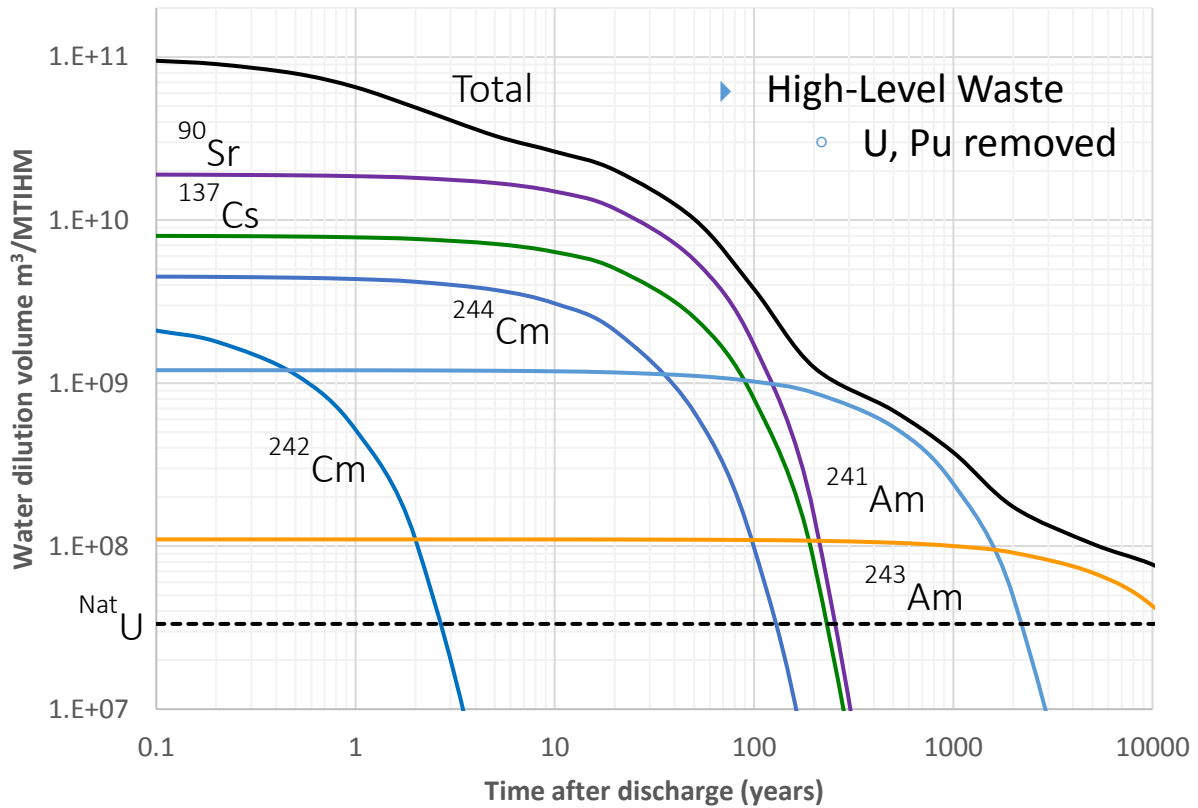


Figure 1: Radiotoxicity (volume of water required to dilute material to within drinking water standards in units of meters cubed per metric ton of initial heavy metal or m³/MTIHM) of high-level waste as a function of time after discharge compared with natural uranium (dotted line)¹³

The presence of americium and curium in high-level waste increases the heat load in geological repositories and results in larger waste volumes. In addition, these elements are the source of a majority of the long-term radiotoxicity in the waste. However, the heat load and long-term radiotoxicity contribution from americium is much greater than the contribution from curium. The most abundant isotope of americium in the used fuel is ^{241}Am ($T_{1/2} = 432.7$ years), which decays to long-lived alpha-emitting ^{237}Np ($T_{1/2} = 2.14 \times 10^6$ years) and contributes significantly to the long-term heat load on the repository and long-term radiotoxicity of the waste¹⁴. The contribution of Cm to the heat load and radiotoxicity of the waste is significant on the same time scale as fission products such as ^{137}Cs and ^{90}Sr .

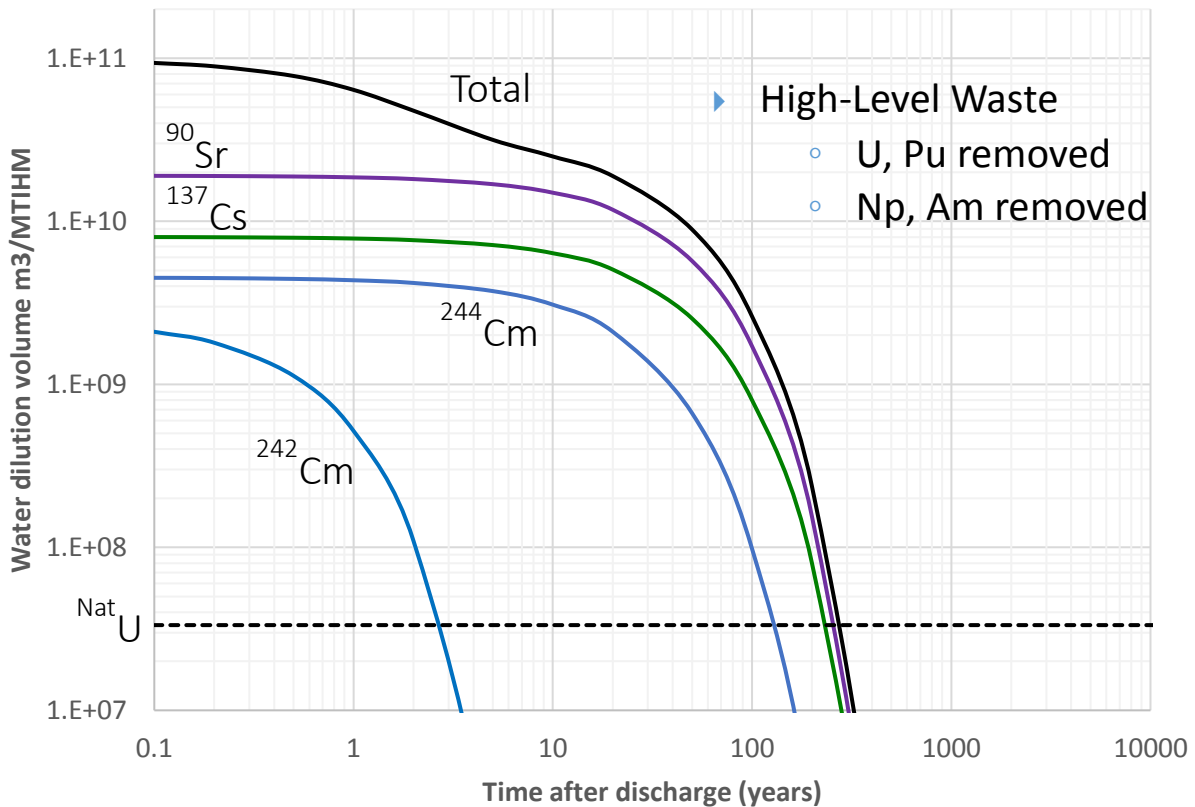


Figure 2: Radiotoxicity of high-level waste over time with americium and neptunium removed¹³

If americium and neptunium are removed from the high-level waste, the material becomes less hazardous than the original uranium sometime between two and three hundred years after discharge as shown in Figure 2. A shorter hazardous-lifetime of the waste would allow increased accuracy in predictions of geological repository performance. If curium is removed from the high-level waste, the material still becomes less hazardous than the original uranium sometime between two and three hundred years as shown in Figure 3. There is no significant reduction in the hazardous lifetime of the waste from removal of curium.

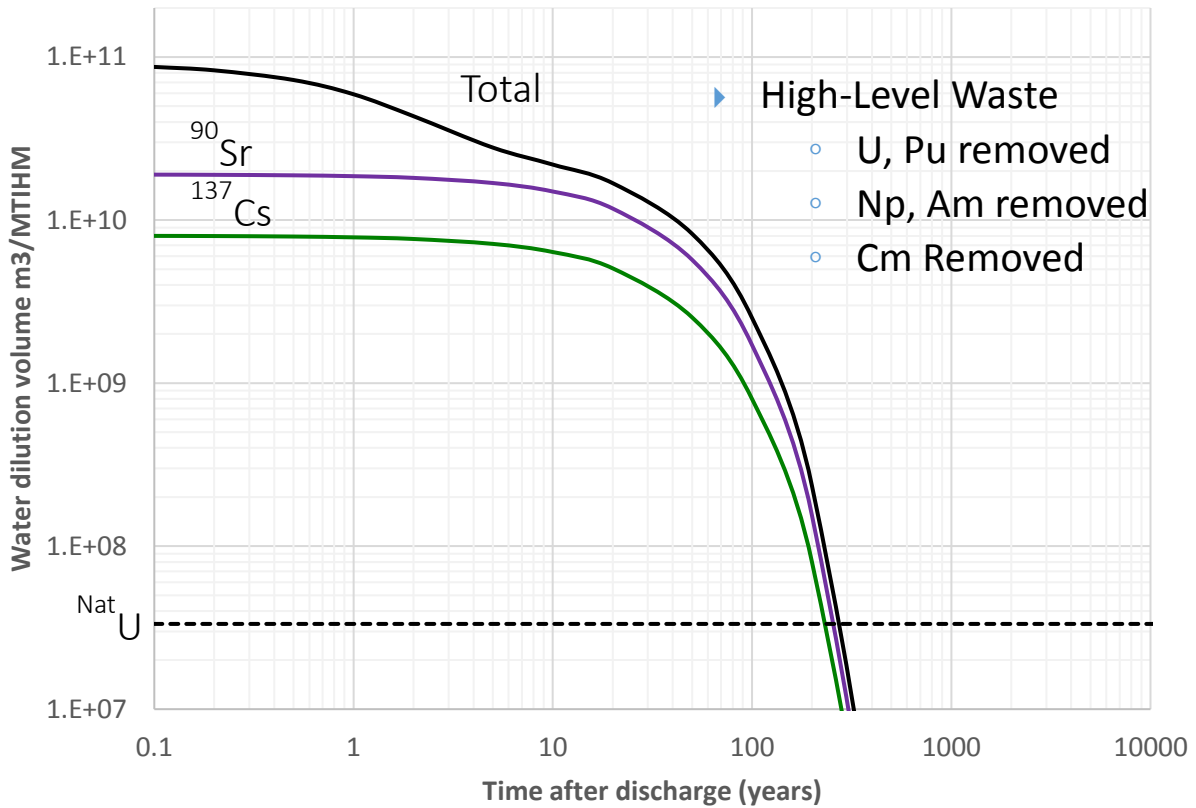


Figure 3: Radiotoxicity of high-level waste over time with neptunium, americium and curium removed¹³

Currently envisioned advanced fuel cycles often include recycling of americium (not necessarily curium) into fast reactor fuel, thus reducing the long-term radiotoxicity of the waste¹. Several curium isotopes present in spent nuclear fuel have significant spontaneous fission activities. On the time-scale of reprocessing and recycling, the most notable isotope would be ²⁴⁴Cm. The presence of neutron-emitting curium in fuel would greatly complicate fuel fabrication and handling, making curium recycling undesirable¹⁵. Efficient minor actinide separations are an imperative capability for the development of advanced nuclear fuel cycles.

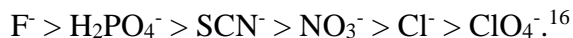
This research focused on minor actinide separations to assist in enabling minimization of waste generation to support the development of a sustainable fuel cycle and advance nuclear power as a resource for our Nation's needs.

1.2 Solution Chemistry of Americium and Curium

1.2.1 Americium

Americium exhibits the III, IV, V, and VI oxidation states in aqueous solutions. All of these oxidation states are accessible to americium in alkaline solution while only the III, V, and VI states are available in acidic media. Trivalent americium is the most common oxidation state in aqueous solution and is present as the Am³⁺ metal ion. Pentavalent and hexavalent americium exist as linear *trans*-dioxo americyl cations.¹⁶

Am³⁺ forms complexes with several anions. Complex stability with monovalent inorganic ligands has been found to follow the sequence:



Trivalent americium forms insoluble fluoride, oxalate, phosphate, and iodate compounds. Similar to other actinide elements, trivalent americium forms hydroxide complexes in aqueous solutions above a pH of 5. These complexes have low solubility therefore most partitioning

technologies applied to spent nuclear fuel use highly acidic conditions. The ionic radius of 6-coordinate trivalent americium is 97.5 pm³.

1.2.2 Curium

Curium exhibits only the III oxidation state in aqueous solutions. Trivalent curium forms insoluble fluoride, oxalate, phosphate, and iodate compounds. Curium forms insoluble hydroxide complexes in almost identical manner to americium. The chloride, iodide, perchlorate, nitrate, and sulfate compounds of trivalent curium are water-soluble.¹⁶ The ionic radius of 6-coordinate trivalent curium is 97.0 pm.³

1.3 Separation of Americium from Curium

Chemical separations of americium from curium are complicated by their similar chemical behavior. Separations are typically performed in acidic media, when using aqueous separation techniques, because americium and curium tend to hydrolyze and form sparingly-soluble hydroxides in alkaline environments³. Americium and curium are predominantly trivalent in acidic media. Curium does not have other oxidation states available in solution; however, americium does have higher oxidation states available¹⁷. Aqueous separations of americium from curium can be sorted into two categories: separation of trivalent americium from curium and separation of americium in high oxidation states from curium.

1.3.1 Separation of Trivalent Americium from Curium

Separation of trivalent americium from curium has been achieved using ion-exchange¹⁸⁻²⁰, extraction chromatography^{21,22}, and solvent extraction techniques^{23,24}. Early separation methods focused mainly on the use of ion exchange. While determining the chemical properties of the newly discovered americium and curium, Glenn Seaborg and Kenneth Street developed a separation procedure using citrate solutions and Dowex-50 cation exchange resin²⁵. This procedure only

afforded fractionation of the americium and curium. This was useful as an analytical tool but was not promising on a larger scale for complete separation. Some significant improvements were made in the sixties with the development of anion-exchange and extraction chromatography-based separation procedures^{19,22}. The anion exchange procedures include strong electrolyte and mixed alcohol-nitric acid mobile phases. The extraction chromatography resin was a high molecular weight quaternary amine used to retain americium more strongly than curium from a strong electrolyte-low acidity solution. The separation factors for these procedures are 2.7 or less, making them difficult to apply on a large scale.

More recently, solvent extraction procedures have been developed^{23,24}. These include diglycolamide and dithiophosphinic acid extractants as well as other complexants. These procedures still have separation factors of approximately only two. This leads to a very sensitive process flowsheet that would be difficult to manage.

The difficulty in achieving high separation factors for the separation of trivalent americium from curium has led to an increased interest in the use of high oxidation states of americium to perform americium-curium separations.

1.3.2 Separation of Americium in High Oxidation States from Curium

Americium can be oxidized to Am(IV), Am(V), or Am(VI) from Am(III)²⁶. The standard reduction potentials are given in Figure 4. Tetravalent americium is only stable in solution in strongly complexing media. Pentavalent americium is typically formed in the presence of strong oxidants, such as peroxydisulfate, in near neutral pH solutions or by reduction from Am(VI) with bromine. It is more stable than Am(IV) or Am(VI). Hexavalent americium can be formed with strong oxidants such as peroxydisulfate, Ag(II), Cu(III) periodate or sodium bismuthate²⁶⁻²⁹.

Sodium bismuthate is one of the only oxidants capable of oxidizing americium to Am(VI) in molar concentrations of nitric acid that would be expected in spent nuclear fuel reprocessing²⁶.

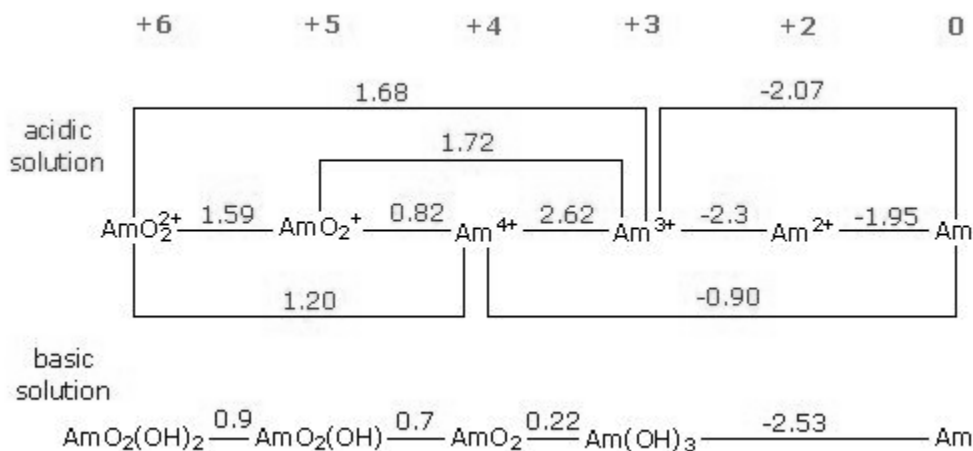


Figure 4: Standard reduction potentials for Am in acidic and basic media¹⁷

Separations involving higher oxidation states of americium include methods such as precipitation³⁰, ion exchange^{18,19}, extraction chromatography^{21,22}, and solvent extraction^{23,24}. There are many methods to oxidize americium²⁶. It is, however, difficult to pair an oxidation method with a suitable separation method because of the relative instability of highly oxidized americium. Americium is often reduced during the separation procedure leading to inefficient or incomplete separation. Maintaining americium in a highly oxidized state throughout a separation procedure is one of the greatest challenges involved in separation of americium in high oxidation states from curium.

Multiple precipitation methods have been reported including oxidation of americium to AmO_2^+ in concentrated K_2CO_3 solution to precipitate $\text{K}_3\text{AmO}_2(\text{CO}_3)_2$ and oxidation of americium to AmO_2^+ or AmO_2^{2+} followed by a lanthanide fluoride coprecipitation of curium^{30,31}. Precipitation,

while effective to some degree, is often very resource intensive and does not produce high decontamination factors.

Several ion-exchange methods have been reported. These methods typically involve oxidation of americium to AmO_2^+ or AmO_2^{2+} , both of which have a much lower charge density than Cm^{3+} , followed by adsorption of curium to the ion exchange material and elution of americium. Some ion-exchange materials utilized include monosodium titanate, zirconium phosphate, as well as pillared metal(IV) phosphate-phosphonate hybrid materials^{18,32-34}. One of the greatest challenges in these methods is preventing the reduction of americium during the separation. When americium is reduced and adsorbed onto the column, it is very difficult to re-oxidize it while on the column. Americium recovery is therefore often incomplete, leading to low decontamination factors for curium.

Solvent extraction techniques have also shown some success. Many methods include oxidation of americium to AmO_2^{2+} , which behaves in a similar manner to UO_2^{2+} , followed by extraction with ligands such as tributylphosphate (TBP) and Diamylamylphosphonate (DAAP)^{31,35}. Other methods include oxidation of americium to AmO_2^+ and extraction of Cm^{3+} with carbamoylmethylphosphine oxide (CMPO)³⁶. These techniques suffer from the instability of americium in high oxidation states in contact with an organic phase as the sodium bismuthate solid must be filtered out prior to performing the solvent extraction. Separations must be performed quickly, often within seconds, to avoid reducing a large fraction of the americium.

Extraction chromatography has been used, in at least one case, to separate americium in high oxidation states from curium³⁴. Americium was oxidized to AmO_2^+ with peroxydisulfate and loaded onto a TRU column from Eichrom Inc. The TRU resin is coated with TBP/CMPO. It was

used to retain the Cm^{3+} and elute the AmO_2^+ . Only a fifty percent yield was observed presumably due to reduction of americium on the column.

These separation methods are all limited by the efficiency of the oxidation method as well as the stability of the oxidized americium throughout the separation procedure. This work describes the development of a novel approach to the separation of americium in high oxidation states from curium.

1.4 Project Goals

The current methods for the partitioning of americium from curium lack the selectivity, efficiency, and cost-effectiveness necessary for successful application to fuel cycle challenges. The aim of this research is to develop a method for the separation of americium from curium that is highly selective, efficient, and cost effective. Selectivity is evaluated by the separation factor of the method. An efficient method would not be time or labor intensive compared to other methods. Cost-effectiveness is determined by factors such as the cost of the materials, the complexity of the method, and the amount of waste generated. In addition to developing a method, this research aims to explore possible applications of the method to nuclear fuel cycle relevant challenges.

1.5 Dissertation Overview

This dissertation describes the work performed to develop and characterize a novel method for the separation of americium from curium as well as studies relevant to its potential application in the nuclear fuel cycle. Chapter 1 describes the need for improved americium-curium separation methods for application in advanced nuclear fuel cycles and outlines past and current partitioning methods. Chapter 2 provides information about the materials, analytical methods and instrumentation used in this research. Chapter 3 describes the initial approach to developing a separation method. This involved extraction chromatography and was unsuccessful according to

the original plan. The information gained in Chapter 3 provides the motivation for Chapter 4, in which the possibility of performing americium-curium separations using sodium bismuthate becomes apparent. Chapter 5 describes the successful development of sodium bismuthate-based separation methods. Chapter 6 further characterizes the sodium bismuthate as a separation medium. Chapter 7 includes all work involving other elements of interest for nuclear fuel cycle applications.

CHAPTER 2: MATERIALS, METHODS, AND INSTRUMENTATION

2.1 Materials

2.1.1 Sodium Bismuthate

Sodium bismuthate (NaBiO_3) is a commercially available strong oxidant. It is insoluble in water and only sparingly soluble in nitric acid²⁹. It has an ilmenite structure³⁷. The bismuth present in the compound is in the Bi(V) state. Its oxidative power comes from the Bi(V) to Bi(III) redox couple with a potential of 2.0 V¹⁷. It is commonly used for the determination of manganese in steel, since it is capable of oxidizing manganese species present to permanganate³⁸. It has also been studied for potential use as a photocatalyst for oxidative treatment of organic material in wastewater³⁹⁻⁴³. Much of the commercially available reagent-grade sodium bismuthate contains residual carbonates and peroxides. Peroxides act as a reducing agent with respect to Am(VI). High purity (93% and peroxide free) sodium bismuthate was obtained from Idaho National Laboratory (Source: ChemSavers). Reagent grade (~80%) sodium bismuthate was also tested and was obtained from Sigma Aldrich. The high purity and reagent-grade sodium bismuthate were used as received.

2.1.2 DGA Resin

DGA resin is a commercially available extraction chromatography resin produced by Eichrom Technologies Inc. The ligand is N,N,N',N'-tetra-n-octyldiglycolamide. A version of the ligand with branched carbon chains exists; however, the straight chain DGA resin was used for this work. The DGA resin has a high affinity for tri- and tetravalent actinides and lanthanides⁴⁴. The structure of the DGA ligand is shown in Figure 5.

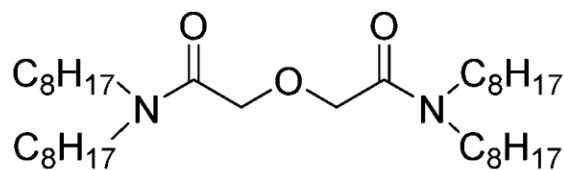


Figure 5: N,N,N',N'-tetra-n-octyldiglycolamide

DGA resin was chosen for this project because of its high affinity for trivalent actinides and low affinity for hexavalent actinides. It would theoretically be able to separate Cm^{3+} and AmO_2^{2+} by retaining the curium and not the americium. The resin used was bulk 50–100 μm particle size DGA resin, normal obtained from Eichrom Technologies Inc.

2.1.3 UTEVA Resin

UTEVA resin is a commercially available extraction chromatography resin produced by Eichrom Technologies Inc. The ligand is diamylamylphosphonate (DAAP). UTEVA resin has a high affinity for tetra- and hexavalent actinides and a low affinity for trivalent actinides⁴⁵. The structure of the DAAP ligand is shown in Figure 6.

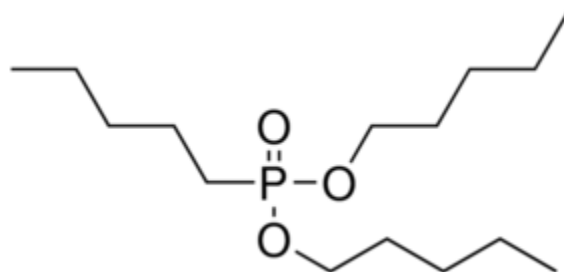


Figure 6: Diamylamylphosphonate

UTEVA resin was chosen for this project because of its high affinity for hexavalent actinides and low affinity for trivalent actinides. It would theoretically be able to separate Cm^{3+} and AmO_2^{2+}

by retaining the americium and not the curium. The resin used was bulk 100–150 μm particle size UTEVA resin obtained from Eichrom Technologies Inc.

2.2 Methods

2.2.1 Solvent Extraction

Solvent extraction is a separation technique in which a solute or solutes are partitioned between two immiscible liquid phases. Typically, the partitioning occurs between an aqueous phase and an immiscible organic phase. The aqueous phase may contain acids, bases, complexing agents, or other constituents based on the separation to be performed. The organic phase typically contains some type of extractant, or ligand, used to remove certain constituents selectively from the aqueous phase.

The distribution ratio is used to measure the effectiveness of a particular solvent extraction system. This value is simply the concentration of the solute of interest in the organic phase divided by its concentration in the aqueous phase. This allows for comparison between solvent extraction systems and is useful in determining which solvent extraction system to use for a given separation or extraction need.

Solvent extraction is used in this work to determine the partitioning of americium between nitric acid and dibutylbutylphosphonate (DBBP) in n-dodecane. Experimental details are given in Chapter 3.

2.2.2 Ion Exchange Chromatography

Ion exchange chromatography is a chemical separation technique in which a mobile phase containing a solute of solutes of interest is passed over a solid phase that has stationary active sites where labile ions can be exchanged. Ion exchange materials are either cation or anion exchangers based on the charge of the labile ion. The surfaces of many natural materials, such as

oxide minerals and clays, have ion exchange properties. Commercial ion exchange resins are also available and are typically composed of permeable polymer beads that have covalently bound ionic functional groups on the polymer chains. Some inorganic ion exchange materials are also available.

Separations can be performed when there is a difference in the strength of interaction between ions of interest and the ion exchange material. The strength of these interactions can be compared using the weight distribution ratio (D_w). This ratio is the same as the distribution ratio used in solvent extraction except it is the concentration of the solute of interest on the ion exchange material (in activity per unit mass) divided by its concentration in the aqueous phase (in activity per unit volume).

A novel ion exchange chromatography technique is presented in this work. Experimental details are given in the chapters.

2.2.3 Extraction Chromatography

Extraction chromatography is, in essence, a combination of solvent extraction and ion exchange. An organic ligand or extractant is loaded onto an inert support material to create a chromatographic resin with partitioning characteristics similar to that of the solvent extraction system. The use of organic ligands or extractants often offers greater selectivity than ion exchange techniques while offering the ease of operation of column chromatography. Many extraction chromatography resins are commercially available.

Weight distribution ratio can be used in extraction chromatography in much the same way as ion exchange. For well-characterized resins, the weight distribution ratio can be converted to a value that estimates the free column volume to peak maximum (k') for that system. This is a simple correction factor and it was used in this work to determine the k' for americium and

curium on commercially available extraction chromatography resins. Experimental details are given in Chapter 3.

2.2.4 Batch Contact Studies

The batch contact method used to determine adsorption provides insight into the potential of a resin or other chromatographic material to perform separations. A tracer is added to the solution, which is then brought into contact with the solid material, under constant mixing provided by a shaker table. The solution is then separated from the solid material and the activity of the analyte remaining in the solution is determined. The activity of the analyte in solution, as well as the mass of the solid material, the volume of solution, and the activity of analyte associated with the solid phase (determined by difference), are put into Equation 1 to determine the weight distribution ratio (D_w).

$$D_w = \frac{A_s/m}{A_{aq}/V} \quad \text{where} \quad A_s = A_o - A_{aq} \quad (1)$$

Activity in the solid phase (A_s) and in solution (A_{aq}) and total activity (A_o) are in units of activity, mass (m) is in grams, and volume (V) is in milliliters. The weight distribution ratio allows for comparison of behavior between various elements on a given chromatographic material. The larger the difference in weight distribution ratio between the respective elements, the greater the separation factor. Experimental details are given in each chapter.

2.2.5 CeF₃ Microprecipitation

Microprecipitation aims to create a very thin sample for alpha spectroscopy through the precipitation of small quantities (0.1 to 1.0 μg) of highly insoluble compounds. This insoluble material is chosen in such a way that coprecipitation of selected actinides occurs and the precipitate is subsequently filtered from solution onto a micropore filter (0.1-0.45 μm pore size). While these

samples are often thicker than electrodeposited samples, the recovery is very consistent. The resolution often approaches that of electrodeposited samples⁴⁶.

Cerium fluoride microprecipitation was chosen as the preferred method for the preparation of actinide samples for alpha spectrometry analysis. To prepare these samples, 0.1 mL of 3.6 mM $\text{Ce}(\text{NO}_3)_{3(\text{aq})}$ is added to the sample solution. One milliliter of concentrated hydrofluoric acid is then added, and the solution is briefly mixed by swirling. The solution is allowed to sit for 30 minutes, after which the sample is filtered through a 0.1 μm polypropylene filter. The Resolve filters used in this work were obtained from Eichrom Technologies Inc. The filter is then dried under a heating lamp, mounted onto a stainless steel planchet, and analyzed.

Disproportionate recovery on the filter was noted for trivalent and tetravalent actinides in molar nitric acid samples. This phenomenon was not observed in chloride matrices. Samples in a nitric acid matrix were therefore evaporated and reconstituted in hydrochloric acid prior to the cerium fluoride microprecipitation procedure.

2.3 Instrumentation

2.3.1 Alpha Spectrometry

Semi-conductor detectors are the most widely used type of detector for charged particles. The fast timing characteristics, wide detectable energy range, relatively low cost, and wide range of good linearity make them a good choice for a wide variety of applications. The intrinsic efficiency of semi-conductor detectors for alpha spectroscopy are essentially 100% since the active volume of the detector results in a thickness that is greater than the range of any naturally occurring alpha particle.

These detectors are solid-state ionizing detectors. The energy from the charged particle is transferred to electrons in the material that are promoted from the valence band to the conduction

band, resulting in electron-hole pairs. The energy required to make an electron-hole pair is significantly smaller than for ionizations in gas-filled detectors. More ionizations occur per interaction with a particle of a given energy, and as a result, improved energy resolution is possible.

The main parameters that are used to characterize silicon charged-particle detectors are resolution, active area, and depletion depth. The resolution can be as low as 12 keV. The compact size of these detectors allows for a wide variety of geometries; however, the most common geometry is a circular disc.

The active area of the disc is determined by the diameter of the circular disc. The depletion depth is synonymous with the sensitive depth of the detector, or the thickness of the silicon disc for a fully depleted detector. The thickness of the disc must be greater than the range of the particle in that material. A fifty-micron thickness of silicon detector is sufficient to stop all naturally occurring alpha particle energies.

A Canberra Alpha Analyst instrument was used to analyze all samples prepared for alpha spectrometry. The detectors in this instrument were passivated implanted planar silicon detectors and had an active area of 450 mm². The samples were counted long enough to provide good statistics for all major peaks (>1000 counts/peak).

2.3.2 Liquid Scintillation Counting

Liquid scintillation counting is a radionuclide counting technique that employs a liquid scintillator to convert the energy from the radiation into light that can be measured with a photomultiplier tube. This technique is most often used with beta-emitting radionuclides but can also be used to measure alpha radiation. The liquid scintillator is an organic molecule whose scintillation properties stem from electronic transitions within the energy levels of the individual molecule. This makes it possible to have functional organic scintillators in a solid, liquid, or

gaseous state. Inorganic scintillators on the other hand rely on electron energy band structure within a crystal lattice and therefore are not functional as liquids.

The radionuclide is dissolved and mixed in with the liquid scintillation “cocktail.” The cocktail is a mixture of an organic scintillator and an appropriate solvent, as well as a waveshifter compound (absorbs photons emitted by the scintillator and re-emits them at a longer wavelength) and an emulsifier that allows for the sample containing the radionuclide to be in a polar or nonpolar solvent.

The fact that the radionuclide is mixed into the scintillator material allows for a 4π counting geometry. Since the vial is placed in a mirrored cavity for measurement of the emitted light, the counting efficiencies are near 100 %. This technique has one of the highest counting efficiencies in radiation detection. The scintillator has a decay time of a few nanoseconds for prompt fluorescence, which allows for rapid pulse processing. Liquid scintillation counting can also be used to measure indirectly ionizing radiation such as gamma rays and neutrons, but additional elements that will enhance the radiation interactions must be added to the cocktail.

The light emitted by the sample is measured by two photomultiplier tubes that are operated in coincidence counting mode. The coincidence counting lowers the background reading and greatly improves the signal to noise ratio. Photomultiplier tubes randomly record events from thermally produced photoelectrons even when no light is present. It is unlikely that two photomultiplier tubes will have these sporadic events simultaneously. However, it is very likely that the light coming from the scintillator will reach both photomultiplier tubes at essentially the same time.

It is possible that some of the radiation will not be converted to light or that the light that is emitted will not reach the detector. This decrease in light output is called quenching. Chemical quench is caused by molecules that absorb energy without emitting light. This reduces the overall

light output. Optical quench is caused by molecules in the sample that absorb light. It is also called color quench because optical quench often occurs in colored samples. The level of quench can be quantitatively measured by a series of Quench Indicating Parameters (QIP). One of these parameters is the Spectral Index of the Sample (SIS). This method measures the shift in the peak of a given beta-emitter spectrum caused by quench. The peak is shifted to lower energies when a quenching agent is present. Another quench indication parameter is called the transformed Spectral Index of the External Standard (t-SIE). This parameter is calculated from the Compton edge of a gamma spectrum induced in the scintillation cocktail by an external gamma source. The SIS is only accurate for samples containing one known radionuclide with a high enough activity to give a clear distribution.

The instrument is calibrated using sources of known activity. The instrument adjusts the voltage of the photomultiplier tubes to optimize performance. This is typically done with a ^{14}C source. This standard, as well as a tritium standard and a blank, are measured and a t-SIE value of 1000 is assigned to these standards. Any value below 1000 indicates that some quench is occurring.

Perkin Elmer Tri-Carb 2800TR and Tri-Carb 5110 TR instruments were used for all liquid scintillation counting measurements. All samples were counted for one hour or until there were 40,000 counts (0.5 % relative uncertainty in the count rate) in the region of interest.

2.3.3 Atomic Emission Spectroscopy

Atomic emission spectroscopy was used to determine the concentration of non-radioactive elements of interest. The sample was introduced into the instrument through an inductively coupled plasma system. Inductively Coupled Plasma – Atomic Emission Spectroscopy (ICP-AES) is frequently used for elemental analysis of solutions. The liquid, typically aqueous, sample is aerosolized and introduced into the inductively coupled plasma in a stream of argon gas. While in

the plasma, the atoms in the sample are excited and ionized. The atoms that are promoted to an excited state decay to lower energy states, resulting in emission of characteristic light that is passed through a monochromator and detected at specific wavelengths. The characteristic wavelengths can be used to determine if a specific element is present in a sample or, if the instrument is calibrated with that element, the intensity of the light can be correlated to the concentration of the element in the solution. In this work, a Perkin Elmer Optima 8000 Spectrometer was used for quantitative analysis of lanthanide elements. All samples were prepared in ~2% v/v nitric acid.

2.3.4 Mass Spectrometry

Inductively Coupled Plasma – Mass Spectrometry (ICP-MS) was used to quantify elements that could not be measured accurately using ICP-AES. The sample preparation and sample introduction is identical to the ICP-AES system. In the ICP-MS the ionized atoms are however injected into a mass separator. In this case, the mass separator is a quadrupole. A quadrupole is considered a mass filter since it only allows ions of a certain mass-to-charge ratio to pass through. A quadrupole mass filter is composed of four parallel rods surrounding the ion path that use radio frequency and direct current voltages on opposing rods to make a stable trajectory for a given mass-to-charge ratio. The settings on the quadrupole are varied to scan through the masses of interest. The instrument used for this work was a Perkin Elmer ELAN DRC ICP-MS.

CHAPTER 3: ADSORPTION BEHAVIOR OF AMERICIUM AND CURIUM ON EXTRACTION CHROMATOGRAPHY RESINS IN THE PRESENCE OF SODIUM BISMUTHATE

3.1 Abstract

The separation of americium from curium is imperative for effective reprocessing of used nuclear fuel. Attempts were made to separate bismuthate-oxidized americium from curium utilizing two different extraction chromatography resins. Both attempts were unsuccessful. The sodium bismuthate raised the pH of solutions with low initial nitric acid concentrations and produced Bi(III) as a competing ion. Americium and curium adsorbed to the surface of the solid sodium bismuthate. While the americium and curium both showed some sorption to the sodium bismuthate solid, the curium is more strongly adsorbed.

3.2 Motivation and Objectives

It has been shown that americium can be extracted successfully from highly acidic solutions using diamylamylphosphonate (DAAP) and tributylphosphate (TBP) as ligands in solvent extraction systems^{31,35}. The success of these extraction systems depends entirely on the efficiency of the oxidation and the stability of the higher oxidation states. Trace reducing agents must be avoided and contact times must be short since contact with organic extractants or diluents can result in reduction of the americium to the trivalent state. Some oxidizing agents commonly used for americium oxidation, including NaBiO₃, are solids that must be present in solution in order to maintain oxidation. In general, large-scale solvent extraction processes are not equipped to operate with solids present in the solution. The presence of additional solids should however not be an issue in an extraction chromatography system.

The resins used in extraction chromatography are highly selective and require little maintenance during operation. In attempting to separate americium and curium with extraction chromatography resins, one can either attempt to selectively extract the americium as Am(VI) or selectively extract curium from americium oxidized to either Am(V) or Am(VI).

An extraction chromatography resin coated in N,N,N',N'-tetra-n-octyldiglycolamide (TODGA), sold as DGA resin from Eichrom Technologies Inc., exhibits a very high affinity for trivalent actinides such as americium and curium with k' values exceeding 10^4 in nitric acid concentrations of 1 M or greater⁴⁴. The affinity of DGA resin for penta- and hexavalent actinide elements is several orders of magnitude lower than for trivalent actinides. Attempts were made to utilize this affinity for trivalent actinides to extract curium selectively from solutions containing oxidized americium.

The ligand diamylamylphosphonate (DAAP) has been shown to extract Am(VI) from nuclear fuel raffinate simulant solution in a solvent extraction system³⁵. The DAAP ligand is also used in extraction chromatography as the extractant on commercially available UTEVA resin sold by Eichrom Technologies Inc. This resin is commonly used in separation of actinide elements due to its affinity for tetra- and hexavalent actinides⁴⁵. The resin has a very low affinity for trivalent actinides. In this work, attempts were made to utilize this affinity in order to achieve selective extraction of Am(VI) from curium. Extraction of Am(VI) with UTEVA resin would provide a good comparison of solvent extraction and extraction chromatography methods since Am(VI) has been extracted by the DAAP ligand in solvent extraction studies.

The objective of the work presented in this chapter was to explore the feasibility of utilizing extraction chromatography to separate americium in high oxidation states from curium. The resins were selected based on the difference in affinity for trivalent, pentavalent, and hexavalent actinide

ions in order to allow for a separation of trivalent curium from higher oxidation states of americium. The oxidant, sodium bismuthate, was chosen based on its ability to oxidize americium in molar concentrations of nitric acid.

3.3 Adsorption Behavior on DGA

3.3.1 Experimental

The affinity of americium and curium for DGA resin as a function of nitric acid concentration was tested using a batch contact method. DGA resin (50.0 ± 0.5 mg) was weighed into 2.0 mL centrifuge tubes. The resin was preconditioned by adding 0.800 mL of nitric acid of known concentration and mixing on a shaker table for one hour. The vials were then allowed to sit overnight. The tracer (0.500 mL of either Am-241 or Cm-244 at ~ 100 Bq/mL in 0.01 M HNO₃) was added to the preconditioned resin and mixed on a shaker table for one hour to establish equilibrium. The samples were then filtered through a 0.45 μ m syringe filter, and a 1.000 mL aliquot of the aqueous phase was removed for analysis by liquid scintillation counting (LSC). The same batch contact procedure was used for DGA with NaBiO₃, except ~ 30 mg of NaBiO₃ were weighed into the centrifuge tube with the DGA resin before preconditioning. In order to determine whether the k' was dependent on the ratio of Bi(III) to resin, the amount of resin and the preconditioning time were varied in the curium system.

Normal DGA resin (50-100 μ m bulk) was purchased from Eichrom Technologies Inc. and was used as received. Nitric acid was reagent grade and was diluted with 18.2 M Ω distilled deionized water from a Millipore water purification system. The sodium bismuthate was high purity (peroxide-free) and was used as received from Idaho National Laboratory (Source: ChemSavers). All data points are the average of three replicates and the error bars show the statistical uncertainty to one standard deviation.

3.3.2 Results and Discussion

3.3.2.1 Americium and Curium on DGA

The results for batch-contact adsorption studies for americium and curium on DGA resin in nitric acid are shown in Figure 7.

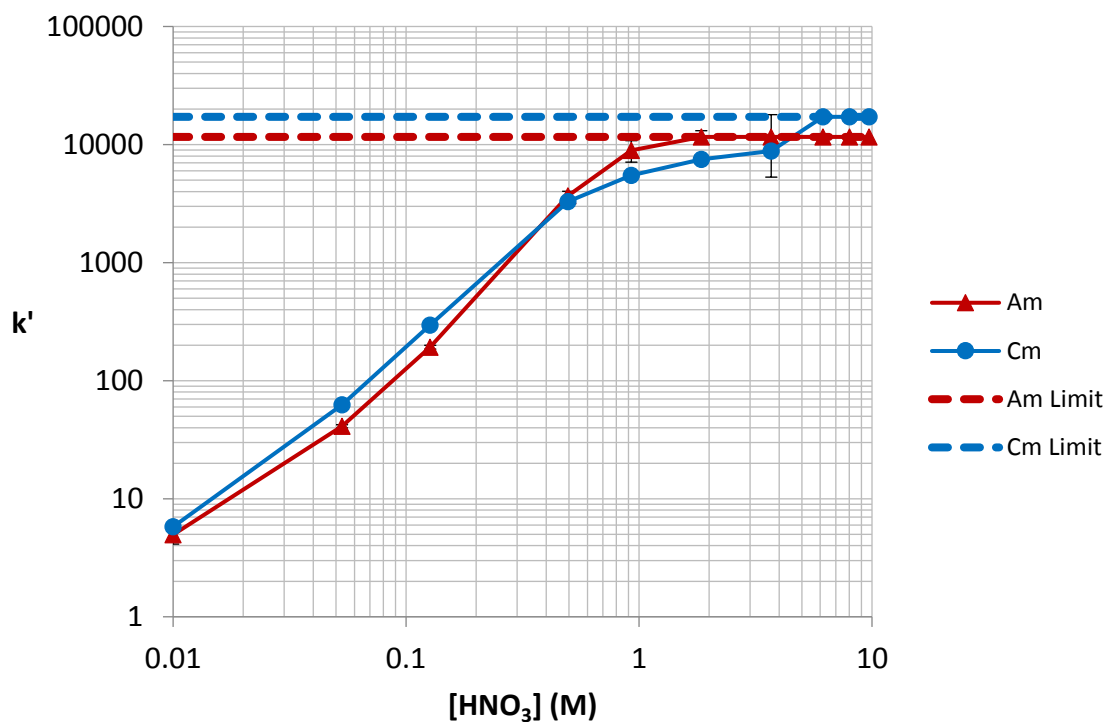


Figure 7: Nitric acid dependency of k' for Am and Cm on DGA resin

The affinity of DGA resin for Am(III) and Cm(III) is very similar. The k' values for both elements increase with increasing acid concentration. These results are in good agreement with previous studies⁴⁴.

3.3.2.2 Americium and Curium on DGA in the presence of NaBiO₃

The results for batch-contact adsorption studies for americium and curium on DGA resin in nitric acid in the presence of sodium bismuthate are shown in Figure 8.

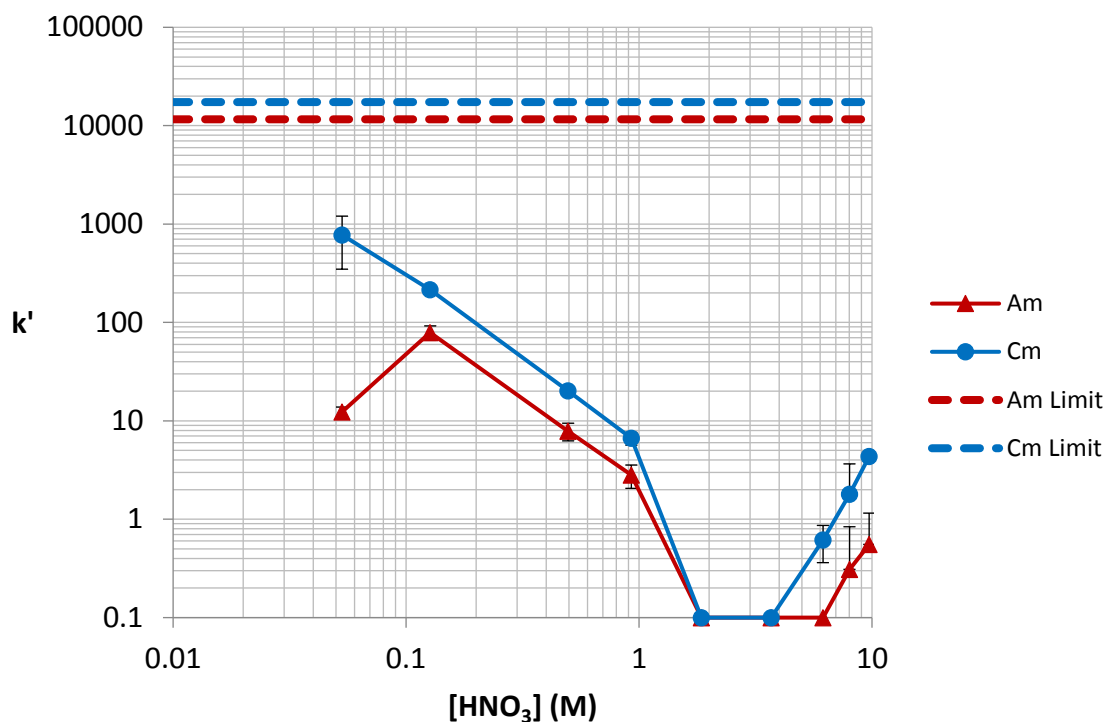


Figure 8: Nitric acid dependency of k' for Am and Cm on DGA in the presence of NaBiO_3

Below 0.1 M HNO_3 , the curium showed higher k' values than would be expected from DGA resin alone. The k' value for americium below 0.1 M HNO_3 was similar to DGA resin alone. Above 0.1 M HNO_3 there is a drop in k' with increasing acid concentration followed by a slight increase in k' above 4 M HNO_3 for both elements. This suggests that the change in k' is not caused by the oxidation of americium. The first data point at 0.01 M HNO_3 was omitted because the 0.01 M HNO_3 samples reached a pH of ~ 7 when in contact with the NaBiO_3 and the actinides may have

been lost from solution by hydrolysis. The oxidant, NaBiO_3 , uses the $\text{Bi(V)} - \text{Bi(III)}$ redox couple. The reduced bismuth is in the trivalent state. The possibility of Bi(III) interference was explored.

3.3.2.3 Bi(III) Interference

The amount of resin used was varied to include 50, 100, and 150 mg. The 100 and 150 mg samples were measured after one hour of contact and after contact overnight. The results for the batch-contact adsorption studies for curium on DGA resin in nitric acid are shown in Figure 9 overlaying the data from Figure 8.

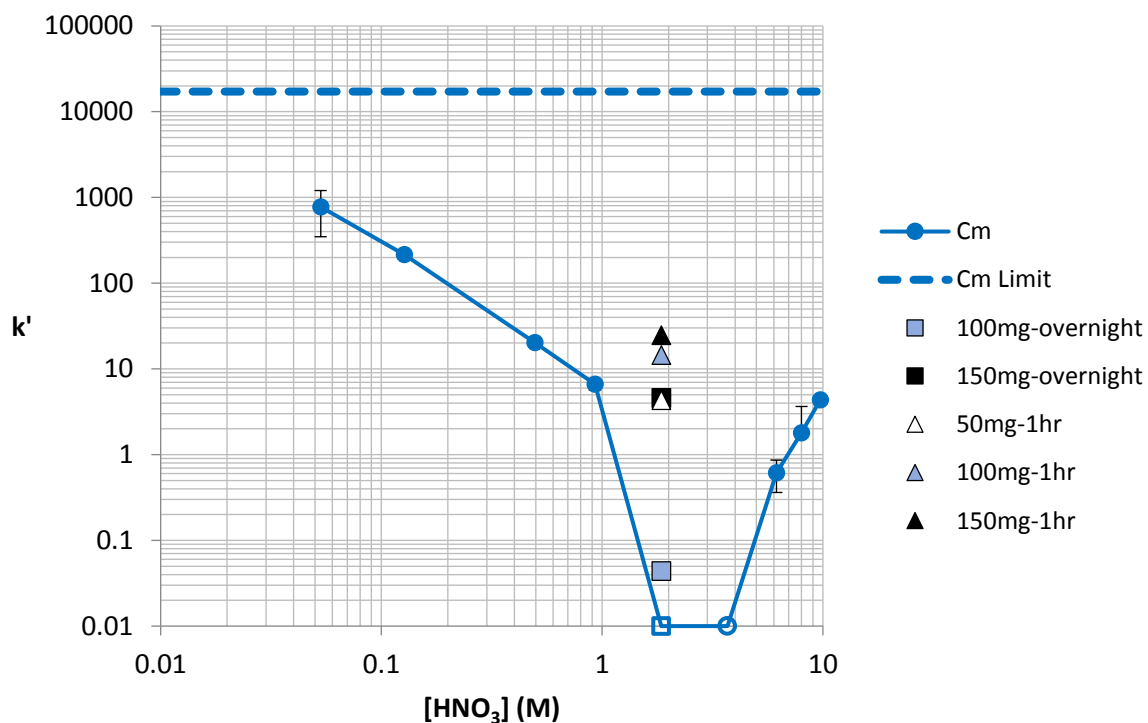


Figure 9: Effect of different preconditioning times and resin masses on k' for Cm on DGA

The k' of Cm on DGA in the presence of NaBiO_3 was dependent on preconditioning time and resin mass. This is consistent with the hypothesis that Bi(III) was acting as a competing ion for the DGA resin. The longer preconditioning times lead to higher Bi(III) concentrations and more resin mass increases the number of binding sites for both the Bi(III) and Cm(III) . As the preconditioning time increased, the k' values decreased for the same amount of resin. As the resin mass was increased, resulting in a higher resin to bismuth ratio, the measured k' values increased. These results supported the hypothesis that ingrowth of Bi(III) was impacting the k' values in this study. The k' of Bi(III) on DGA has been measured by Horwitz et al., and the acid dependency plot is shown in Figure 10.

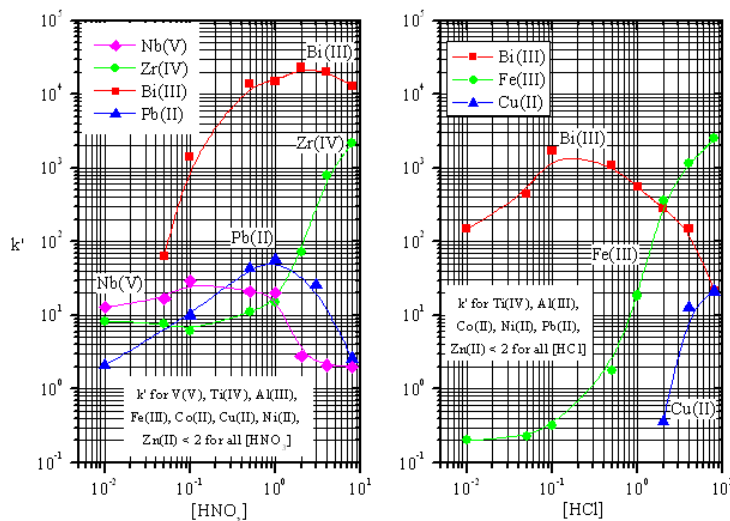


Figure 10: k' for selected transition and post transition elements on DGA resin⁴⁴

The k' value for Bi(III) in nitric acid is even greater than that of Cm(III) or Am(III) in the mid-range nitric acid concentrations. This is also where the k' for Am and Cm was the lowest for the

DGA-BiO₃ system. This suggests that the Bi(III) produced from the reduction of NaBiO₃ acts as a competing ion for the DGA resin.

3.4 Adsorption Behavior on UTEVA

3.4.1 Experimental

The affinity of americium and curium for UTEVA resin as a function of nitric acid concentration was tested using a batch contact method. UTEVA resin (50.0 ± 0.5 mg) was weighed into 2.0 mL centrifuge tubes. The resin was preconditioned by adding 0.800 mL of nitric acid of known concentration and mixing on a shaker table for one hour. The vials were then allowed to sit overnight. The tracer (0.500 mL of either Am-241 or Cm-244 at ~ 100 Bq/mL in 0.01 M HNO₃) was then added to the preconditioned resin and mixed on a shaker table for one hour to establish equilibrium. The samples were then filtered through a 0.45 μ m syringe filter, and a 1.000 mL aliquot of the aqueous phase was removed for analysis by liquid scintillation counting (LSC). The same batch contact procedure was used for UTEVA with NaBiO₃, except ~ 30 mg of NaBiO₃ were weighed into the centrifuge tube with the UTEVA resin before preconditioning.

UTEVA resin (50-100 μ m bulk) was purchased from Eichrom Technologies Inc. and was used as received. Nitric acid was reagent grade and was diluted with 18.2 M Ω distilled deionized water from a Millipore water purification system. The sodium bismuthate was high purity (peroxide-free) and was used as received from Idaho National Laboratory (Source: Chem Savers). All data points are the average of three replicates, and the error bars show the statistical uncertainty to one standard deviation.

3.4.2 Results and Discussion

3.4.2.1 Americium and Curium on UTEVA

The results of the batch studies in the absence of NaBiO₃ are shown in Figure 11.

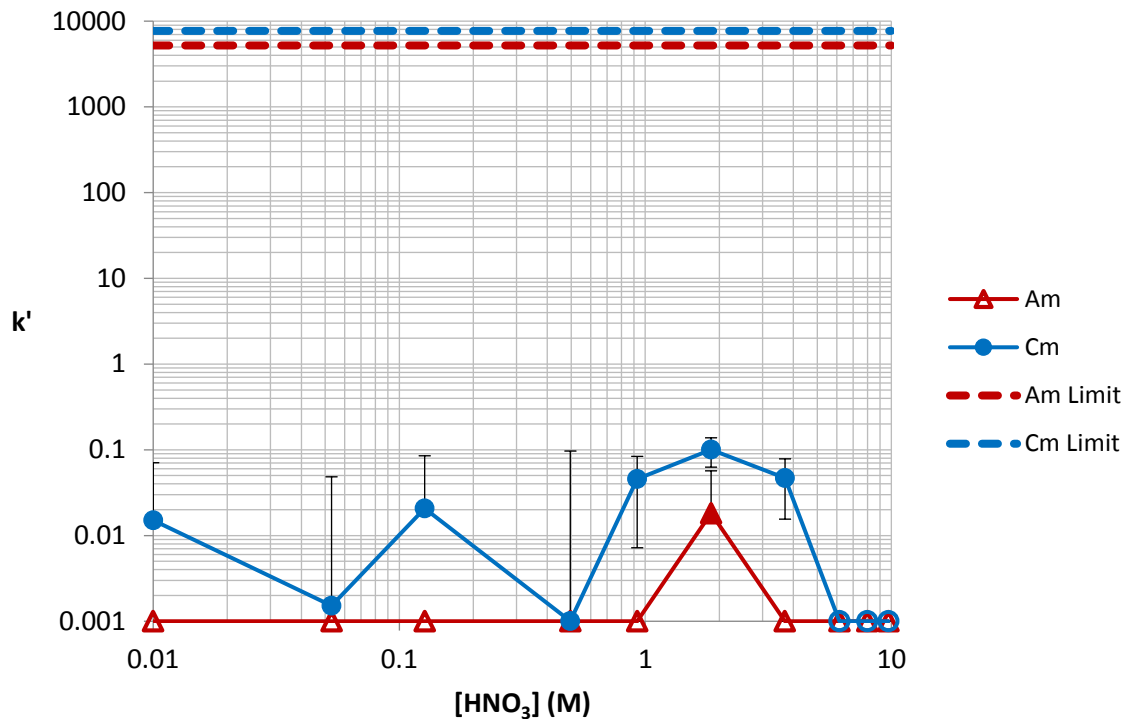


Figure 11: Nitric acid dependency of k' for Am and Cm on UTEVA resin

The k' values for both Am and Cm were very low for all acid concentrations with a peak at ~2M HNO₃ for both elements. This is as expected from literature³⁵.

3.4.2.2 Americium and Curium on UTEVA in the presence of NaBiO₃

The batch contact procedure was repeated with NaBiO₃ for UTEVA resin. The results are shown in Figure 12.

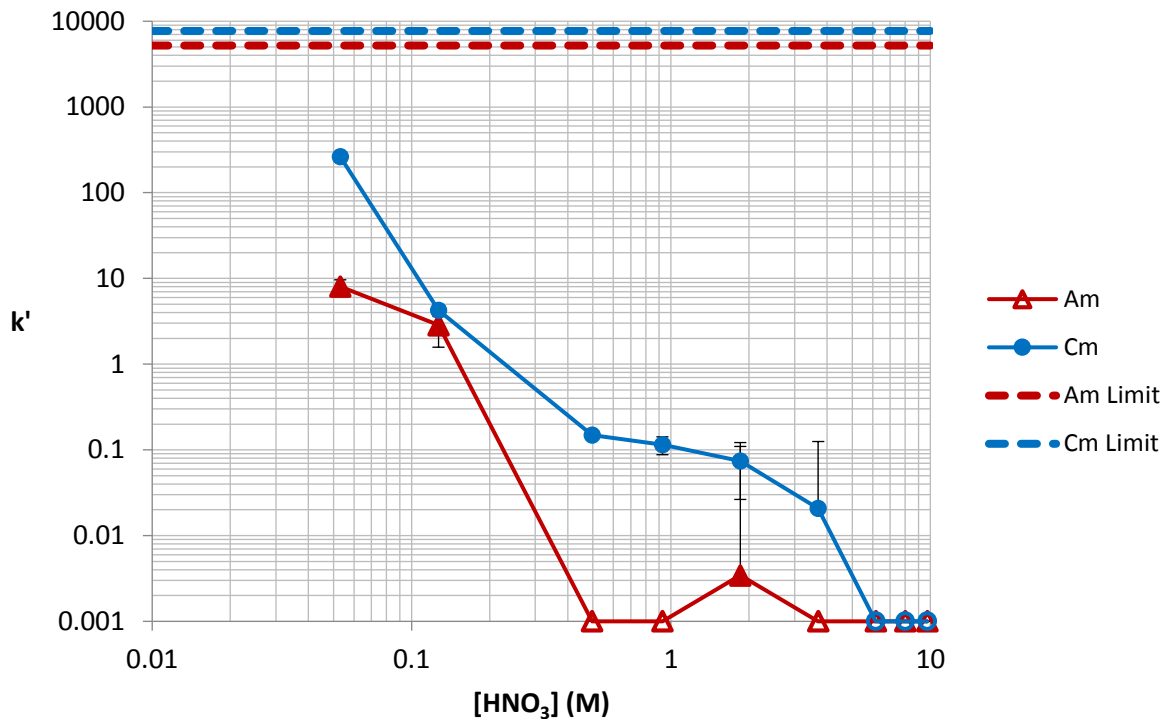


Figure 12: Nitric acid dependency of k' for Am and Cm on UTEVA in the presence of NaBiO₃

The k' values from ~2 M HNO₃ through the higher concentrations appeared to behave similarly to the system without NaBiO₃ while at lower concentrations there is an increase in the measured k' values as the nitric acid concentration decreases similar to the behavior seen in the DGA-NaBiO₃ system. The ligand used in UTEVA resin has been shown to extract bismuthate-oxidized Am(VI) from nitric acid solutions in solvent extraction systems³⁵. It was decided that an attempt to replicate the solvent extraction results could provide valuable information as well as provide a good starting point to understanding the behavior of bismuthate-oxidized Am in an extraction chromatography system.

3.5 DBBP Solvent Extraction of Bismuthate-Oxidized Am

3.5.1 Experimental

The procedure outlined by Bruce Mincher et al. in their paper “Diamylamylphosphonate Solvent Extraction of Am(VI) from Nuclear Fuel Raffinate Simulant Solution”³⁵ was replicated with some minor variations. The aqueous phase was prepared by adding the appropriate amount of water, Trace Select Nitric acid, and tracer (0.400 mL of ~200 Bq/mL ²⁴¹Am in 0.1 M HNO₃) to make 0.800 mL of aqueous phase in the appropriate nitric acid concentration to a 2.0 mL centrifuge tube with ~20 mg of NaBiO₃. The aqueous phase was shaken on a shaker table for two hours. The organic phase was 0.800 mL of 1 M dibutylbutylphosphonate in n-dodecane that was contacted with 0.800 mL of nitric acid of the same concentration as the aqueous phase with ~20 mg of NaBiO₃ for 2 hours. The aqueous and organic phases were separated from the oxidant by centrifugation and 0.600 mL of each phase was added to a 2.0 mL centrifuge tube, contacted on a vortex mixer for 15 seconds, and immediately separated by centrifugation. Aliquots (0.500 mL) were taken from each phase and counted by LSC. The distribution ratio was then calculated as the concentration of Am in the organic phase divided by the concentration in the aqueous phase.

3.5.2 Results and Discussion

One test measurement was run with 6.0 M HNO₃. The experiment was run in triplicate and the distribution ratio (D_{Am}) was found to be $D_{Am} = 0.19$. This is lower than the values reported by Mincher et al. However, the concentration of Am in their experiments was orders of magnitude higher than the concentration that was used in this work. It was noted in their work that the distribution ratio increased at higher americium concentrations. A comparison of the americium concentrations and distribution ratios reported by Mincher and the value obtained in this work are shown in Table 1 and Figure 13.

Table 1: Comparison of americium D-values at different concentrations extracted by DBBP

$[Am](M)$	D_{Am}	Source
2.30×10^{-3}	13.5	Mincher ³⁵
3.00×10^{-5}	3.6	Mincher ³⁵
3.27×10^{-9}	0.2	Richards

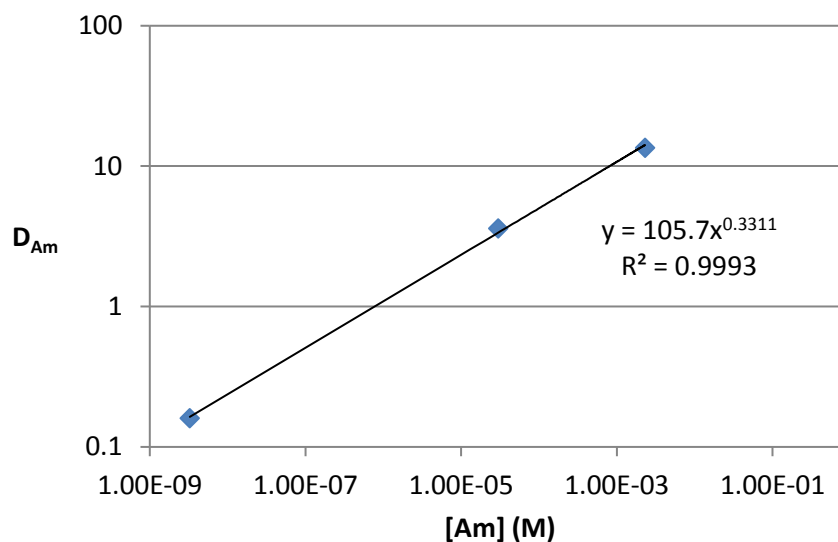


Figure 13: D_{Am} plotted against Am concentration

The value of D_{Am} appears to have a correlation to the concentration of Am in the solvent extraction system with the distribution ratio being lower at lower concentrations. Whether this is due to a difference in Am oxidation efficiency as is proposed in the paper by Mincher et al. or another reason, such as kinetics is still unknown. Further study and experimentation would be required to understand the implications of this possible correlation.

3.6 Conclusions

Separation of bismuthate-oxidized americium from curium utilizing extraction chromatography was unsuccessful in this work. The presence of Bi(III) proved to be problematic

in the DGA- NaBiO_3 system. The UTEVA- NaBiO_3 system did not show the predicted extraction of americium at high nitric acid concentrations. The results from both the DGA and UTEVA experiments provided evidence that americium and curium were being lost from solution at low acid concentrations. The possibility of hydrolysis was ruled out because samples that had an initial nitric acid concentration above 0.01 M had a measured pH lower than 2. The increase in pH seen in low initial acid concentration samples was found to be almost instantaneous, not gradual as would be expected from decomposition of NaBiO_3 . This led to the hypothesis that the surface of the solid sodium bismuthate was basic and acting as an ion-exchange material and that the americium and curium were adsorbing to the surface of the undissolved bismuthate.

CHAPTER 4: ADSORPTION OF AMERICIUM AND CURIUM TO SODIUM

BISMUTHATE SOLID

4.1 Abstract

Unexplained loss of americium and curium from dilute nitric acid solutions was observed in studies aimed at utilizing extraction chromatography to separate bismuthate-oxidized americium from curium. Adsorption of americium and curium on the undissolved sodium bismuthate solid was hypothesized as a possible cause. The results of a detailed study of the adsorption of americium and curium to solid sodium bismuthate are presented here. The sorption behavior of americium was found to be very different from the sorption behavior of curium.

4.2 Motivation and Objectives

Studies aimed at utilizing extraction chromatography to separate bismuthate-oxidized americium from curium showed significant deviation from the expected metal ion behavior at nitric acid concentrations below one molar. This led to the hypothesis that the surface of the undissolved sodium bismuthate could play an active role in the behavior of the metal ions. The objective of the work presented in this chapter was to determine and quantify the interaction of the americium and curium metal ions with the surface of the undissolved sodium bismuthate.

4.3 Nitric Acid Dependency of Adsorption

4.3.1 Experimental

4.3.1.1 Americium and Curium on NaBiO₃

The affinity of americium and curium for NaBiO₃ as a function of nitric acid concentration was tested using a batch contact method. The NaBiO₃ (50.0±0.5 mg) was weighed into 2.0 mL centrifuge tubes. The appropriate amount of water and TraceSELECT nitric acid and tracer (either Am-241 or Cm-244 at ~200 Bq/mL in 0.1 M HNO₃) and was added to give the desired final acid

concentration. The samples were mixed with the shaker table for an hour and were then filtered through a 0.45 μm syringe filter, and an aliquot of the aqueous phase was removed for analysis by liquid scintillation counting (LSC). All data points are the average of two replicates, and the error bars show the statistical uncertainty to one standard deviation.

4.3.1.2 Americium and Curium on Preconditioned NaBiO_3

The same procedure was used as described previously except that the NaBiO_3 was initially washed with 1.000 mL of the appropriate acid concentration, then separated by centrifugation and 0.800 mL was subsequently removed. Another 0.800 mL of fresh acid was added and then separated. This was repeated once more, and then the appropriate amount of water, nitric acid (TraceSELECT), and tracer was added to perform the batch contact experiment. The aqueous phase was analyzed by liquid scintillation counting (LSC). All data points are the average of three replicates, and the error bars show the statistical uncertainty to one standard deviation.

4.3.2 Results and Discussion

The results of the batch contact study of americium and curium on sodium bismuthate solid is presented in Figure 14. The results of the batch contact study of americium and curium on preconditioned sodium bismuthate solid is presented in Figure 15.

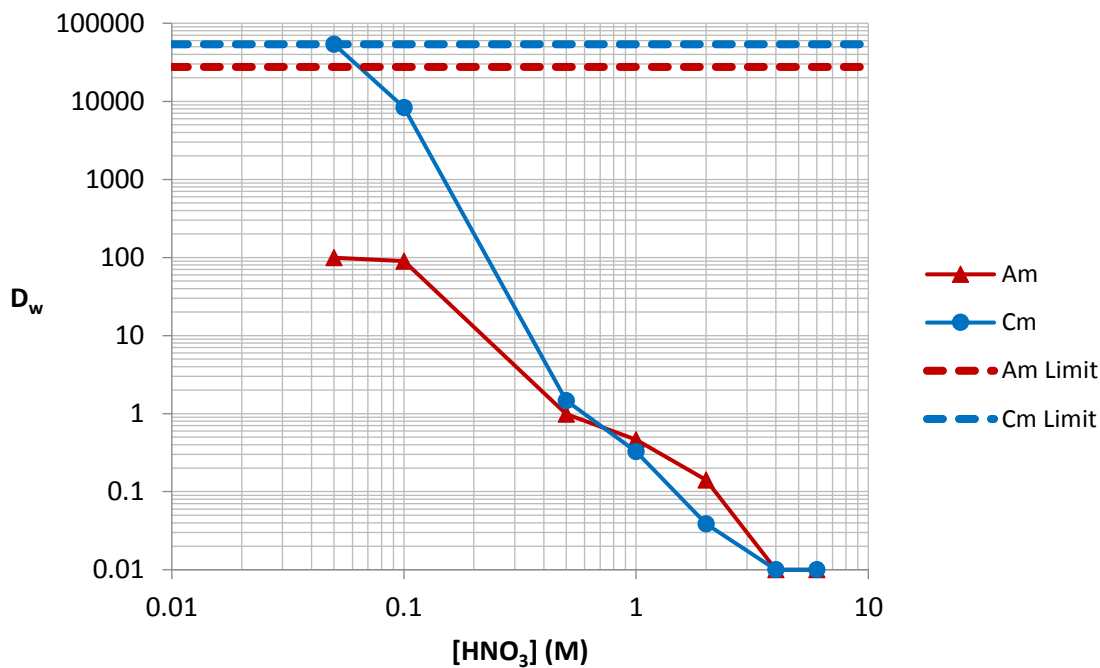


Figure 14: Nitric acid dependency of D_w for Am and Cm on $NaBiO_3$ powder

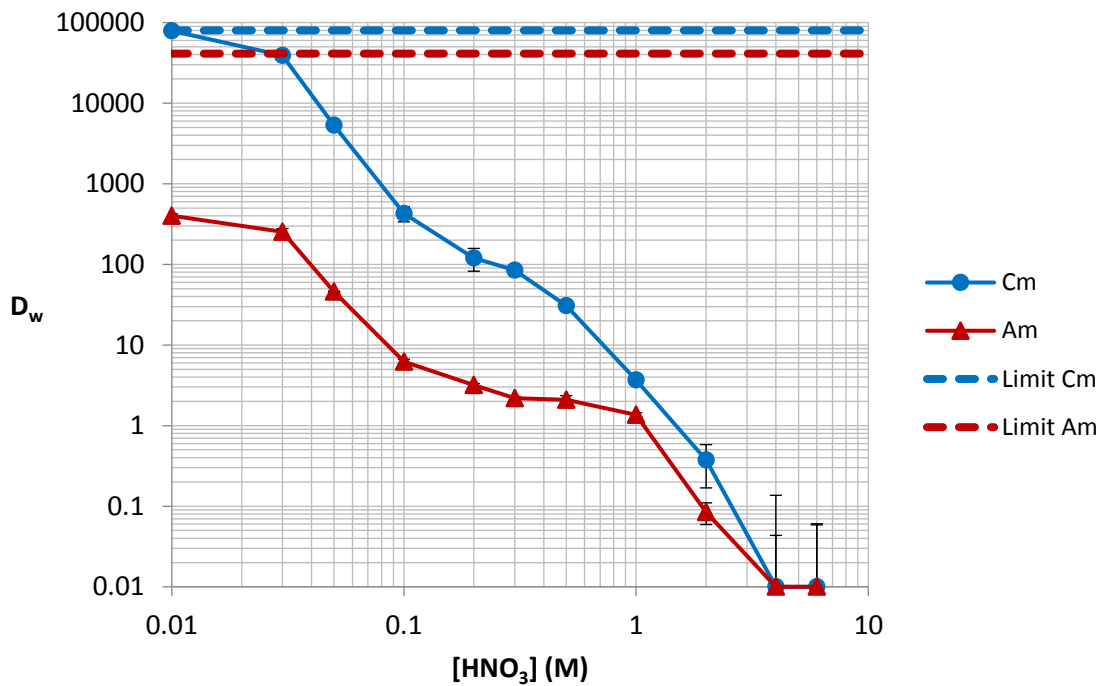


Figure 15: Nitric acid dependency of D_w for Am and Cm on preconditioned $NaBiO_3$ solid

The weight distribution ratios of americium and curium on sodium bismuthate show strong adsorption below 0.1 M HNO₃ with the adsorption being about 100 times larger for curium. Above 0.1 M HNO₃ the adsorption drops off rapidly with increase acid concentration. When the preconditioning step is added the decrease in D_w values is less drastic than the non-preconditioned case but the adsorption for curium remains about 100 times higher for curium than for americium.

The structure of sodium bismuthate is quite similar to that of aluminum oxide³⁷. The sodium bismuthate solid can behave like an ion exchange material. The dry material is quite basic. When NaBiO₃ is mixed with DI water the resulting pH is around nine or ten. This property would explain the differences observed when the preconditioning step is added in the batch study experiments. At low acid concentrations, the pH is raised significantly by the dry bismuthate. When the sodium bismuthate is preconditioned with nitric acid the adsorption of curium is significantly higher than that of americium at nitric acid concentrations below 1 M.

4.4 Time Dependence of Adsorption

4.4.1 Experimental

The affinity of americium and curium for NaBiO₃ as a function of time in 0.1 M nitric acid concentration was tested using a batch contact method. The NaBiO₃ (50.0±0.5 mg) was weighed into 2.0 mL centrifuge tubes. The NaBiO₃ was washed with 1.000 mL of 0.1 M nitric acid then separated by centrifugation, and 0.800 mL was removed. Another 0.800 mL of 0.1 M nitric acid was then added and separated. This was repeated once more for a total of three preconditioning washes. The tracer (0.400 mL of either Am-241 or Cm-244 at ~200 Bq/mL in 0.1 M HNO₃) and 0.400 mL 0.1 M nitric acid was added to give a final volume of 1.000 mL. The samples were mixed for a set amount of time (1 – 120 minutes) and were filtered through a 0.45 µm syringe

filter, and an aliquot of the aqueous phase was removed for analysis by liquid scintillation counting (LSC). All data points are the average of three replicates, and the error bars show the statistical uncertainty to one standard deviation.

4.4.2 Results and Discussion

The results of the study on the time dependence of adsorption of americium and curium on preconditioned sodium bismuthate in 0.1 M HNO₃ are presented in Figure 16.

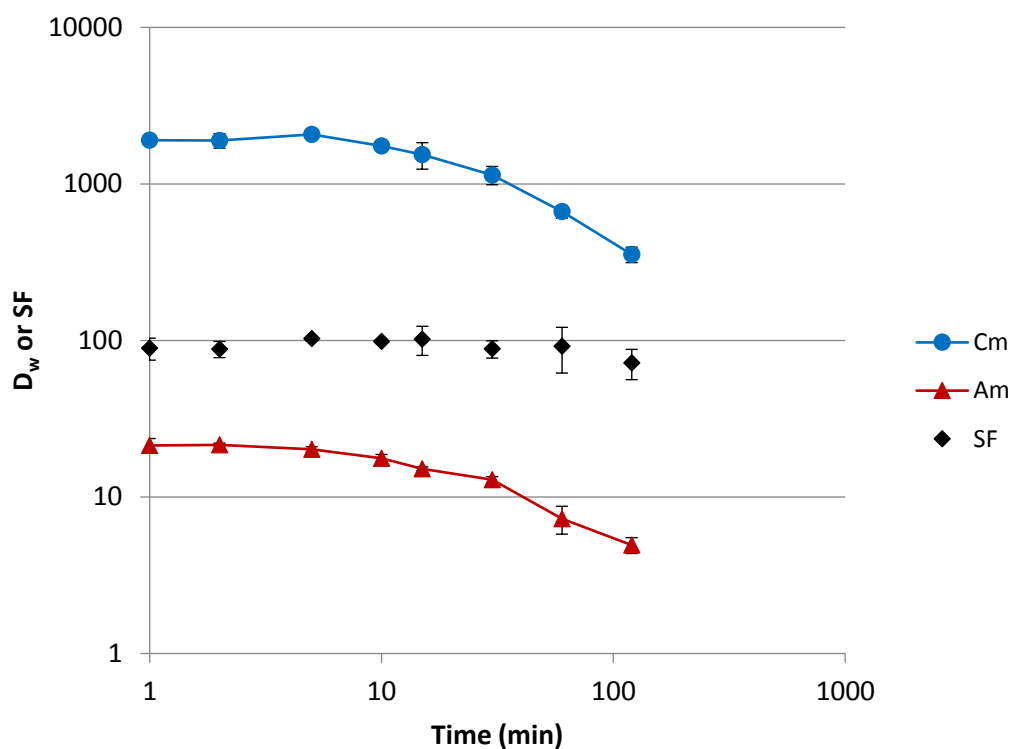


Figure 16: Time dependence of D_w of Am and Cm in 0.1 M HNO₃ on NaBiO₃

The separation factor of ~90 seen in the nitric acid dependency studies of Am and Cm on sodium bismuthate is seen within the first minute of contact. As contact time increases, the D_w for americium and curium decrease. This results in a changing D_w for both americium and curium, but

a relatively constant separation factor (SF) over the course of the first two hours of contact. This decrease in D_w over time could be due to the ingrowth of Bi(III) as the sodium bismuthate is dissolved and reduced in the nitric acid solution. It is likely that Bi(III) would show similar behavior to Cm(III) on the solid sodium bismuthate and therefore behave as a competing ion.

4.5 Nitric Acid Dependency of Sorption with Short Contact Time

4.5.1 Experimental

The sorption experiment described in section 4.3 *Americium and Curium on Preconditioned NaBiO₃* was repeated with a contact time of 10 minutes instead of 1 hour. All data points are the average of three replicates, and the error bars show the statistical uncertainty to one standard deviation.

4.5.2 Results and Discussion

The results of the 10-minute batch contact study of americium and curium on sodium bismuthate is presented in Figure 17.

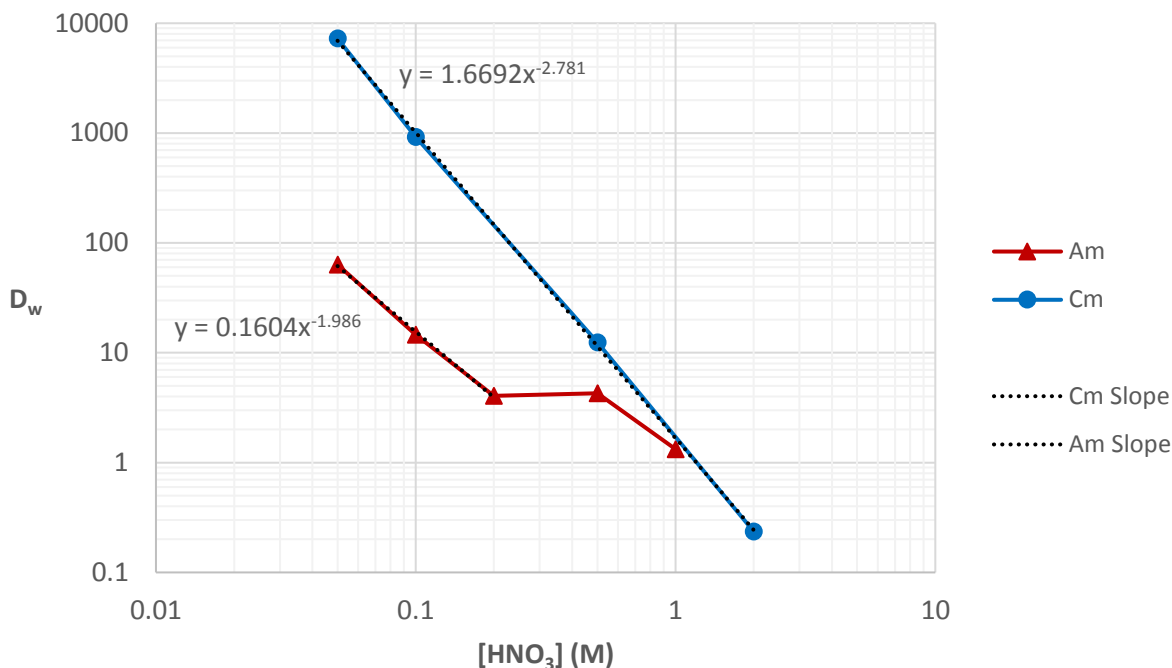


Figure 17: Nitric acid dependency of D_w for Am and Cm on preconditioned NaBiO_3 solid with a contact time of 10 minutes

The overall trends in americium and curium behaviors with a 10-minute contact time are the same as those seen with a 1-hour contact time. This D_w values for curium increase quickly with decreasing nitric acid concentration while, below 1 M, the values for americium are significantly lower. The nitric acid dependency curve for curium was more linear in the 10-minute contact time study compared with the 1-hour contact time study. This is likely due to the reduced interference of Bi(III) with shorter contact time. The slope of the curve on a log-log scale is -3, which is consistent with the expected trivalent behavior of curium. The nitric acid dependency curve for americium follows a linear correlation on a log-log plot between 0.05 and 0.2 M nitric acid. The slope of this line is -2, which is consistent with divalent americium (AmO_2^{2+}) behavior. The D_w for americium approaches values similar to D_w for curium as the nitric acid concentration increases.

At 1 M nitric acid, the americium behavior is no longer distinguishable from curium. It appears that americium follows hexavalent actinide behavior at low acid concentrations while following trivalent behavior at higher nitric acid concentrations on the surface of sodium bismuthate under these conditions.

4.6 Nitrate Dependence of Sorption

4.6.1 Experimental

Batch studies were performed to determine the nitrate dependence of Cm adsorption on NaBiO₃ with constant acid concentration of 0.05 M HNO₃. The procedure was identical to the batch studies performed for the 10-minute contact time studies for nitric acid dependency, except sodium nitrate solution was added instead of nitric acid to give the desired overall nitrate concentration. All data points are the average of three replicates, and the error bars show the statistical uncertainty to one standard deviation.

4.6.2 Results and Discussion

The results of the nitrate dependence study are shown in Figure 18 compared with the nitric acid dependency results.

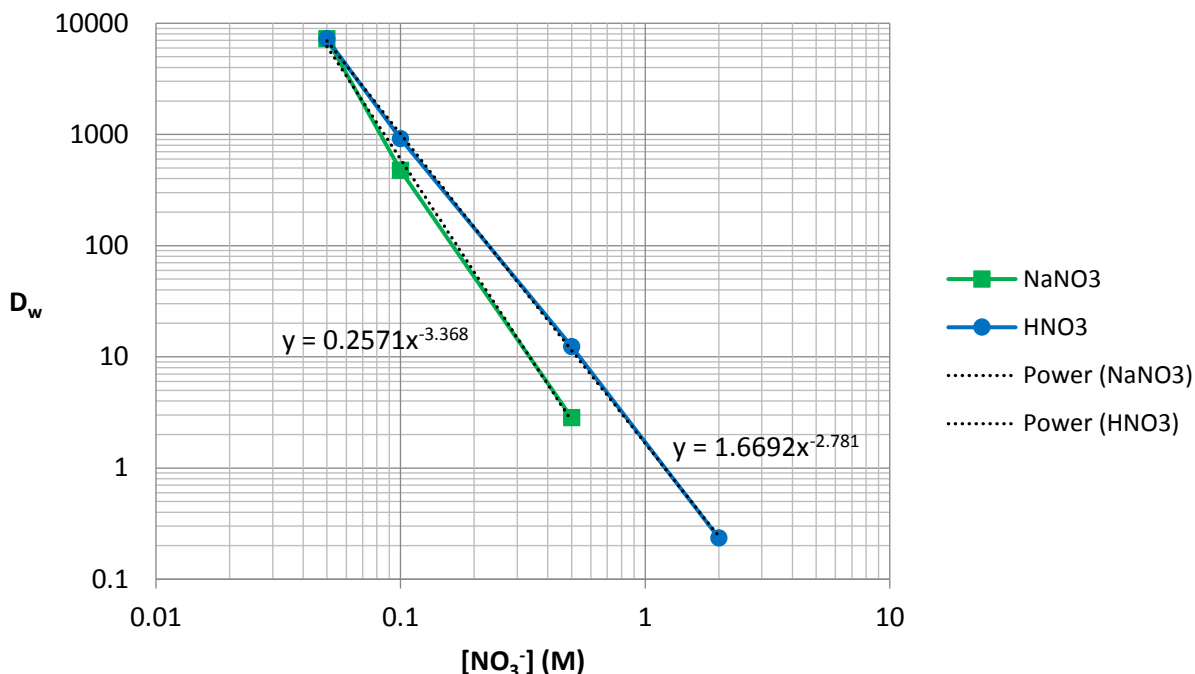


Figure 18: Nitrate dependency of D_w for Cm on preconditioned NaBiO_3 solid compared with nitric acid dependency

The nitrate dependence of curium sorption at a fixed acid concentration is very similar to the nitric acid dependence of curium sorption on sodium bismuthate solid. This suggests that the behavior seen is a result of the competition between active sites on the surface of the sodium bismuthate and nitrate complexation. This also shows that sorption will not occur when high concentrations of nitrate are present, even if the acid concentration is low.

4.7 Conclusions

It was found that americium and curium in nitric acid adsorb to the surface of solid sodium bismuthate. This adsorption appears to be the result of the ion exchange properties of the surface of the undissolved sodium bismuthate. Americium and curium are retained differently at nitric acid concentrations below 1 M. The difference in adsorption leads to a separation factor of ~90 at 0.1

M nitric acid. This separation factor is evident within the first minutes of contact and continues for at least two hours. The sorption of americium and curium decreases over time. This is thought to be due to the dissolution of sodium bismuthate and the corresponding increase of trivalent bismuth in solution. When contact time is kept short, americium exhibits hexavalent actinyl behavior (AmO_2^{2+}) at low nitric acid concentrations (<0.5 M). At higher concentrations of nitric acid, the americium behavior appears to be more like trivalent americium. Curium exhibits trivalent behavior across all concentrations of nitric acid in which adsorption was measurable. Above 2 M nitric acid, no adsorption of either americium or curium was seen. The sorption behavior of curium was found to be dependent on the concentration of nitrate in the system, suggesting that the sorption behavior is a result of competition between active sites on the surface of the solid sodium bismuthate and nitrate complexation in solution.

CHAPTER 5: SEPARATION OF AMERICIUM FROM CURIUM UTILIZING SODIUM BISMUTHATE

5.1 Abstract

A novel method for the separation of americium from curium in nitric acid media was developed using sodium bismuthate to perform both the oxidation and separation. Sodium bismuthate is shown to be a promising material for performing a simple and rapid separation. Curium is more strongly retained than americium on the undissolved sodium bismuthate at nitric acid concentrations below 1.0 M. A separation factor of ~ 90 was obtained in 0.1 M nitric acid. Separations using sodium bismuthate were performed using solid-liquid extraction as well as column chromatography.

5.2 Motivation and Objectives

One of the most significant challenges to any separation involving higher oxidation states of americium is maintaining oxidation throughout the separation procedure. By utilizing the surface chemistry of the undissolved sodium bismuthate, the oxidation and separation can be performed using the same material. Americium cannot interact with the separation medium without interacting with the oxidant simultaneously. This allows for a very reproducible higher oxidation state behavior of americium during the separation. Trace reducing agents are consumed by interaction with the sodium bismuthate and separations can be performed at room temperature using only nitric acid and sodium bismuthate.

5.3 Batch Solid-Liquid Separation Method

5.3.1 Experimental

A known amount of sodium bismuthate (20.0 ± 0.5 mg) was added to two 2.0 mL microcentrifuge tubes (Solid-1 and Solid-2). A 0.2 mL aliquot of 0.1 M nitric acid was added to

the sodium bismuthate samples (Solid-1 and Solid-2). The resulting mixtures were then contacted with three 1.3 mL solutions of 0.1 M nitric acid and separated by centrifugation after each 1.3 mL solution in order to acidify the surface of the sodium bismuthate. The appropriate amounts of tracer (~100 Bq each ^{241}Am and ^{244}Cm per mL in 0.1 M nitric acid) and 0.1 M nitric acid were added to Solid-1 to give a total volume of 1.5 mL. The sample was contacted on a shaker table for 10 min and separated by centrifugation. A 1.3 mL portion of the solution was removed from Solid-1 and added to Solid-2, and 1.3 mL of fresh 0.1 M nitric acid were added to Solid-1 to again give a total volume of 1.5 mL. The samples were contacted for 10 more minutes and separated by centrifugation. A 1.3 mL portion was removed from Solid-2 for analysis, a 1.3 mL aliquot of solution was removed from Solid-1 and added to Solid-2, and 1.3 mL of 0.1 M nitric acid were added to Solid-1. This process was repeated until Solid-1 and Solid-2 had been contacted with the original tracer solution plus four solutions of 0.1 M nitric acid each. Finally, the sodium bismuthate was contacted with 4.0 M nitric acid for 10 min to remove any remaining americium or curium, after which the solution was separated by filtration through a 0.45 μm PTFE syringe filter. All five 0.1 M nitric acid solutions were filtered through 0.45 μm syringe filters prior to analysis. The resulting solutions were analyzed using alpha spectrometry. Prior to sample preparation by cerium fluoride microprecipitation, each sample was spiked with a 1 mL of ^{242}Pu (2.17 Bq/mL) as an internal standard to account for losses during precipitation and differences in counting efficiency, and 0.5 mL of 30% hydrogen peroxide were added to ensure complete reduction of the Am. All data points are the average of three replicates, and the error bars show the statistical uncertainty to one standard deviation.

5.3.2 Results and Discussion

The separation was performed with two solid phases and five solution phases at room temperature and was completed in less than 2 hours. Americium was detected in all five solutions of 0.1 M nitric acid. Americium accounted for $100 \pm 4\%$ of the activity in the five solution phases. Curium accounted for $95 \pm 3\%$ of the activity recovered from the two solid phases, the remaining activity being from residual americium. In this separation system, $97 \pm 3\%$ of the americium and $95 \pm 2\%$ of the curium were recovered. Recovery in the microprecipitation step was high enough that within a few hours there were sufficient counts for all major peaks in the alpha spectrum to reduce the counting uncertainty to well below the replicate uncertainty.

5.4 Sodium Bismuthate Chromatography Separation Method

5.4.1 Experimental

The sodium bismuthate powder used was very fine and, as such, was difficult to use as a chromatographic material without modification. Celite 535 was used to aid in filtration and to improve flow properties of the material. Columns were slurry packed into 2 mL polypropylene columns from Eichrom Technologies Inc. using 0.1 M nitric acid. First, 75 mg of Celite were packed to form a Celite plug onto which 500 mg of a mixture of Celite and sodium bismuthate

powder (5% sodium bismuthate by weight) was packed (Figure 19). The Celite/sodium bismuthate mixture was homogenized by shaking in 0.1 M HNO₃ prior to slurry packing.

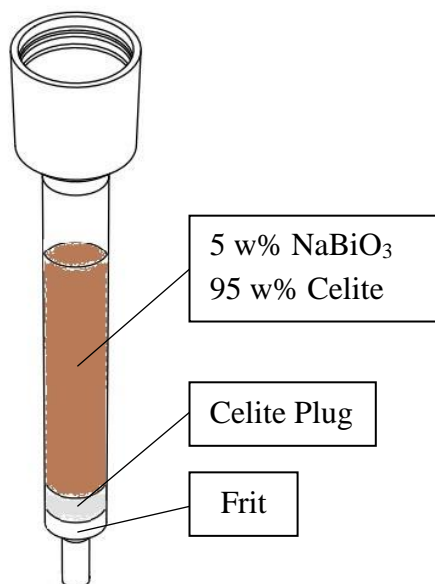


Figure 19: Sodium bismuthate chromatography column setup

Columns were placed on a vacuum box (Eichrom Part No. AR-12-BOX) and washed with 10 mL of 0.1 M nitric acid to ensure acidification of the mixture. A 1.0 mL sample containing a mixture of americium and curium (~100 Bq each) was loaded onto the column followed by 15 mL of 0.1 M nitric acid to elute the americium, which was collected in a single fraction in order to maintain a consistent flow rate. The curium was then eluted with 15 mL of 2.0 M nitric acid and was collected in a single fraction as well. The fractions were analyzed using alpha spectrometry. Prior to sample preparation by cerium fluoride microprecipitation, each sample was spiked with 1 mL of ²⁴²Pu (2.17 Bq/mL) as an internal standard to account for losses during precipitation and differences in counting efficiency then evaporated to near dryness and reconstituted in hydrochloric acid. A volume of 0.5 mL of 30% hydrogen peroxide was added to ensure reduction

of the americium. All data points are the average of three replicates, and the error bars show the statistical uncertainty to one standard deviation.

5.4.2 Results and Discussion

The chromatographic separation was performed using a column made with 25 mg of sodium bismuthate powder dispersed in 475 mg of Celite (27 mm bed height). The vacuum was kept at 5–7 in. Hg vac, and the flow rate was 1.5–2.0 mL/min. The separation procedure was completed in under half an hour and was performed at room temperature. Americium accounted for $100 \pm 3\%$ of the activity in the 0.1 M nitric acid fraction. Curium accounted for $98 \pm 4\%$ of the activity in the 2.0 M nitric acid fraction, the remaining activity being from americium (see Figure 20). Recovery in the microprecipitation step was high enough that within a few hours there were sufficient counts for all major peaks in the alpha spectrum to reduce the counting uncertainty to well below the replicate uncertainty.

Mincher and co-workers recently reported a separation of americium from curium on TRU resin utilizing Am(V)³⁴. The Am(V) was produced using an ammonium peroxydisulfate oxidation method. That separation procedure achieved only a 50% yield and ~70% recovery

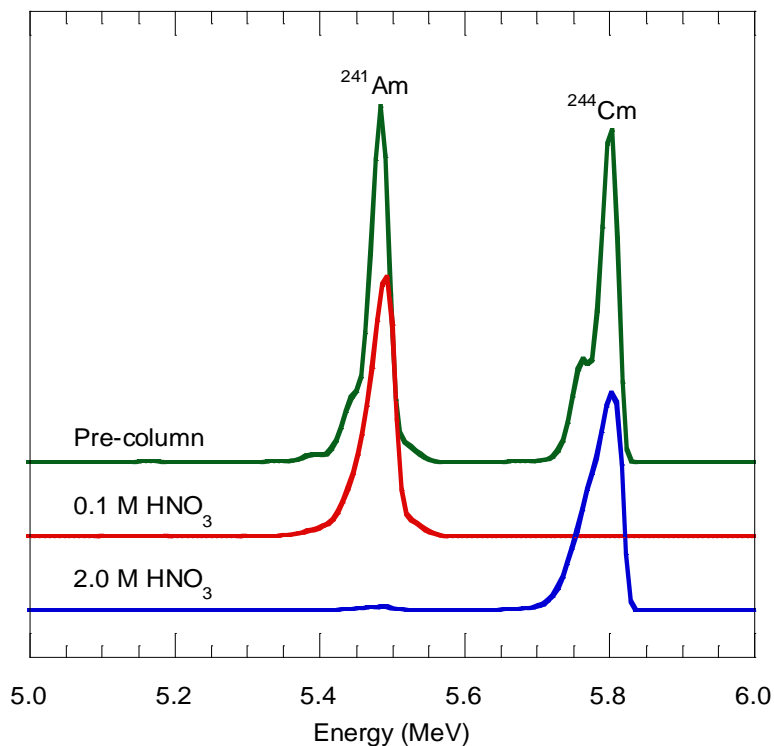


Figure 20: Alpha spectrum of the pre-separation mixture (green), the 0.1 M fraction (red) and the 2.0 M fraction (blue)

following elution of curium. In this separation system $97 \pm 2\%$ of the americium and $98 \pm 2\%$ of the curium were recovered. During the course of the separation, visible amounts of gas evolved in the column, possibly from the reaction of bismuthate with the solutions. The separation, however, did not appear to be adversely affected by this phenomenon.

5.5 Conclusions

The ion exchange behavior of sodium bismuthate was successfully used to separate americium from curium in nitric acid. A solid-liquid extraction method was successfully employed resulting in greater than 90% purity and recovery of both americium and curium. These values could be improved with the addition of more stages. The results are consistent with expected behavior from batch contact studies. Separation by chromatography was faster than solid-liquid extraction and

resulted in purity and recovery of over 97% for both americium and curium in one pass through a column.

CHAPTER 6: PROPERTIES OF SODIUM BISMUTHATE AS A SEPARATION MEDIUM

6.1 Abstract

The previous chapter illustrated how a separation of americium from curium utilizing sodium bismuthate as a solid-oxidant ion-exchange material was successfully achieved. A clear understanding of the properties of sodium bismuthate as a separation medium is however imperative for the successful application of this novel separation method. The adsorption capacity of sodium bismuthate for trivalent metal ions, the dissolution of sodium bismuthate in nitric acid, and particle size were all explored. A comparison was also made between the behavior of americium and curium on high purity and reagent-grade sodium bismuthate.

6.2 Motivation and Objectives

Americium and curium were successfully separated from each other utilizing sodium bismuthate as an ion-exchange medium. Separations were performed using a solid-liquid batch contact method as well as a chromatography setup. The solid-liquid extraction method resulted in greater than 90% purity and recovery of both americium and curium. Separation by chromatography was faster than solid-liquid extraction and gave improved separation and recovery.

A greater understanding of the properties of sodium bismuthate as a separation medium is required if it is to be applied to challenges in the nuclear fuel cycle. The objective of this chapter is to address some of the properties of sodium bismuthate that would be of interest in separation systems.

As in any separation system, the adsorption capacity of the material must be understood in order to apply the separation in analytical applications where the concentration is unknown or in industrial applications where capacity would be utilized to the greatest extent possible.

While sodium bismuthate has very low solubility, even in nitric acid, its solubility is not negligible when using it to perform separations. For this reason, the dissolution of sodium bismuthate in nitric acid must be understood in order to account for loss of the separation medium as well as sodium and bismuth contamination in the americium and curium fractions.

If the material in a separation can be reused, it can improve the cost effectiveness of the separation system. Since sodium bismuthate has non-negligible solubility in the system, it is important to explore the possibility of reusing the undissolved sodium bismuthate solid left over from a separation. Two properties that could change as the material is dissolving would be the particle size and surface area of the material. An understanding of the particle size and surface area of the material would be important in predicting behavior of the system.

6.3 Adsorption Capacity

6.3.1 Experimental

Solutions of lanthanum nitrate in 0.1 M nitric acid were contacted with 20 mg of preconditioned sodium bismuthate for a contact time of ten minutes. Lanthanum concentrations were varied from 10 ppm to 80 ppm. Each lanthanum concentration was run in triplicate. Final lanthanum concentrations were measured by inductively coupled plasma atomic emission spectroscopy (ICP-AES).

6.3.2 Results and Discussion

The adsorption behavior was measured and is shown in a plot of μg La adsorbed versus La concentration in parts per million (Figure 21).

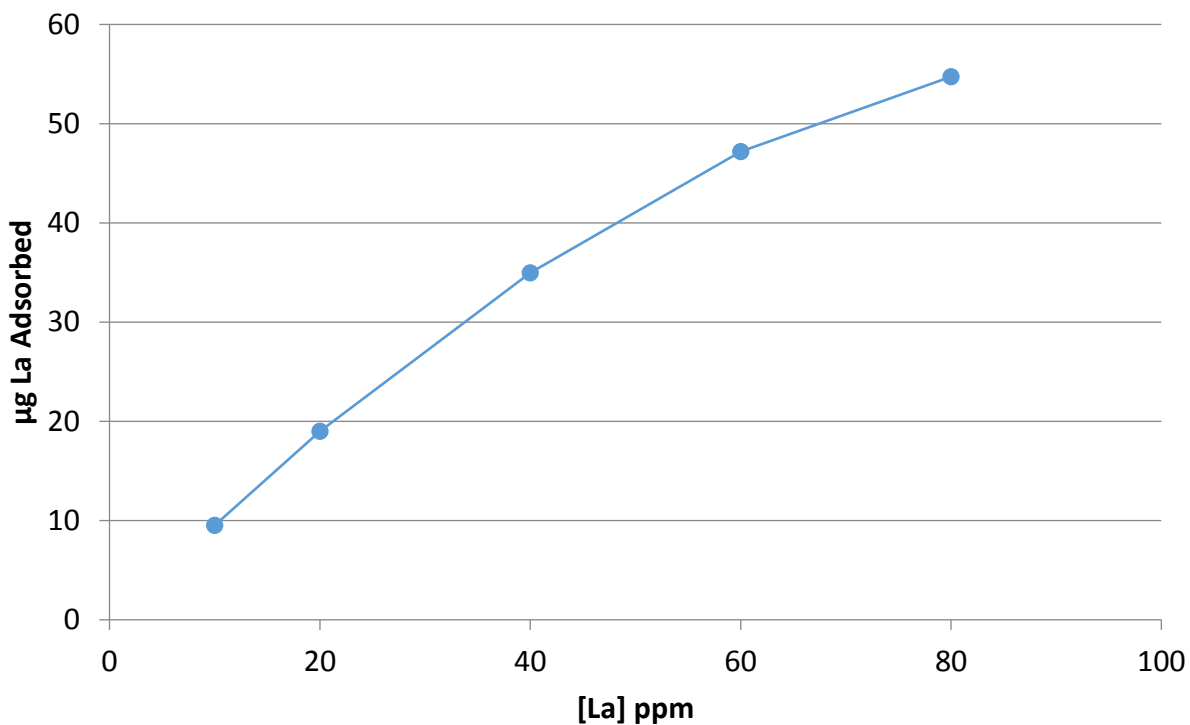


Figure 21: Mass of lanthanum adsorbed versus lanthanum concentration in solution

The adsorption behavior is not linear. The shape of the curve in Figure 21 suggests that the Langmuir adsorption isotherm model would describe the system well. The Langmuir Isotherm Model, or Langmuir Adsorption Isotherm, was used to determine the adsorption capacity of lanthanum on sodium bismuthate. The Langmuir isotherm model is a simple model that assumes that the surface of the material is homogeneous and that the ions adsorb to sites on the surface and that only one ion adsorbs per site. This allows the adsorption capacity to be calculated by varying the concentration of the metal ion and measuring the concentration of the metal ion after contact with sodium bismuthate. The relationship between the metal ion concentration and the adsorption is given by Equation 2.

$$q_e = \frac{Q_M K_{ad} C_e}{1 + K_{ad} C_e} \quad (2)$$

Where q_e is the amount of solute adsorbed per unit mass of solid at equilibrium (mg/mg). Q_M is the maximum adsorption capacity in mg adsorbate/mg adsorbent. K_{ad} is the adsorption constant in L/mg. C_e is the concentration of solute in solution at equilibrium with the adsorbent (mg/L or ppm). Rearrangement of equation 2 gives rise to a linear form shown in equation 3.

$$\frac{C_e}{q_e} = \frac{C_e}{Q_M} + \frac{1}{K_{ad} Q_M} \quad (3)$$

Plotting C_e/q_e versus C_e should result in a straight line with a slope of $1/Q_M$. For the lanthanum-sodium bismuthate system, C_e/q_e versus C_e is plotted in Figure 22.

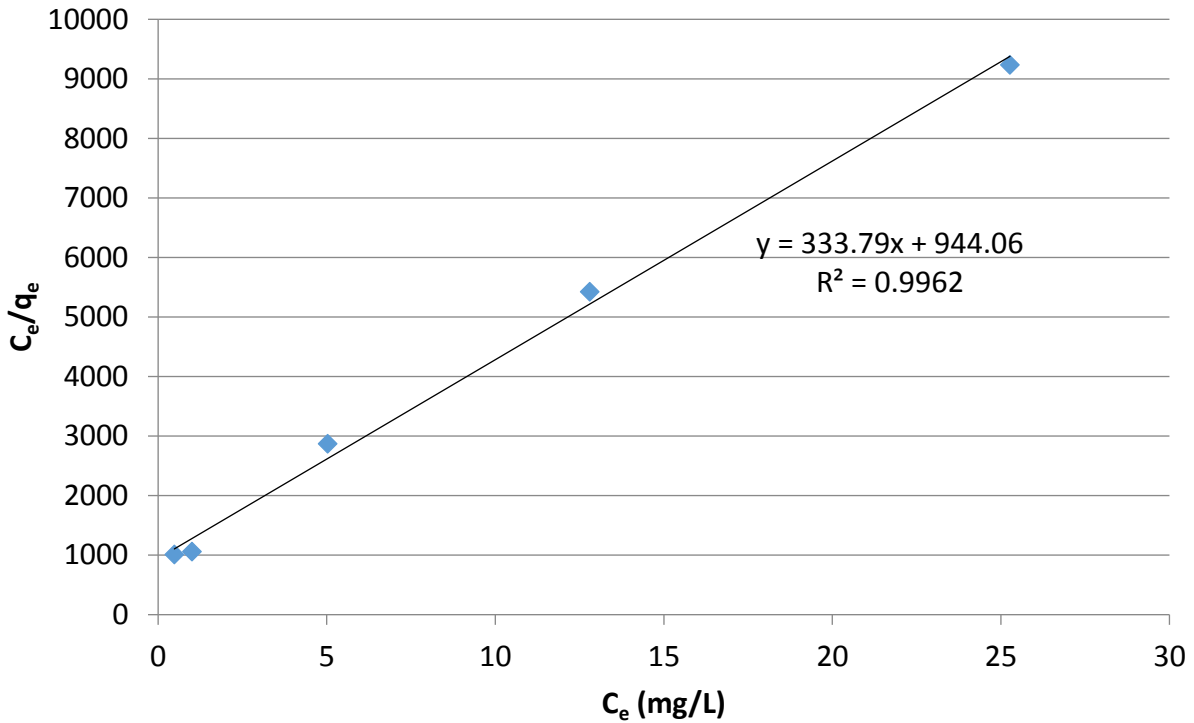


Figure 22: C_e/q_e versus C_e for lanthanum on sodium bismuthate in 0.1 M nitric acid with a 10-minute contact time

Because sodium bismuthate-based separations are not performed at equilibrium, as is shown in the studies on time dependence of adsorption, the contact time was fixed at ten minutes. Therefore, the adsorption capacity found here may not be identical for different contact times. The slope of the C_e/q_e versus C_e plot is 333.79, giving an adsorption capacity of 3.0 mg La/g NaBiO₃ or 0.022 mmol La³⁺/g NaBiO₃. Organic cation exchange resins typically have a capacity of ~1-2 meq/mL by wetted bed volume. Since lanthanum is trivalent, the capacity of the sodium bismuthate is 0.066 meq/g. The sodium bismuthate is very dense; however, once dispersed into diatomaceous earth at about ten weight percent, there are about 100 mg of sodium bismuthate per two milliliters of bed volume. This gives a capacity of ~0.003 meq/mL by wetted bed volume. If a solid-liquid separation method were used, the sodium bismuthate would not be dispersed into diatomaceous earth. This would result in a capacity of 0.43 meq/mL assuming a density of 6.5 g/cm³. In its pure form, the sodium bismuthate used in this work would have a capacity (in meq/mL) about half that of conventional organic ion-exchange materials.

6.4 Surface Area and Particle Size

6.4.1 Experimental

The surface area of the sodium bismuthate was measured using a NOVA-1000 BET surface area analyzer. Sodium bismuthate was analyzed as received.

Particle size measurement was also attempted with a dynamic light scattering particle sizer. Measurements were attempted with sodium bismuthate dispersed in water, 10 mM sodium nitrate, and 100 mM nitric acid.

6.4.2 Results and Discussion

Results of a 6-point BET analysis gave a surface area of 23.7 m²/g using a 0.1194 g sample. Macroporous polymeric resins used in extraction chromatography have larger surface area per unit mass. Amberchrom CG71 resin⁴⁷, which is commonly used in extraction chromatography, has a specific surface area of 500 m²/g. It should be noted that sodium bismuthate has a significantly higher density (NaBiO₃ ρ = 6.5 g/cm³, Amberchrom CG71 ρ = 1.3 g/cm³). When adjusted for density, the surface area per unit volume of sodium bismuthate is 154.05 m²/cm³ while Amberchrom CG71 resin has a surface area per unit volume of 650 m²/cm³. Amberlite XAD-4 and Amberlite XAD-7 have similar specific surface areas (725 and 450 m²/g respectively)^{48,49}.

The particle size analysis was unsuccessful due to the high density of sodium bismuthate (6.5 g/cm³) and particle size large enough that settling occurred too quickly to create a measurable suspension. None of the sodium bismuthate appeared to pass through 0.45 μm filter. A small amount of material passed through a 3-μm filter. The particle size is >0.45 μm and the smallest particles are on the order of 1-3 microns.

6.5 Dissolution of Sodium Bismuthate in Nitric Acid

6.5.1 Experimental

Sodium bismuthate dissolution was measured by contacting 1.0 mL of nitric acid and sodium nitrate (0.1 M nitric acid, 2.0 M nitric acid, and 0.1 M nitric acid/2.0 M sodium nitrate) with 20 mg of sodium bismuthate for 5, 10, 30, 60, 120, 180, and 240 minutes, respectively, and measuring the bismuth concentration in the supernatant by ICP-AES. All concentrations and contact times were run in triplicate.

6.5.2 Results and Discussion

The bismuth concentration in solution as a function of time for the three nitrate media is shown in Figure 23.

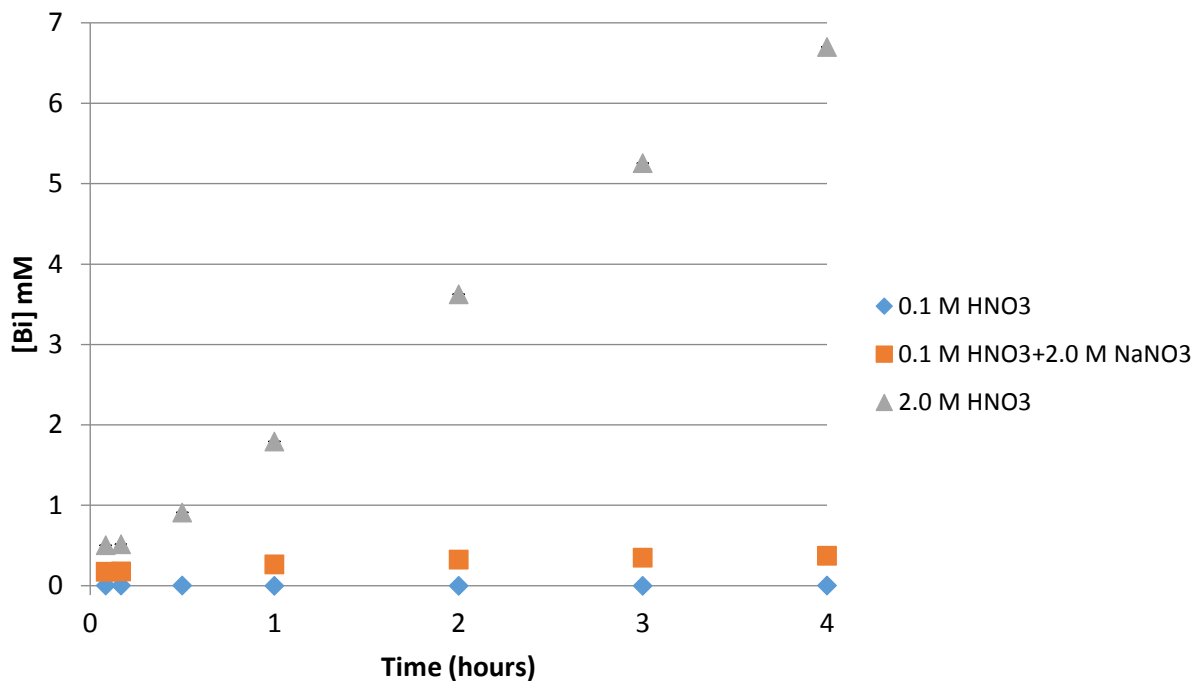


Figure 23: Bismuth concentration in nitrate media in contact with sodium bismuthate over the course of four hours

The ingrowth of dissolved bismuth in the 2.0 M nitric acid solution in contact with sodium bismuthate proceeds in a relatively linear fashion with the concentration of dissolved bismuth increasing at a rate of about 1.6 mM per hour. More bismuth is found in the 5-minute samples than would be expected from linear extrapolation of the data. This could be a result of the preconditioning procedure used to ensure a reproducible nitric acid concentration. Very little dissolved bismuth is seen in the 0.1 M nitric acid solution (More detail in Figure 24).

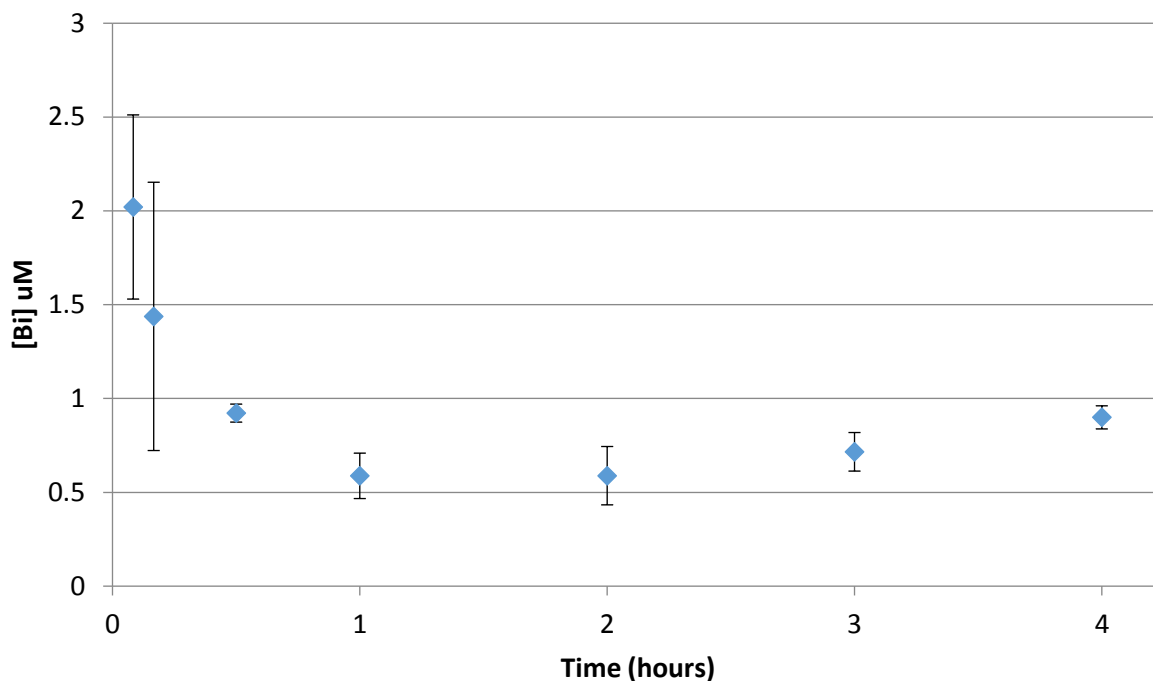


Figure 24: Dissolved bismuth in 0.1 M nitric acid in contact with preconditioned sodium bismuthate over the course of four hours

Dissolved bismuth has no clear trend in the 0.1 M nitric acid samples and averages a concentration of about 1 μM . The elevated and variable results in the 5 and 10-minute samples were not a result of memory effects in the ICP-AES setup. Blanks were analyzed between the standard and the samples and between samples to ensure that the bismuth signal returned to background before proceeding to the next sample. The overall low bismuth concentration in solution is to be expected as Bi(III) likely has a similar behavior to other trivalent metal ions on sodium bismuth and would adsorb to the surface of the sodium bismuthate.

The concentration of dissolved bismuth in the nitric acid-sodium nitrate mixture fits between the 0.1 M and 2.0 M nitric acid cases. This makes sense, because these samples had the same acid

concentration as the 0.1 M nitric acid samples and a similar nitrate concentration to the 2.0 M nitric acid samples (More detail in Figure 25).

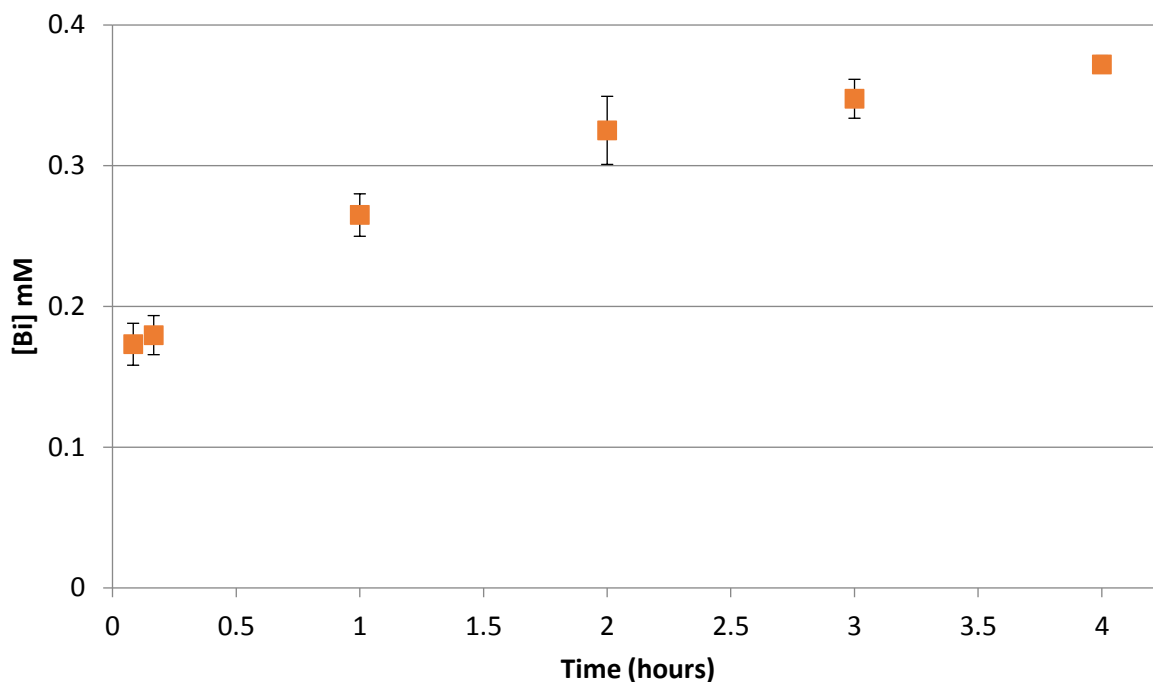


Figure 25: Dissolved bismuth in 0.1 M nitric acid/2.0 M NaNO₃ in contact with preconditioned sodium bismuthate over the course of four hours

6.6 Comparison of High Purity and Reagent Grade NaBiO₃

6.6.1 Experimental

A batch study comparison of americium and curium behavior on high purity and reagent-grade sodium bismuthate was carried out. The same procedure as described in Section 4.3 for preconditioned sodium bismuthate was used for this analysis. Analysis was performed at nitric acid concentrations of 0.1, 0.5, and 2.0 M.

6.6.2 Results and Discussion

The results of the batch study are shown in Figure 26.

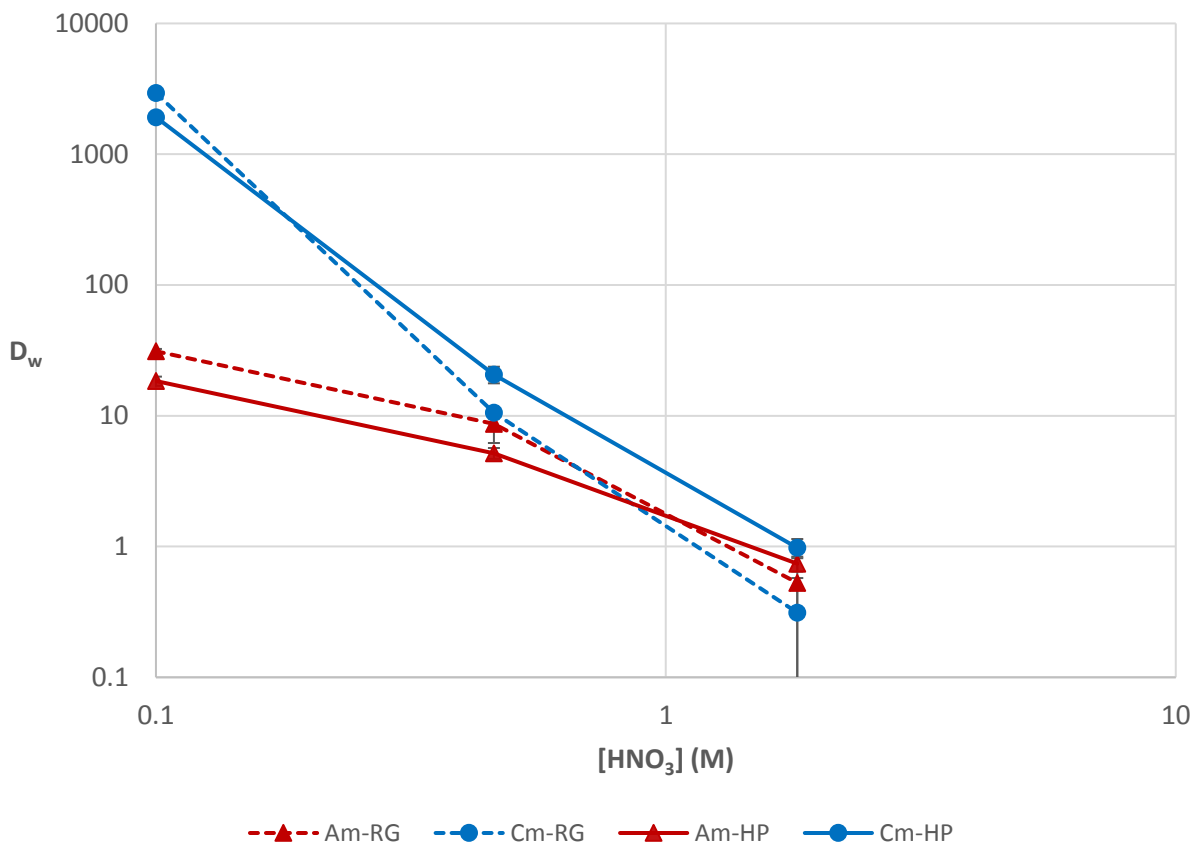


Figure 26: Comparison of D_w values for americium and curium on reagent grade (RG) and high purity (HP) sodium bismuthate

One of the first differences that was noted about the reagent-grade sodium bismuthate was the increased effervescence in contact with nitric acid. This did not disrupt batch study experiments, but the lower purity of the sodium bismuthate could interrupt column performance through excessive gas buildup in the column. The adsorption results for reagent grade and high purity sodium bismuthate were however quite similar. A large separation factor still exists at 0.1 M nitric acid and both elements show little retention at 2.0 M nitric acid. This suggests that trace reducing

agents such as peroxide, which are often detrimental in oxidation procedures, do not adversely affect this americium-curium separation procedure. This would allow an application of this method on a large scale to be much more cost effective.

6.7 Conclusions

Several properties of sodium bismuthate that would affect its performance as a separation medium were explored. Sodium bismuthate was found to be quite similar to other chromatographic materials with respect to properties such as adsorption capacity and surface area.

The adsorption capacity of the sodium bismuthate used in this work was calculated from measured values of lanthanum adsorption using the Langmuir Isotherm Model. The adsorption capacity of La(III) on sodium bismuthate is 3.0 mg La/g NaBiO₃ or 0.022 mmol La/g NaBiO₃. When adjusted for density, the adsorption capacity of sodium bismuthate is similar to that of a conventional cation exchange column.

The specific surface area of the sodium bismuthate used is lower than that of chromatographic materials used in extraction chromatography. The difference is less drastic when adjusted for the difference in density of the materials. The specific surface area of the sodium bismuthate used in this work is 23.7 m²/g. An accurate determination of particle size range was not successful. The particle size is greater than 0.45 μm and some of the smaller particles are less than three microns as evidenced by small amounts of material passing through a 3-μm filter.

While sodium bismuthate solubility is very low, it is significantly higher than that of most chromatographic materials. This leads to some dissolution of the sodium bismuthate during the separation procedure. The dissolved sodium bismuthate contaminates the column effluent. However, the amount of bismuth contamination in the 0.1 M nitric acid fraction of a separation is three orders of magnitude smaller than that found in the 2.0 M nitric acid fraction. This is in part

due to the affinity of sodium bismuthate for trivalent metal ions. The dissolved bismuth is reduced to Bi(III), which is retained on the sodium bismuthate in a similar manner to curium. This leads to a significantly higher purity in the americium fraction than in the curium fraction.

It is quite difficult to synthesize pure sodium bismuthate. It is almost inevitable that the sodium bismuthate will have some impurities. The tolerance of the separation method for intrinsic impurities was tested by comparing the batch contact results of americium and curium on high purity (93%) and reagent grade (80%) sodium bismuthate. The method showed a surprisingly high tolerance for the use of impure sodium bismuthate to perform separations. The behaviors of americium and curium were not adversely affected by the use of lower purity material.

Overall, the properties of sodium bismuthate are conducive enough for it to be used as a chromatographic material. Some drawbacks are its reactivity and effervescence in aqueous systems, as well as its solubility. However, these properties do not prevent the separation of americium from curium.

CHAPTER 7: APPLICATION OF SODIUM BISMUTHATE CHROMATOGRAPHY TO CHALLENGES IN ADVANCED PARTITIONING OF USED NUCLEAR FUEL

7.1 Abstract

Sodium bismuthate chromatography has a unique capability to easily separate americium from curium. This could be very advantageous in advanced partitioning of used nuclear fuel. In order to determine where this method could be applied to partitioning challenges, the behavior of several fuel cycle relevant elements in sodium bismuthate chromatography was explored. The applicability of this method to currently proposed used nuclear fuel partitioning technologies is discussed. This includes application after an actinide lanthanide separation, after non-lanthanide/rare-earth fission product removal (TRUEX), and directly after the PUREX process.

7.2 Motivation and Objectives

With the successful separation of americium from curium utilizing sodium bismuthate as an ion exchange medium, applicability of this novel separation to nuclear science challenges must be determined. The application explored in this work is the advanced partitioning of used nuclear fuel. Advanced partitioning of used nuclear fuel aims to increase resource sustainability and minimize waste. While many of the proposed methods for the partitioning of used nuclear fuel separate actinides from fission products, few of these methods are capable of separating americium and curium. This is due to the chemical similarity of americium and curium in typical processing conditions.

Removal of americium from the waste would reduce the hazardous lifetime of the waste, making it easier to predict repository conditions for the lifetime of the waste and reducing the likelihood of eventual release of hazardous material. Removal of curium from the waste would not significantly reduce the hazardous lifetime of the waste. The relatively short half-lives of the

curium isotopes give them higher specific activities that would make handling of curium containing fuel hazardous from increased gamma radiation, heat generation, and neutron emission. Removal of americium from the waste and separation of americium from curium would be ideal in advanced partitioning of used nuclear fuel.

A sodium bismuthate-based separation of americium from curium could be implemented at different points in the process of partitioning. If implemented after a separation of the actinides from the lanthanides (TALSPEAK, ALSEP, GANEX), the separation could be performed as described for just americium and curium. If applied after removal of non-lanthanide/rare earth fission products (TRUEX) the behavior of lanthanides and other rare earths would need to be understood. If applied directly after a PUREX separation, the behavior of fission product elements would also need to be considered. The behavior of these elements and other factors involved in application of sodium bismuthate chromatography to advanced partitioning of used nuclear fuel are explored in this chapter.

7.3 Sorption of Lanthanides on Sodium Bismuthate Solid

7.3.1 Experimental

The affinity of lanthanides for NaBiO_3 as a function of nitric acid concentration was tested using the batch contact method described in Section 4.3 with preconditioning of the sodium bismuthate. Lanthanide nitrate solutions were made at a concentration of about 10 ppm in 0.1 M nitric acid for all lanthanides except promethium. The concentration of each lanthanide in contact with the sodium bismuthate was approximately 1 ppm. Each was measured in triplicate and analyzed by ICP-AES. Each lanthanide was initially tested separately. An interference study was then performed with all lanthanides in one solution.

7.3.2 Results and Discussion

The calculated weight distribution ratios for the lanthanides, measured individually, are shown in Figure 27. The calculated weight distribution ratios for the lanthanides in an interference study, with all lanthanides in one solution, are shown in Figure 28.

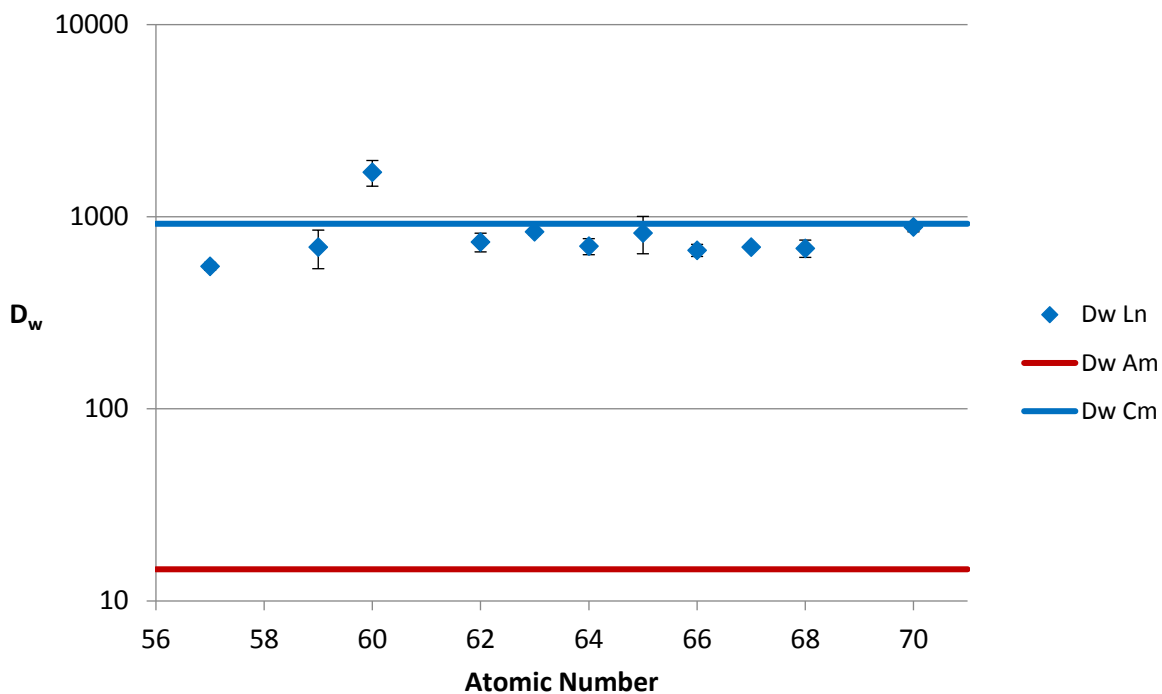


Figure 27: D_w of lanthanides on NaBiO_3 solid in 0.1 M HNO_3 (individually tested)

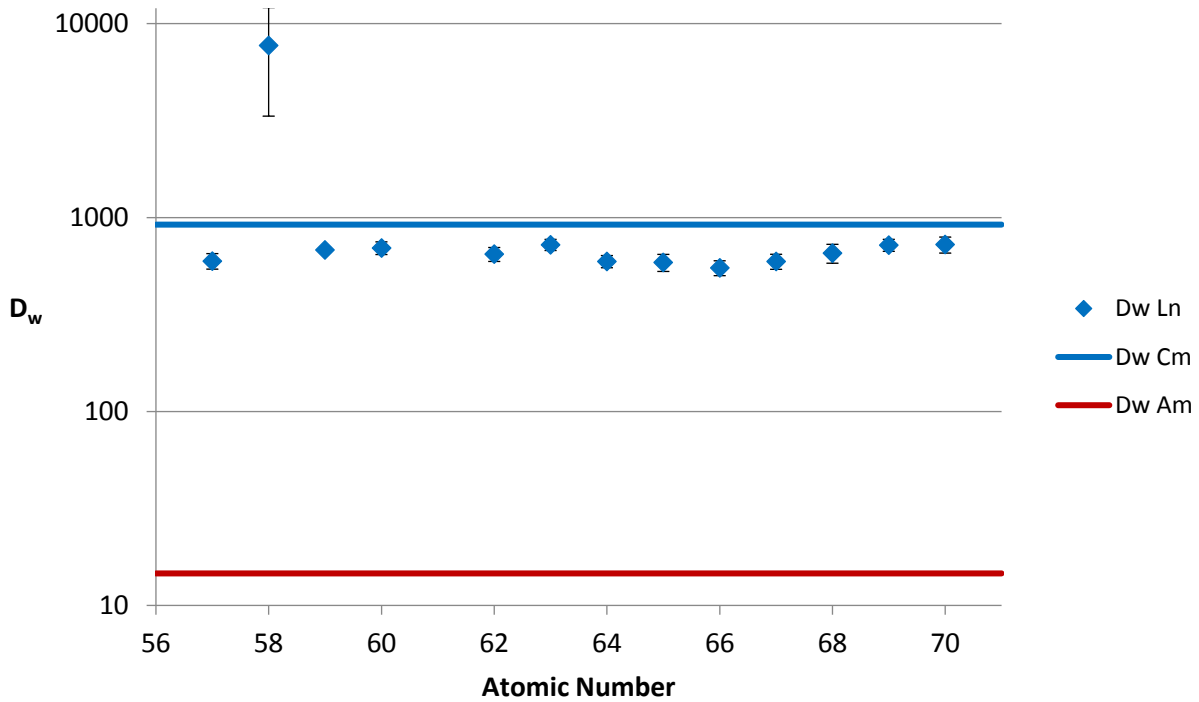


Figure 28: D_w of lanthanides on NaBiO_3 solid in 0.1 M HNO_3 (interference study)

The behavior of the lanthanides is very similar to that of curium, with the exception of cerium. This similarity in behavior is common for trivalent actinides and lanthanides. Cerium is retained to a greater degree than the other lanthanides in 0.1 M nitric acid, sometimes to the point that its concentration in solution is below the detection limit of the instrument. This is most likely due to the oxidation of cerium to the tetravalent state.

Sodium bismuthate is a strong enough oxidant to oxidize trivalent cerium to tetravalent¹⁷. The charge density of tetravalent cerium is greater than that of trivalent cerium. Greater charge density would lead to a stronger electrostatic interaction with the surface of the sodium bismuthate. This strong affinity for cerium could make reusability of the sodium bismuthate as a separation medium difficult in waste streams containing lanthanide fission products.

With good agreement between the interference study and the individual measurements of lanthanides, the interference study was expanded to include other acid concentrations. The results are shown in Figure 29.

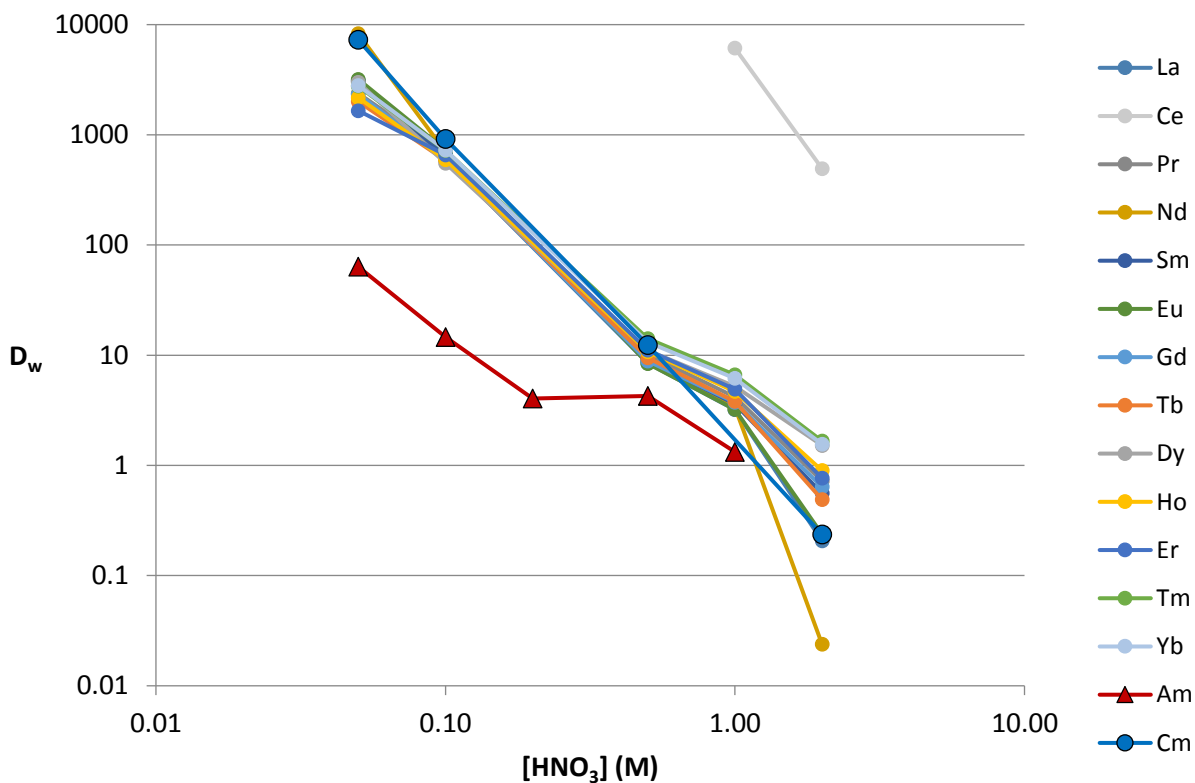


Figure 29: Nitric acid dependency of D_w (0.05, 0.1, 0.5, 1.0, 2.0 M) of lanthanides on sodium bismuthate with a 10-minute contact time compared with americium and curium

The behavior of the lanthanide elements follows curium closely at low acid concentrations, showing the same decreasing trend in D_w . Behaviors begin to diverge at concentrations above 1.0 M nitric acid. This is not particularly significant in a separation procedure as the D_w values are very low and only cerium would be retained at those acid concentrations.

7.4 Sorption of Uranium, Plutonium, and Technetium on Sodium Bismuthate Solid

7.4.1 Experimental

The affinity of uranium and plutonium for NaBiO_3 as a function of nitric acid concentration was tested using the batch contact method described in Section 4.3 with preconditioning of the sodium bismuthate. Uranium, plutonium and technetium tracers in 0.1 M nitric acid were used (100 Bq/mL ^{233}U , 100 Bq/mL ^{239}Pu , 100 Bq/mL ^{99}Tc). Samples at each acid concentration were measured in triplicate and analyzed by LSC.

7.4.2 Results and Discussion

The calculated weight distribution ratios for the uranium and plutonium are shown in Figure 30.

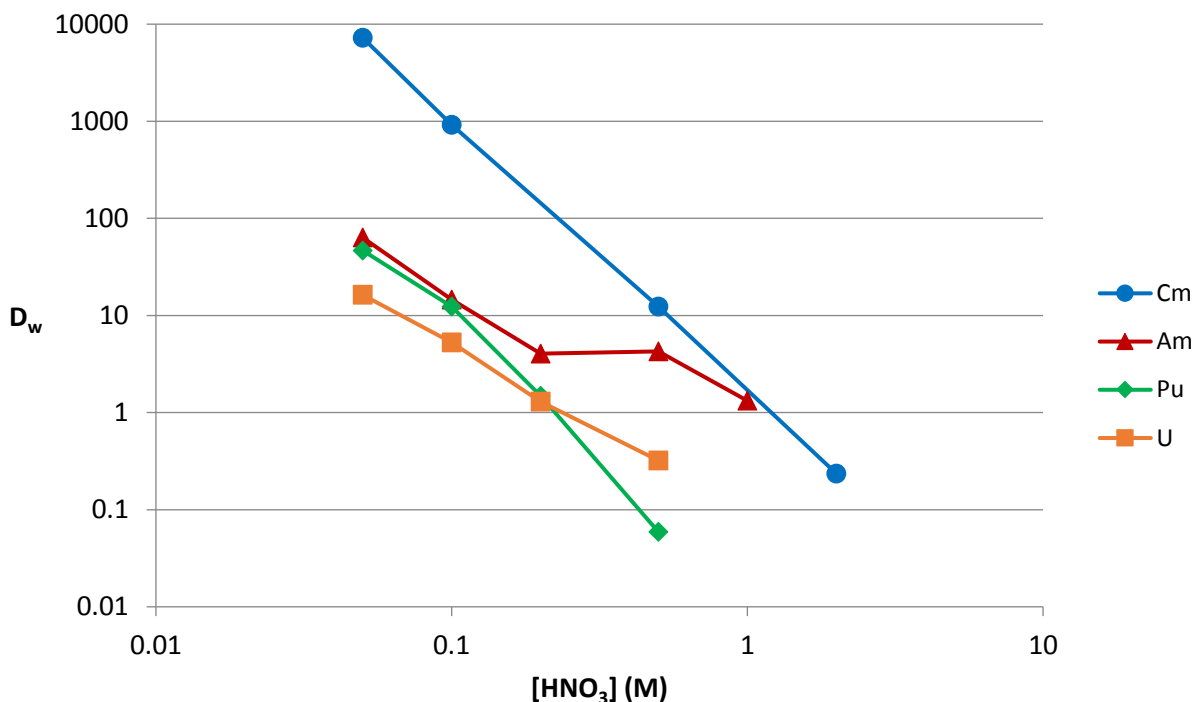


Figure 30: Nitric acid dependency of D_w of uranium and plutonium on sodium bismuthate with a 10-minute contact time compared with americium and curium

At concentrations of nitric acid around 0.1 M the uranium and plutonium show D_w values and slopes similar to americium. This suggests that these actinides are all behaving as divalent actinyl ions. There is some evidence of the actinide contraction leading to higher D_w values for actinyl ions of later actinides. Neptunium would be expected to have a D_w value somewhere between uranium and plutonium. The D_w value for uranium continues on a slope of -2 up to 0.5 M nitric acid suggesting consistent uranyl behavior across the acid concentrations measured. Plutonium shows a more significant decline in weight distribution ratio at high acid concentrations. No technetium adsorption was observed at 0.1 or 2.0 M nitric acid.

7.5 Post-TRUOX Application

7.5.1 Experimental

A non-radioactive TRUOX strip solution simulant was prepared in 0.05 M HNO_3 with the composition given in Table 2. The simulant was adjusted to either 0.1 or 2.0 M nitric acid and was diluted to 1/100th of the original concentration and contacted with 20 mg sodium bismuthate for 10 minutes in a batch contact study. Samples were run in triplicate and elements were measured by ICP-AES.

7.5.2 Results and Discussion

The composition of the TRUOX strip solution simulant was based on the concentrations of TRUOX extracted elements in PUREX raffinate from light-water reactor fuel with a burn-up of 50 GigaWatt-days and a cooling time of 5 years. The results of the batch contact study of TRUOX strip solution simulant on sodium bismuthate is shown in Table 2.

Table 2: TRUEX strip solution simulant composition and D_w at 0.1 and 2.0 M HNO_3

Constituent	Concentration (mM)	D_w (0.1 M HNO_3)	D_w (2.0 M HNO_3)
HNO_3	50	-	-
Ce	4.37	>10,000	4200 ± 750
Eu	0.28	767 ± 33	<0.1
Gd	0.10	776 ± 97	5 ± 1
La	2.26	693 ± 37	<0.1
Nd	7.21	820 ± 60	<0.1
Sm	1.41	764 ± 45	<0.1
Y	1.29	682 ± 32	0.5 ± 1

For the most part, all elements behaved as expected. Cerium was adsorbed very strongly at both acid concentrations. The behavior of the other lanthanides was consistent with an average D_w of 750 ± 50 in 0.1 M nitric acid. Gadolinium was the only lanthanide that showed some adsorption at 2.0 M nitric acid. Further study would be needed to understand this result. The separation, however, would be unaffected by this deviation. Yttrium has very similar behavior to that of lanthanum.

One obvious challenge of a post-TRUEX application of sodium bismuthate chromatography would be the buildup of cerium on the sodium bismuthate. This would limit the reusability of the sodium bismuthate material in the process and would also drive up cost and waste volume.

7.6 Post-PUREX Application

7.6.1 Experimental

A non-radioactive PUREX raffinate simulant solution was prepared in 3 M HNO_3 with the composition given in Table 3. The simulant was adjusted to 0.1 M nitric acid with distilled deionized water and diluted 50-fold from the original concentration (PR-50). This solution was used in batch contact and column chromatography studies.

Batch studies were performed with 0.5 mL of the PR-50 solution diluted to 1 mL with 0.1 M nitric acid in contact with 50 mg of sodium bismuthate for 10 minutes. After 1 minute of

centrifugation at 3000 rpm, 0.800 mL of the supernatant was removed for analysis. Nitric acid and water were added to give a final nitric acid concentration of 2.0 M nitric acid and volume of 1.000 mL. The samples were contacted for 10, 30, 60, and 120 minutes to determine desorption kinetics. The sodium bismuthate was filtered and the supernatant was collected for analysis. The supernatant was analyzed by ICP-MS.

Two 10 w% NaBiO₃/90 w% Celite 535 columns were prepared as described in Section 5.4.1 and preconditioned with 10 mL of 0.1 M nitric acid. A load solution of 1.0 mL of PR-50 solution was loaded onto the columns, and 25 mL of 0.1 M nitric acid were added and collected in 5 mL fractions. A 2.0 M nitric acid solution (25 mL) was then added to the column and collected in 5 mL fractions. Fractions were analyzed by ICP-MS.

7.6.2 Results and Discussion

The composition of the PUREX raffinate simulant solution was based on the concentrations of elements in PUREX raffinate from light-water reactor fuel with a burn-up of 50 GigaWatt-days and a cooling time of 5 years. The D_w values for the elements in the PUREX raffinate simulant solution at 0.1 M nitric acid as calculated from the batch contact data are given in Table 3 ordered from highest to lowest D_w value.

Table 3: PUREX raffinate simulant composition and D_w at 0.1 M HNO_3

Constituent	Concentration (mM)	D_w (0.1 M HNO_3)
HNO_3	3000	-
Ce	4.37	>10,000
Zr	9.48	>10,000
Pd	0.04	>10,000
Sn	0.20	3400 ± 5900
Gd	0.10	1061 ± 80
Y	1.29	971 ± 85
Nd	7.21	728 ± 45
Eu	0.28	727 ± 45
Pr	2.03	714 ± 59
Mo	4.47	660 ± 63
La	2.26	609 ± 55
Sm	1.41	501 ± 79
Ru	~3	92 ± 7
Sr	2.34	69 ± 5
Rb	1.03	55 ± 3
Se	0.18	22 ± 6
Cs	4.99	18 ± 1

Results of the desorption kinetics in 2.0 M nitric acid portion of the batch study experiments are given in Figure 31.

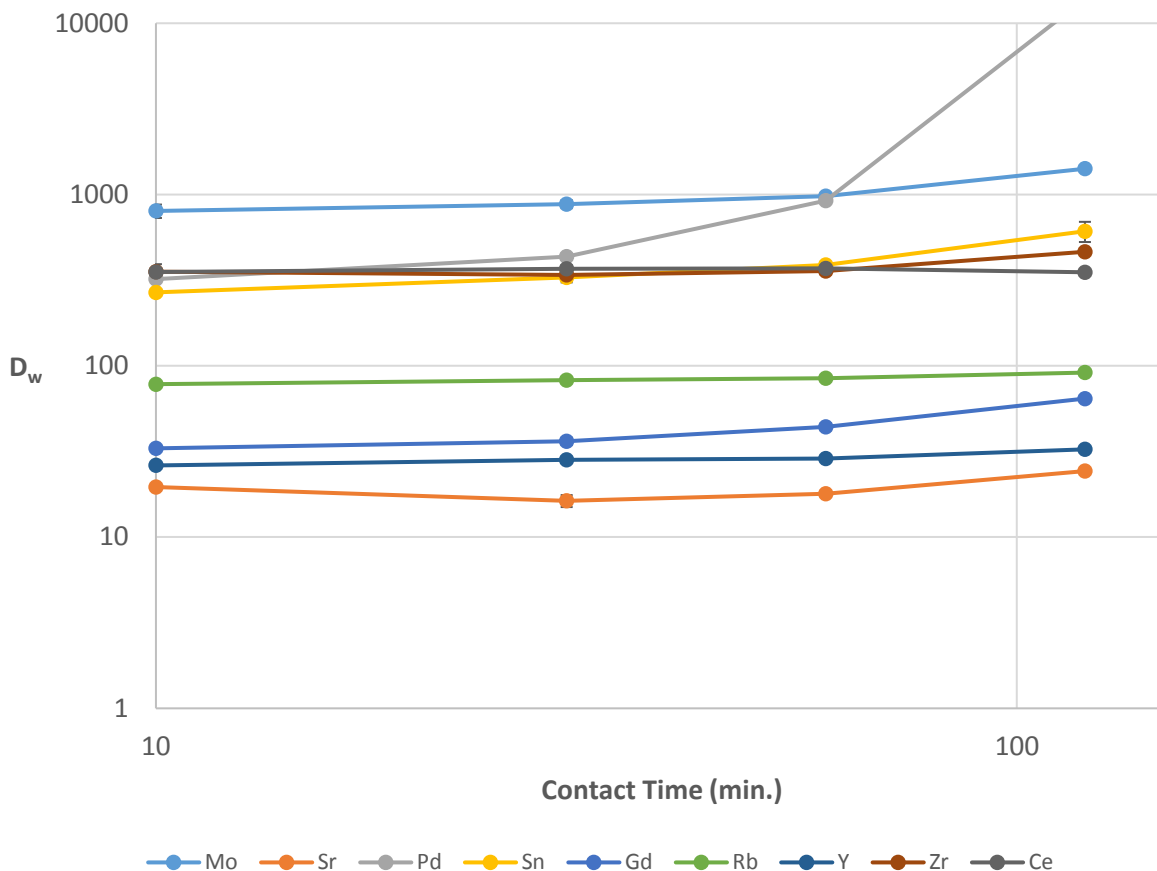


Figure 31: Measured D_w values for PR-50 elements with significant D_w at 2.0 M HNO_3 over time in 2.0 M HNO_3 after adsorption in 0.1 M HNO_3

There is negligible change in D_w value over the course of 2 hours for all elements with significant D_w values in 2.0 M nitric acid except palladium. The D_w for palladium increases to the point that after 2 hours the element was no longer measurable. The only trend visible in other elements is a slight upward trend. This is the opposite of the trend seen with americium and curium in 0.1 M nitric acid. In 2.0 M nitric acid Bi(III) is no longer retained on the surface of the sodium bismuthate and is no longer competing for sites. It is difficult to determine the specific reason for this increase. The surface area of the sodium bismuthate could be changing significantly at 2.0 M nitric acid as some of the sodium bismuthate is dissolved. The speciation of some of these elements

could be changing, however, no clear correlation exists between elements that have potential for hydrolysis and those that don't. For example, the D_w for rubidium changes very little and is expected to only be Rb(I). The D_w of gadolinium, on the other hand, increases over the course of 2 hours and is also expected to be in only one oxidation state, Gd(III). A graph showing the measured D_w values of PUREX raffinate simulant elements and measured actinide elements on sodium bismuthate in 0.1 M nitric acid is given in Figure 32.

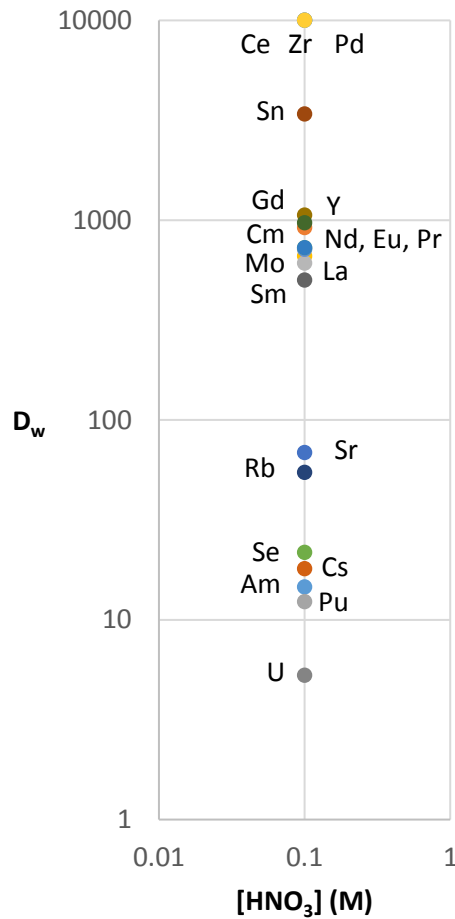


Figure 32: D_w of PUREX-relevant elements on sodium bismuthate in 0.1 M nitric acid

All elements with D_w greater than or equal to samarium would be expected to follow curium. All elements with D_w values less than or equal to strontium would be expected to follow americium. None of the elements analyzed have a D_w value between these elements. This allows for predictable separation results.

The elution profile of the column separation of PUREX raffinate elements is shown in Figure 33.

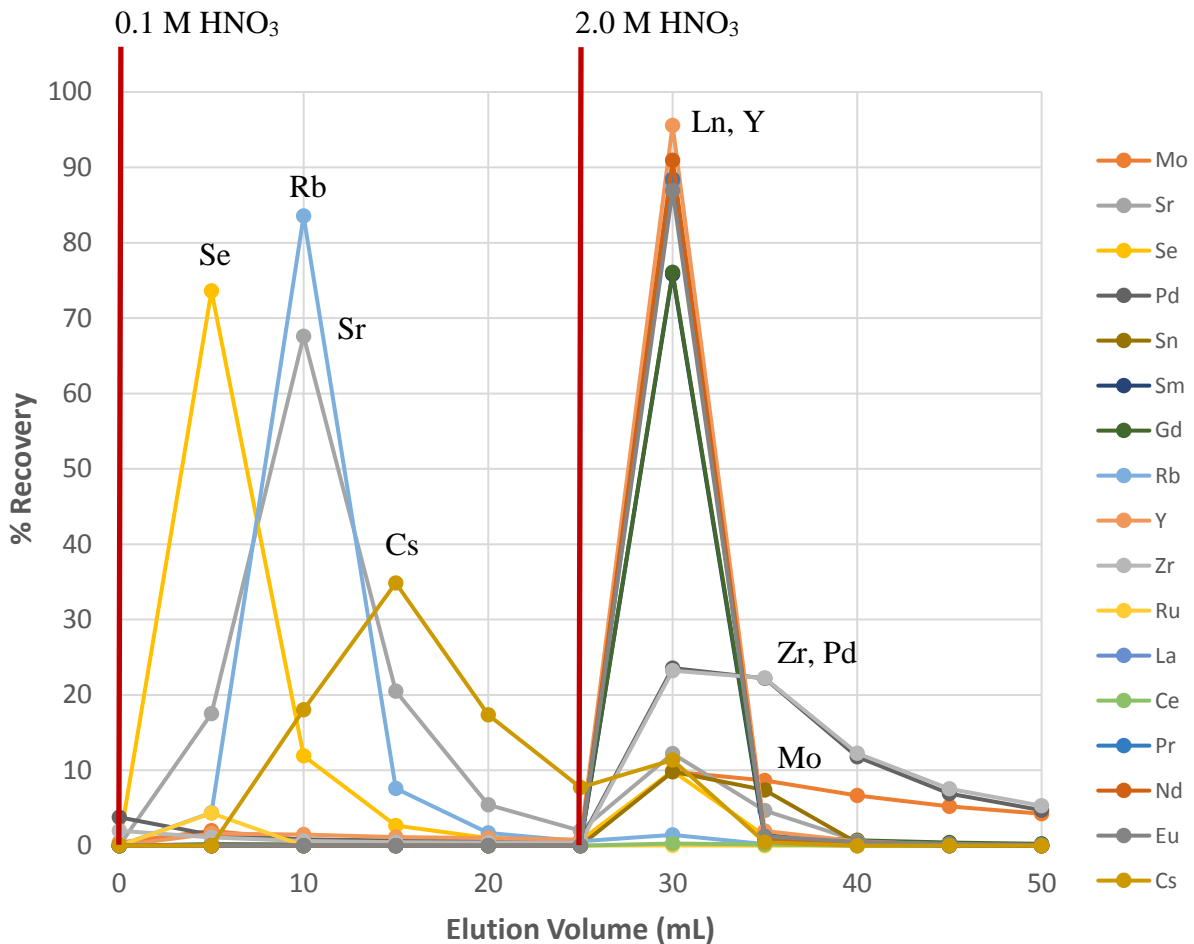


Figure 33: Elution profile of PUREX raffinate elements in a sodium bismuthate chromatography separation

Selenium, rubidium, strontium, and cesium eluted in the 0.1 M nitric acid fraction, or americium fraction, as would be expected by the measured D_w values. Ruthenium also has a low D_w value, though it was not detected in the 0.1 or 2.0 M nitric acid fractions. This is likely due to the behavior of ruthenium in the presence of sodium bismuthate and nitric acid. While the chemistry of ruthenium is quite complex in nitric acid, with at least nine different species being formed under normal conditions⁵⁰⁻⁵², sodium bismuthate is sufficiently oxidizing to convert these ruthenium species to ruthenium tetroxide¹⁷. Ruthenium tetroxide is a neutral and non-polar species that would not be retained by electrostatic interactions. While ruthenium tetroxide most likely eluted in the 0.1 M nitric acid fraction, its relatively high vapor pressure and tendency to reduce to insoluble ruthenium dioxide in contact with plastic make it likely that all ruthenium that was eluted was no longer in solution by the time the fractions were analyzed. It would be beneficial to remove the ruthenium tetroxide in a controlled manner after contact with sodium bismuthate in a separation procedure. This could be accomplished with organic solvent impregnated imbibor beads (IBH-20) as discussed in “Selective Partitioning of Ruthenium from Nitric Acid Media”⁵³. The presence of ruthenium has been shown to be detrimental to some separation procedures involving the use of hexavalent americium. The D_w of americium on sodium bismuthate in 0.1 M nitric acid was measured in the presence and absence of 3 mM ruthenium and no effect was observed. The presence of ruthenium should not affect the behavior of americium in these separation systems.

The elution of all lanthanides besides cerium, as well as the elution of yttrium with the lanthanides was expected. Cerium and tin were not seen in either fraction. This is reasonable since both elements have relatively high D_w values in 2.0 M nitric acid in this mixture; however, zirconium, palladium, and molybdenum have similar D_w values in 2.0 M nitric acid, and these

show a small gradual elution. This suggests that multiple species may be forming for some of the elements, leading to elution of some forms and no elution of others.

Because several elements did not elute in 2.0 M nitric acid, it is unlikely that this material could be reused in separation procedures containing these elements, namely cerium, tin, zirconium, palladium, and molybdenum. While the sodium bismuthate material may not be suitable for reuse as a separation medium in a post-PUREX application, it could still be used as long as there is a suitable way to handle the saturated sodium bismuthate.

Sodium bismuthate readily dissolves in hydrochloric acid and produces chlorine gas in the process. If hydrogen peroxide is added to the hydrochloric acid, this chlorine is converted back to chloride, and oxygen gas is evolved instead. The dissolved bismuth can then be precipitated as bismuth oxide. Curium and fission product elements adsorbed on the sodium bismuthate could be co-precipitated with the bismuth oxide and incorporated into a bismuth-silicate glass for final disposal^{54,55}. An example of what a separation process like this may look like is given in Figure 34.

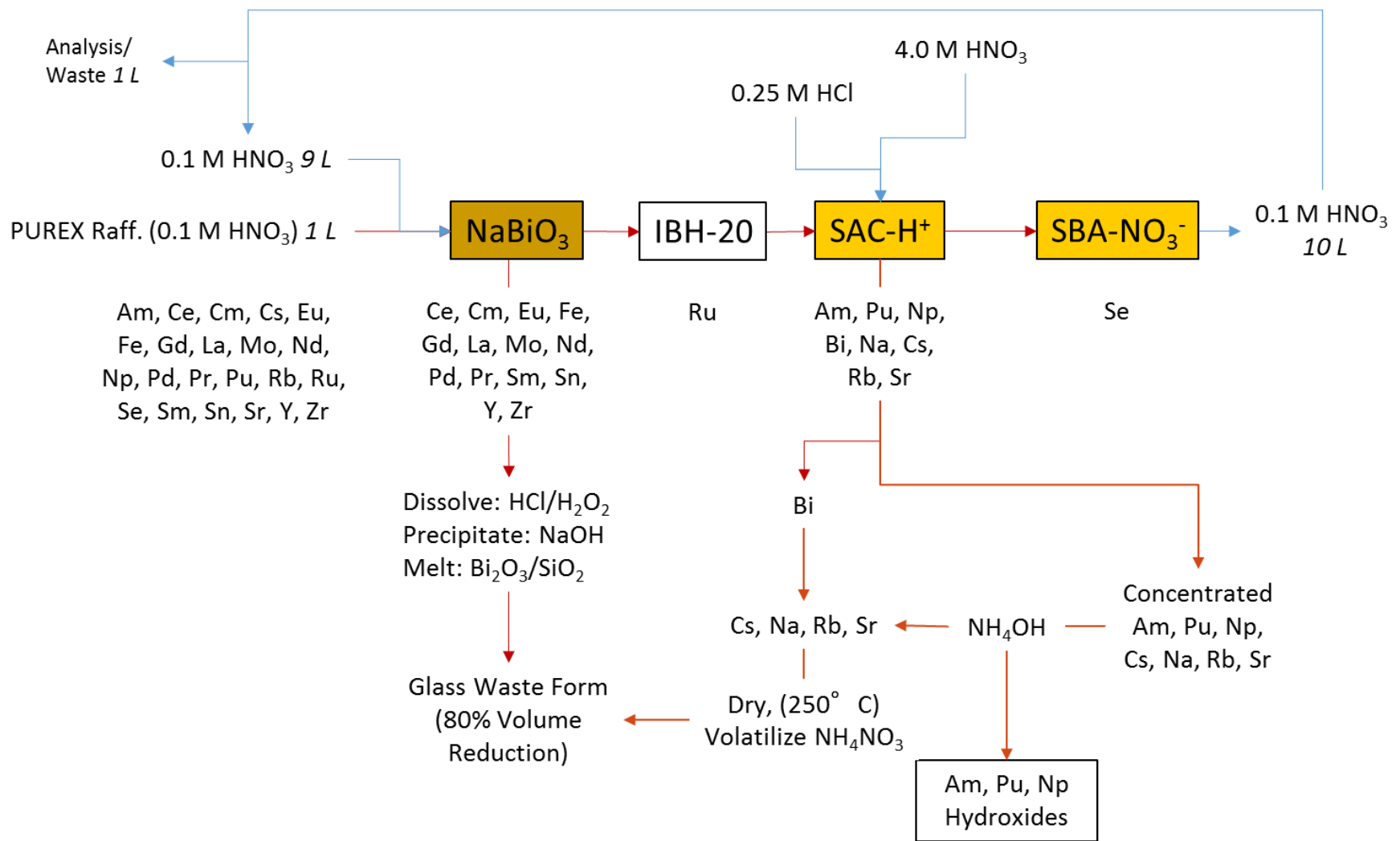


Figure 34: Proposed process scheme for isolation of americium from PUREX raffinate using sodium bismuthate chromatography

7.7 Conclusions

The capabilities of sodium bismuthate chromatography can be expanded to include elements beyond americium and curium. The similarity in behavior of curium and the lanthanides allows for isolation of americium from curium and the lanthanides. Plutonium, uranium and technetium follow americium. This makes a post TRUEX application of sodium bismuthate chromatography possible. One difficulty with post-TRUEX application of this separation is the high D_w value of cerium in 2.0 M nitric acid. Higher acidities would dissolve the sodium bismuthate making reuse of the sodium bismuthate material for separations quite limited.

While there is significant variation in the D_w values of fission product elements on sodium bismuthate in 0.1 M nitric acid, a significant gap exists between the mono and divalent species and the tri and tetravalent species. In the initial separation step, anionic, mono, and divalent species follow americium and tri and tetravalent species follow curium. This makes a separation of PUREX raffinate elements predictable. Separation of americium from the elements that follow americium in sodium bismuthate chromatography is quite simple compared to separations involving trivalent actinides and lanthanides. Similar to post-TRUEX application, several fission product elements from PUREX raffinate are not eluted in 2.0 M nitric acid. This makes reuse of the sodium bismuthate material for separations difficult if not impossible. If sodium bismuthate chromatography were to be applied to isolation of americium from PUREX raffinate, it would be advantageous to incorporate the bismuthate into the waste form to eliminate the need for complicated additional separations.

Sodium bismuthate chromatography is a novel and promising technology that has the capability to isolate americium from curium, lanthanides, and some fission product elements. This

method could be applied at various stages throughout the proposed processes involved in spent nuclear fuel processing.

CHAPTER 8: CONCLUSIONS AND IMPLICATIONS

The primary goal of this project was to develop and characterize a highly selective, efficient, and cost effective method for the separation of americium from curium and explore possible applications of the method to fuel cycle relevant challenges.

8.1 Extraction Chromatography

The first partitioning method attempted was a combination of a sodium bismuthate oxidation and an extraction chromatography separation using commercially available resins. This technique was unsuccessful. The dissolved sodium bismuthate resulted in high levels of Bi(III) that acted as a competing ion in the DGA system. Americium did not exhibit oxidized behavior in the UTEVA system. During the course of these experiments, it was however observed that there was much lower recovery of americium and curium when in contact with sodium bismuthate at low acid concentrations.

The pH of the samples with nitric acid concentrations above 0.01 M was one or lower, making the possibility of hydrolysis very low. The 0.01 M nitric acid samples showed an increase in pH to about seven or eight. This increase in pH was instantaneous when the solution was brought into contact with sodium bismuthate. This suggests that the surface of the sodium bismuthate is basic and that the pH change is not a result of decomposition of the sodium bismuthate. This behavior is similar to that of inorganic ion exchange materials. It was hypothesized that the americium and curium were adsorbing to the surface of the sodium bismuthate through electrostatic interactions.

8.2 Sorption of Am and Cm on NaBiO₃

Americium and curium adsorb to the surface of sodium bismuthate at nitric acid concentrations below 2.0 M. This is presumed to be an ion exchange process. At nitric acid concentrations below 1.0 M the behavior of americium becomes quite different from that of curium. Americium adopts

hexavalent americium (AmO_2^{2+}) behavior, while curium maintains trivalent behavior. At 0.1 M nitric acid, the difference in weight distribution ratio gives rise to a separation factor of 90 between americium and curium. This separation factor demonstrates the high selectivity of this material for this partitioning. Curium is more strongly retained. The adsorption behavior of curium is nitrate dependent, suggesting that adsorption behavior is a competition between electrostatic interaction with the sodium bismuthate surface and nitrate complexation of the metal ion.

8.3 Separation of Am and Cm with NaBiO_3

Sodium bismuthate was successfully used as an ion exchange material for the separation of americium from curium in 0.1 M nitric acid. A solid-liquid separation technique resulted in greater than 90% recovery and purity of americium and curium. Greater purity could be obtained with increased contact stages. A chromatography method was also developed. The use of a filter aid was however required to achieve acceptable flow properties. The recovery and purity of the americium and curium fractions was higher (>97%) than in the solid-liquid batch contact separation and only required one pass through the column. The chromatographic method is efficient as it can be completed in less than half an hour and results in good purity and recovery with only one pass through the column. The method has the potential to be cost-effective, as it only requires a few inexpensive, commercially available materials. Cost-effectiveness would depend on application.

8.4 Properties of Sodium Bismuthate

The efficacy of sodium bismuthate as a separation medium is dependent on many properties. Several of these properties were explored and sodium bismuthate was found to be comparable to other chromatographic materials in many ways.

The adsorption capacity of sodium bismuthate for trivalent metal ions was determined by analyzing the adsorption of lanthanum at varying concentrations on sodium bismuthate. The adsorption capacity was determined using the Langmuir Isotherm Model and was found to be 3.0 mg La/g NaBiO₃ or 0.022 mmol La/g NaBiO₃. This value is only valid at a contact time of ten minutes, as the system never reaches equilibrium during a separation. The adsorption capacity of sodium bismuthate, when adjusted for density, is comparable to that of conventional ion exchange resins.

The sodium bismuthate used in this study has a lower specific surface area than chromatographic materials used in extraction chromatography even when adjusted for density. However, the surface area is sufficient to provide comparable capacity. The specific surface area of the sodium bismuthate used in this work was found to be 23.7 m²/g. While an accurate determination of particle size was not successful, the particle size can be somewhat inferred from the filtration behavior. The particles are greater than 0.45 μm, and some of the smallest particles are less than 3 μm. The average particle size is presumed to be on the order of a few microns.

Sodium bismuthate has non-negligible solubility in nitric acid and some dissolution occurs during the separation procedure. This results in bismuth contamination in the effluent streams. The bismuth concentration in the americium (0.1 M nitric acid) fraction is kept quite low (~100 ppb) as a result of the good retention of trivalent species, including Bi(III), by the surface of the sodium bismuthate. The bismuth contamination in the curium fraction (2.0 M nitric acid) is much higher (~100 ppm) as there is little retention of dissolved bismuth.

It is very common for sodium bismuthate to be sold with purities of approximately 80%. This is due to the difficulty of synthesizing pure sodium bismuthate. The effect of these intrinsic impurities on the separation was tested in a comparison of the behavior of americium and curium

on high purity (93%) and reagent grade (80%) sodium bismuthate. The behavior of americium and curium on reagent-grade sodium bismuthate was very similar to the behavior on the high purity sodium bismuthate. The separation factor was not adversely affected by the presence of greater levels of impurities. The reagent grade sodium bismuthate showed more effervescence in the presence of nitric acid, which could lead to difficulties in using reagent grade materials for column chromatography.

Sodium bismuthate has benefits and drawbacks as a separation material. The drawbacks include the production of gases in nitric acid and the gradual dissolution of the material during the separation. The main benefit is that this separation method greatly simplifies one of the most challenging separations in radiochemistry, the separation of americium from curium.

8.5 Application of Sodium Bismuthate Chromatography

In order for sodium bismuthate chromatography to be applied to challenges in advanced nuclear fuel cycles the method must be tolerant of other elements in the separation. It was found that the capabilities of sodium bismuthate chromatography include many elements beyond americium and curium. Americium can be isolated from mixtures of curium, lanthanides, and rare earths due to the similar chemical behavior of these elements. This chemical similarity, combined with the low nitric acid concentration typical of TRUEX strip solutions, makes post-TRUEX application of sodium bismuthate chromatography an attractive option. The major challenge with post-TRUEX application involves cerium. Sodium bismuthate is capable of oxidizing cerium to Ce(IV). The D_w value of Ce(IV) in 0.1 M nitric acid is much higher than that of trivalent lanthanides, and it is not eluted from the column with 2.0 M nitric acid. This would make the reuse of sodium bismuthate columns quite limited.

Fission product elements expected to be present in PUREX raffinate vary greatly in their weight distribution values for contact with sodium bismuthate in 0.1 M nitric acid. While these values vary greatly, there is a significant gap between the mono- and divalent species and the tri- and tetravalent species. This large separation in behaviors allows for predictable outcomes in separation procedures. The anionic, mono, and divalent species end up in the americium fraction and the tri and tetravalent species follow curium. Isolation of americium from the elements in the americium fraction is significantly simpler than separation of americium from curium and the lanthanides. Several elements are not eluted from the column in 2.0 M nitric acid. This makes reuse of the columns difficult if not impossible. It could be possible to incorporate the bismuthate into a glass-based waste form such as bismuth silicate glass or into grout. This would eliminate the need for complicated separations to remove the retained elements from the bismuthate. Sodium bismuthate chromatography could be applied at various stages throughout the proposed processes involved in spent nuclear fuel processing.

8.6 Proposed Future Work

Sodium bismuthate chromatography is a novel and promising technology that has the capability to isolate americium from curium, lanthanides and some fission product elements. Much still remains to be learned about this novel separation method. Future work should include further characterization and optimization of the separation method as well as expansion and discovery of the capabilities of this method to address challenges in chemical separations.

In order to further characterize and optimize this separation method, more chemical properties should be determined. Particle size could be analyzed using microscopy techniques such as scanning electron microscopy (SEM). This analysis could be performed prior to and following a separation procedure to understand the changes in particle shape and morphology during a

separation procedure. More sources of sodium bismuthate could be tested to determine needs in purity and composition to maintain separation efficiency. Many bismuthate compounds are reported in the literature⁵⁶⁻⁵⁸. Some can be made with much higher purities⁵⁷. Exploring the possible use of these other bismuthate compounds as chromatography materials would be beneficial. It could be possible to find a material with lower solubility or one that produces less gas in contact with nitric acid. Comparison of different bismuthate compounds could lead to greater understanding of the influence that the structure of the material has on the properties of the material as a separation medium.

Other filter aids or column setups could be tested as well. If a method could be developed to cover a chromatographic material with a bismuthate coating, capacity and flow properties could be improved. Sodium bismuthate could be incorporated into polyacrylonitrile as in the commercially available MnO₂-PAN resin sold by Triskem Inc⁵⁹. The use of other filter aids or column setups could help mitigate the problem of effervescence. It would also be beneficial to test these separations with higher concentrations of americium.

The separation relies heavily upon the behavior of americium and all experiments done in this work were performed at trace level. In order for this method to be successfully applied to fuel cycle challenges, the behavior of americium at higher concentrations would need to be similar.

This work focuses on application of this method to challenges in the nuclear fuel cycle, however, many other potential applications exist for this method. A rapid separation of americium from curium could allow for greater understanding of the neutron capture properties of ²⁴¹Am that are of interest in stockpile stewardship. A rapid separation of americium from curium could also allow for removal of isobaric interferences in nuclear forensic analysis of materials containing americium and curium. It could also be applied in environmental monitoring. The requirements

and challenges in these applications would be quite different from those in nuclear fuel cycle applications. In environmental and forensic work, the behavior of elements found in soil and debris would need to be explored to determine the chemical preparations that would be required to make this method successful in separating americium from curium. In application to neutron-capture properties, the method would have to be as rapid as possible to be able to perform an accurate analysis. This method could possibly be applied outside of nuclear science in any other separation requiring ion-exchange separation in a highly oxidizing environment.

APPENDIX: RAW DATA FOR FIGURES

Table 4: Raw Data for Figure 7

[HNO ₃] (M)	k' (Am)	k' (Cm)
0.01	5.0 ± 0.3	5.8 ± 0.8
0.05	41.1 ± 1.1	62.4 ± 1.3
0.13	192.4 ± 8.9	296.7 ± 7.0
0.50	3690.5 ± 487.8	3282.1 ± 328.0
0.93	8939.8 ± 5858.6	5502.8 ± 1844.0
1.85	>10000	7475.3 ± 1490.9
3.70	>10000	8830.1 ± 6308.4
6.16	>10000	>10000
8.00	>10000	>10000
9.73	>10000	>10000

Table 5: Raw Data for Figure 8

[HNO ₃] (M)	k' (Am)	k' (Cm)
0.01	hydrolysis	hydrolysis
0.05	12.3 ± 1.5	776.2 ± 428.2
0.13	79.0 ± 13.2	215.9 ± 15.1
0.50	7.9 ± 1.6	20.2 ± 1.2
0.93	2.8 ± 0.7	6.7 ± 1.0
1.85	<0.10	<0.1
3.70	<0.10	<0.1
6.16	<0.10	0.6 ± 0.3
8.00	0.3 ± 0.5	1.8 ± 1.8
9.73	0.6 ± 0.6	4.4 ± 0.5

Table 6: Raw Data for Figure 9

[HNO ₃] (M)	k' (Cm)	50 mg 1 hr.	100 mg 1 hr.	150 mg 1 hr.	100 mg 12 hr.	150 mg 12 hr.
0.01	hydrolysis					
0.05	776.2 ± 428.2					
0.13	215.9 ± 15.1					
0.50	20.2 ± 1.2					
0.93	6.7 ± 1.0					
1.85	<0.1	7.5 ± 4.3	25.5 ± 14.5	43.3 ± 24.7	0.08 ± 0.04	8.0 ± 4.6
3.70	<0.1					
6.16	0.6 ± 0.3					
8.00	1.8 ± 1.8					
9.73	4.4 ± 0.5					

Table 7: Raw Data for Figure 11

[HNO ₃] (M)	k' (Am)	k' (Cm)
0.01	<0.01	0.02 ± 0.06
0.05	<0.01	<0.01
0.13	<0.01	0.02 ± 0.06
0.50	<0.01	<0.01
0.93	<0.01	0.05 ± 0.04
1.85	0.02 ± 0.04	0.10 ± 0.04
3.70	<0.01	0.05 ± 0.03
6.16	<0.01	<0.01
8.00	<0.01	<0.01
9.73	<0.01	<0.01

Table 8: Raw Data for Figure 12

[HNO ₃] (M)	k' (Am)	k' (Cm)
0.01	hydrolysis	hydrolysis
0.05	8.03 ± 1.60	263.25 ± 32.97
0.13	2.86 ± 1.28	4.24 ± 0.65
0.50	<0.01	0.15 ± 0.01
0.93	<0.01	0.11 ± 0.03
1.85	<0.01	0.07 ± 0.05
3.70	<0.01	0.02 ± 0.10
6.16	<0.01	<0.01
8.00	<0.01	<0.01
9.73	<0.01	<0.01

Table 9: Raw Data for Figure 14

[HNO ₃] (M)	D _w (Am)	D _w (Cm)
0.05	99.19 ± 4.06	>50000
0.10	90.02 ± 1.17	8364.65 ± 337.98
0.50	0.99 ± 0.01	1.46 ± 0.01
1.00	0.46 ± 0.01	0.33 ± 0.01
2.00	0.14 ± 0.01	0.04 ± 0.01
4.00	<0.01	<0.01
6.00	<0.01	<0.01

Table 10: Raw Data for Figure 15

[HNO ₃] (M)	D _w (Am)	D _w (Cm)
0.01	401.33 ± 22.81	>75000
0.03	253.18 ± 25.14	39025.50 ± 407.37
0.05	45.79 ± 0.82	5336.22 ± 95.04
0.10	6.22 ± 0.43	428.71 ± 91.52
0.20	3.19 ± 0.14	120.07 ± 37.72
0.30	2.18 ± 0.12	85.08 ± 13.14
0.50	2.10 ± 0.25	30.78 ± 2.19
1.00	1.37 ± 0.08	3.68 ± 0.25
2.00	0.08 ± 0.03	0.26 ± 0.06
4.00	<0.01	<0.01
6.00	<0.01	<0.01

Table 11: Raw Data for Figure 16

Time (min.)	D _w (Am)	D _w (Cm)
1	21.3 ± 2.3	1901.0 ± 100.2
2	21.5 ± 0.6	1895.5 ± 200.6
5	20.2 ± 0.7	2071.6 ± 141.5
10	17.7 ± 1.0	1745.9 ± 103.2
15	15.1 ± 0.4	1538.2 ± 295.8
30	12.9 ± 0.6	1140.8 ± 152.9
60	7.3 ± 1.5	664.6 ± 59.0
120	4.9 ± 0.6	354.3 ± 40.1

Table 12: Raw Data for Figure 17

[HNO ₃] (M)	D _w (Am)	D _w (Cm)
0.05	63.44 ± 1.5	7258.61 ± 245.03
0.10	14.62 ± 0.07	919.15 ± 71.23
0.20	4.04 ± 0.01	-
0.50	4.28 ± 0.06	12.39 ± 0.26
1.00	1.33 ± 0.02	-
2.00	<0.01	0.24 ± 0.01
4.00	<0.01	<0.01

Table 13: Raw Data for Figure 18

[HNO ₃] (M)	D _w (Cm)	[NO ₃ ⁻] (M) (0.1 M HNO ₃)	D _w (Cm)
0.05	7258.61 ± 245.03	0.05	7258.61 ± 245.03
0.10	919.15 ± 71.23	0.10	476.60 ± 18.05
0.50	12.39 ± 0.26	0.50	2.84 ± 0.06
2.00	0.24 ± 0.01	2.00	<0.01
4.00	<0.01	4.00	<0.01

Table 14: Raw Data for Figure 21

[La] (ppm)	La Adsorbed (μg)
10	9.5 ± 0.8
20	19.0 ± 0.2
40	35.0 ± 3.0
60	47.2 ± 1.9
80	54.7 ± 1.8
100	62.9 ± 1.1

Table 15: Raw Data for Figure 22

C _e (mg/L)	C _e /q _e
0.48	1009.65
1.01	1060.39
5.02	2872.70
12.80	5424.27
25.27	9234.07
37.11	11803.24

Table 16: Raw Data for Figure 23

Time (hours)	[Bi] μM		[Bi] μM
	0.1 M HNO ₃	0.1 M HNO ₃ +2.0 M HNO ₃	2.0 M HNO ₃
0.08	2.0 ± 0.5	173.2 ± 14.9	502.6 ± 31.6
0.17	1.4 ± 0.7	179.6 ± 13.9	515.9 ± 34.2
0.5	0.9 ± 0.1	-	912.1 ± 19.1
1	0.6 ± 0.1	264.9 ± 15.1	1794.4 ± 13.8
2	0.6 ± 0.2	325.1 ± 24.2	3625.0 ± 72.1
3	0.7 ± 0.1	347.6 ± 13.8	5254.0 ± 72.3
4	0.9 ± 0.1	372.0 ± 6.2	6700.1 ± 54.2

Table 17: Raw Data for Figure 24

Time (hours)	[Bi] μM 0.1 M HNO_3
0.08	2.0 ± 0.5
0.17	1.4 ± 0.7
0.5	0.9 ± 0.1
1	0.6 ± 0.1
2	0.6 ± 0.2
3	0.7 ± 0.1
4	0.9 ± 0.1

Table 18: Raw Data for Figure 25

Time (hours)	[Bi] μM 0.1 M HNO_3 +2.0 M HNO_3
0.08	173.2 ± 14.9
0.17	179.6 ± 13.9
0.5	-
1	264.9 ± 15.1
2	325.1 ± 24.2
3	347.6 ± 13.8
4	372.0 ± 6.2

Table 19: Raw Data for Figure 26

[HNO_3] (M)	D_w (Am) High Purity	D_w (Cm) High Purity	D_w (Am) Reagent Grade	D_w (Cm) Reagent Grade
0.1	18.4 ± 1.5	1919.4 ± 179.9	31.1 ± 1.3	2933.8 ± 197.5
0.46	5.2 ± 0.5	20.7 ± 3.0	8.7 ± 2.5	10.6 ± 1.1
1.8	0.7 ± 0.1	1.0 ± 0.2	0.5 ± 0.5	0.3 ± 0.3

Table 20: Raw Data for Figure 27

Element	D_w (0.1 M HNO ₃)
La	552.7 ± 25.7
Ce	-
Pr	694.3 ± 157.8
Nd	1701.9 ± 260.1
Pm	-
Sm	738.5 ± 82.7
Eu	833.5 ± 30.0
Gd	701.7 ± 67.4
Tb	822.6 ± 181.1
Dy	669.5 ± 48.4
Ho	695.0 ± 18.1
Er	685.2 ± 70.9
Tm	-
Yb	884.1 ± 49.6

Table 21: Raw Data for Figure 28

Element	D_w (0.1 M HNO ₃)
La	596.9 ± 54.7
Ce	7713.9 ± 4379.9
Pr	681.6 ± 22.6
Nd	696.5 ± 52.1
Pm	-
Sm	647.1 ± 53.4
Eu	723.8 ± 47.8
Gd	593.9 ± 42.8
Tb	586.4 ± 59.2
Dy	549.8 ± 48.4
Ho	593.6 ± 52.9
Er	654.5 ± 73.0
Tm	720.6 ± 51.2
Yb	724.6 ± 68.6

Table 22: Raw Data for Figure 29

[HNO ₃] (M)	D _w (Am)	D _w (Cm)	D _w (La)	D _w (Ce)
0.05	63.44 ± 1.5	7258.61 ± 245.03	3107.2 ± 200.3	>10000
0.10	14.62 ± 0.07	919.15 ± 71.23	596.9 ± 54.7	>10000
0.50	4.28 ± 0.06	12.39 ± 0.26	8.5 ± 0.2	>10000
1.00	1.33 ± 0.02	-	3.2 ± 0.1	6116.8 ± 1049.5
2.00	<0.01	0.24 ± 0.01	0.2 ± 0.1	492.9 ± 76.7

[HNO ₃] (M)	D _w (Pr)	D _w (Nd)	D _w (Sm)	D _w (Eu)
0.05	2374.8 ± 691.4	8246.8 ± 6040.3	3057.7 ± 391.0	3187.5 ± 137.3
0.10	681.6 ± 22.6	696.5 ± 52.1	647.1 ± 53.4	723.8 ± 47.8
0.50	10.1 ± 0.2	9.2 ± 0.2	8.9 ± 0.2	8.4 ± 0.1
1.00	4.2 ± 0.1	3.4 ± 0.3	3.6 ± 0.1	3.2 ± 0.1
2.00	0.7 ± 0.1	<0.1	0.5 ± 0.1	0.2 ± 0.1

[HNO ₃] (M)	D _w (Gd)	D _w (Tb)	D _w (Dy)	D _w (Ho)
0.05	2335.2 ± 313.4	2000.1 ± 114.2	2987.4 ± 119.5	2174.5 ± 142.9
0.10	593.9 ± 42.8	586.4 ± 59.2	549.8 ± 48.4	593.6 ± 52.9
0.50	8.8 ± 0.2	9.5 ± 0.1	11.0 ± 0.3	10.8 ± 0.2
1.00	3.7 ± 0.1	3.8 ± 0.1	5.2 ± 0.1	4.7 ± 0.1
2.00	0.6 ± 0.1	0.5 ± 0.1	1.5 ± 0.1	0.9 ± 0.1

[HNO ₃] (M)	D _w (Er)	D _w (Tm)	D _w (Yb)
0.05	1655.6 ± 69.3	2753.5 ± 113.8	2798.7 ± 178.8
0.10	654.5 ± 73.0	720.6 ± 51.2	724.6 ± 68.6
0.50	11.1 ± 0.2	14.1 ± 0.4	13.1 ± 0.3
1.00	4.9 ± 0.1	6.6 ± 0.1	6.1 ± 0.1
2.00	0.8 ± 0.1	1.7 ± 0.1	1.5 ± 0.1

Table 23: Raw Data for Figure 30

[HNO ₃] (M)	D _w (Am)	D _w (Cm)	D _w (Pu)	D _w (U)
0.05	63.44 ± 1.5	7258.61 ± 245.03	46.76 ± 2.05	16.29 ± 0.05
0.10	14.62 ± 0.07	919.15 ± 71.23	12.33 ± 0.07	5.28 ± 0.17
0.20	4.04 ± 0.01	-	1.49 ± 0.03	1.30 ± 0.01
0.50	4.28 ± 0.06	12.39 ± 0.26	0.06 ± 0.01	0.32 ± 0.01
1.00	1.33 ± 0.02	-	<0.01	<0.01
2.00	<0.01	0.24 ± 0.01	<0.01	-

Table 24: Raw Data for Figure 31

Time (min.)	D _w (Mo)	D _w (Sr)	D _w (Pd)
10	801.7 ± 72.1	19.6 ± 0.9	320.7 ± 58.9
30	879.6 ± 47.8	16.3 ± 1.3	433.9 ± 48.5
60	978.8 ± 39.5	17.9 ± 0.4	920.6 ± 161.8
120	1413.9 ± 48.2	24.3 ± 0.3	>10000

Time (min.)	D _w (Sn)	D _w (Gd)	D _w (Rb)
10	268.3 ± 4.3	33.0 ± 1.3	78.1 ± 0.7
30	327.6 ± 20.9	36.2 ± 1.8	82.3 ± 1.7
60	388.6 ± 14.2	44.1 ± 2.1	84.7 ± 1.3
120	610.3 ± 82.2	64.3 ± 2.2	91.2 ± 0.5

Time (min.)	D _w (Y)	D _w (Zr)	D _w (Ce)
10	26.2 ± 0.4	353.7 ± 38.3	353.5 ± 16.5
30	28.3 ± 0.5	339.1 ± 25.0	368.8 ± 18.0
60	28.7 ± 0.1	357.4 ± 16.3	370.5 ± 16.9
120	32.5 ± 0.3	463.1 ± 9.2	351.6 ± 9.0

Table 25: Raw Data for Figure 33

Element	5 mL	10 mL	15 mL	20 mL	25 mL
Mo	1.59 ± 0.43	0.32 ± 0.23	0.22 ± 0.21	0.20 ± 0.18	0.22 ± 0.14
Sr	17.52 ± 7.07	67.59 ± 1.53	20.51 ± 0.13	5.43 ± 0.43	2.00 ± 0.07
Se	73.45 ± 3.87	11.78 ± 1.19	2.51 ± 0.31	0.87 ± 0.03	0.52 ± 0.04
Pd	<LLD	<LLD	<LLD	<LLD	<LLD
Sn	<LLD	<LLD	<LLD	<LLD	<LLD
Sm	<LLD	<LLD	<LLD	<LLD	<LLD
Gd	0.21 ± 0.01	0.17 ± 0.01	0.10 ± 0.01	0.07 ± 0.02	0.05 ± 0.04
Rb	4.37 ± 5.89	83.53 ± 5.01	7.60 ± 0.14	1.68 ± 0.10	0.57 ± 0.03
Y	1.59 ± 0.06	1.47 ± 0.13	1.15 ± 0.01	1.00 ± 0.28	0.78 ± 0.32
Zr	<LLD	<LLD	<LLD	<LLD	<LLD
Ru	4.30 ± 0.88	<LLD	<LLD	<LLD	<LLD
La	<LLD	<LLD	<LLD	<LLD	<LLD
Ce	<LLD	<LLD	<LLD	<LLD	<LLD
Pr	<LLD	<LLD	<LLD	<LLD	<LLD
Nd	<LLD	<LLD	<LLD	<LLD	<LLD
Eu	<LLD	<LLD	<LLD	<LLD	<LLD
Cs	<LLD	18.04 ± 5.61	34.85 ± 2.84	17.35 ± 0.42	7.71 ± 0.80

Table 25 (cont.): Raw Data for Figure 33

Element	30 mL	35 mL	40 mL	45 mL	50 mL
Mo	9.42 ± 1.06	8.23 ± 0.37	6.26 ± 0.42	4.82 ± 0.47	3.85 ± 0.37
Sr	12.23 ± 0.81	4.64 ± 0.21	0.65 ± 0.06	<LLD	<LLD
Se	9.77 ± 1.59	1.16 ± 0.41	0.10 ± 0.25	<LLD	<LLD
Pd	19.80 ± 0.72	18.42 ± 2.79	8.03 ± 2.42	3.16 ± 2.40	0.94 ± 2.24
Sn	9.81 ± 6.30	7.36 ± 2.02	0.39 ± 0.01	<LLD	<LLD
Sm	75.83 ± 2.15	0.86 ± 0.06	0.34 ± 0.04	0.09 ± 0.01	<LLD
Gd	76.06 ± 1.65	1.32 ± 0.07	0.71 ± 0.02	0.40 ± 0.01	0.24 ± 0.01
Rb	1.44 ± 0.07	0.19 ± 0.01	<LLD	<LLD	<LLD
Y	95.57 ± 6.44	1.93 ± 0.28	0.56 ± 0.12	0.12 ± 0.02	<LLD
Zr	21.24 ± 0.68	20.26 ± 2.68	10.29 ± 1.72	5.56 ± 1.22	3.32 ± 1.13
Ru	0.03 ± 0.03	<LLD	<LLD	<LLD	<LLD
La	88.15 ± 8.06	1.20 ± 0.24	0.31 ± 0.06	<LLD	<LLD
Ce	0.28 ± 0.12	0.16 ± 0.16	<LLD	<LLD	<LLD
Pr	88.44 ± 7.35	1.00 ± 0.14	0.14 ± 0.20	<LLD	<LLD
Nd	90.95 ± 7.11	1.02 ± 0.18	0.29 ± 0.05	0.02 ± 0.03	<LLD
Eu	86.89 ± 3.05	1.21 ± 0.12	0.50 ± 0.04	0.24 ± 0.02	0.11 ± 0.01
Cs	11.35 ± 1.20	0.47 ± 0.19	<LLD	<LLD	<LLD

REFERENCES

- (1) Wigeland, R.; Taiwo, T.; Ludewig, H.; Todosow, M.; Halsey, W.; Gehin, J.; Jubin, R.; Buelt, J.; Stockinger, S.; Jenni, K.; et al. Nuclear Fuel Cycle Evaluation and Screening – Final Report. US Department of Energy 2014.
- (2) Lanham, W. B.; Runion, T. C. PUREX Process for Plutonium and Uranium Recovery. *ORNL-479*. Oak Ridge, TN 1949.
- (3) Greenwood, N. N.; Earnshaw, A. *Chemistry of the Elements*; 1997.
- (4) Dam, H. H.; Reinhoudt, D. N.; Verboom, W. Multicoordinate ligands for actinide / lanthanide separations. *Chem. Soc. Rev.* **2007**, *36* (2), 367–377.
- (5) Whittaker, D. M.; Gri, T. L.; Helliwell, M.; Swinburne, A. N.; Natrajan, L. S.; Lewis, F. W.; Harwood, L. M.; Parry, S. A.; Sharrad, C. A. Lanthanide Speciation in Potential SANEX and GANEX Actinide/ Lanthanide Separations Using Tetra-N-Donor Extractants. *Inorg. Chem.* **2013**, *52* (7), 3429–3444.
- (6) Gelis, A. V; Lumetta, G. J. Actinide Lanthanide Separation Process ALSEP. *Ind. &Engineering Chem. Res.* **2014**, *53* (4), 1624–1631.
- (7) Kolarik, Z. Complexation and Separation of Lanthanides (III) and Actinides (III) by Heterocyclic N-Donors in Solutions. *Chem. Rev.* **2008**, *108* (10), 4208–4252.
- (8) Braley, J. C.; Grimes, T. S.; Nash, K. L. Alternatives to HDEHP and DTPA for Simplified TALSPEAK Separations. *Ind. &Engineering Chem. Res.* **2012**, *51* (2), 629–638.
- (9) Nilsson, M.; Nash, K. L. Review Article: A Review of the Development and Operational Characteristics of the TALSPEAK Process. *Solvent Extr. Ion Exch.* **2007**, *25* (6), 665–701.
- (10) Ionova, G.; Ionov, S.; Rabbe, C.; Hill, C.; Madic, C.; Guillaumont, R.; Krupa, J. C. Mechanism of trivalent actinide/lanthanide separation using bis(2,4,4-trimethylpentyl) dithiophosphinic acid (Cyanex 301) and neutral O-bearing co-extractant synergistic mixtures. *Solvent Extr. Ion Exch.* **2001**, *19* (3), 391–414.
- (11) Mincher, B. J.; Wai, C. M.; Fox, R. V.; Baek, D. L.; Yen, C.; Case, M. E. The separation of lanthanides and actinides in supercritical fluid carbon dioxide. *J. Radioanal. Nucl. Chem.* **2016**, *307* (3), 2543–2547.
- (12) Definitions. *Code of Federal Regulations*, Section 60.2, Title 10, **2011**.
- (13) Management, N. R. C. (US) B. on R. W. A Study of the Isolation System for Geologic Disposal of Radioactive Wastes. National Academies 1983.
- (14) Cohen, B. L. High-level radioactive waste from light-water reactors. *Rev. Mod. Phys.* **1977**, *49* (1), 1–20.

- (15) Salvatores, M.; Palmiotti, G. Radioactive waste partitioning and transmutation within advanced fuel cycles : Achievements and challenges. *Prog. Part. Nucl. Phys.* **2011**, *66* (1), 144–166.
- (16) Morss, L. R.; Edelstein, N. M.; Fuger, J. *The Chemistry of the Actinide and Transactinide Elements*, 3rd ed.; Springer: Dordrecht, The Netherlands, 2006.
- (17) Bard, A. J. A. J.; Parsons, R.; Jordan, J. *Standard Potentials in Aqueous Solutions*, Vol. 6.; CRC Press: New York, 1985.
- (18) Moore, F. L. New Method for Separation of Americium from Curium and Associated Elements in the Zirconium Phosphate-Nitric Acid System. *Anal. Chem.* **1971**, *43* (3), 487–489.
- (19) Kraak, W.; Van Der Heijden, W. A. Anion exchange separation between americium and curium and between several lanthanide elements. *J. Inorg. Nucl. Chem.* **1966**, *28* (1), 221–224.
- (20) Lebedev, I.; Myasoedov, B.; Guseva, L. Use of alcoholic solutions for the isolation and purification of americium and curium with anion-exchangers. *J. Radioanal. Nucl. Chem.* **1974**, *21* (1), 259–266.
- (21) Suzuki, T.; Otake, K.; Sato, M.; Ikeda, A.; Aida, M.; Fujii, Y.; Hara, M.; Mitsugashira, T.; Ozawa, M. Separation of americium and curium by use of tertiary pyradine resin in nitric acid/methanol mixed solvent system. *J. Radioanal. Nucl. Chem.* **2007**, *272* (2), 257–262.
- (22) Horwitz, P. E.; Orlandini, K. A.; Bloomquist, C. A. A. The Separation of Americium and Curium by Extraction Chromatography Using a High Molecular Weight Quaternary Ammonium Nitrate. *Inorg. Nucl. Chem. Lett.* **1966**, *2* (4), 87–91.
- (23) Modolo, G.; Kluxen, P.; Geist, A. Demonstration of the LUCA process for the separation of americium(III) from curium(III), californium(III), and lanthanides(III) in acidic solution using a synergistic mixture of bis(chlorophenyl)dithiophosphinic acid and tris(2-ethylhexyl)phosphonate. *Radiochim. Acta* **2010**, *98* (4), 193–201.
- (24) Chapron, S.; Marie, C.; Arrachart, G.; Miguirditchian, M.; Pellet-Rostaing, S. New Insight into the Americium/Curium Separation by Solvent Extraction using Diglycolamides. *Solvent Extr. Ion Exch.* **2015**, *33* (3), 236–248.
- (25) Street, K.; Seaborg, G. T. The Separation of Americium and Curium from the Rare Earth Elements. *J. Am. Chem. Soc.* **1950**, *72* (6), 2790–2792.
- (26) Runde, W. H.; Mincher, B. J. Higher oxidation states of americium: Preparation, characterization and use for separations. *Chem. Rev.* **2011**, *111* (9), 5723–5741.
- (27) Lumetta, G. J.; Sinkov, S. I. Americium(III) oxidation by copper(III) periodate in nitric acid solution as compared with the action of Bi(V) compounds of sodium. *Radiochim. Acta* **2015**, *103* (8), 541–552.

- (28) Mccann, K.; Brigham, D. M.; Morrison, S.; Braley, J. C. Hexavalent Americium Recovery Using Copper(III) Periodate. *Inorg. Chem.* **2016**, *55* (22), 11971–11978.
- (29) Hara, M.; Suzuki, S. Oxidation of americium (III) with sodium bismuthate. *J. Radioanal. Chem.* **1977**, *36* (1), 95–104.
- (30) Burney, G. A. Separation of Americium from Curium by Precipitation of $K_3AmO_2(CO_3)_2$. *Nucl. Appl.* **1968**, *4* (4), 217–221.
- (31) Mincher, B. J.; Martin, L. R.; Schmitt, N. C. Tributylphosphate extraction behavior of bismuthate-oxidized americium. *Inorg. Chem.* **2008**, *47* (15), 6984–6989.
- (32) Burns, J. D.; Borkowski, M.; Clearfield, a.; Reed, D. T. Separation of oxidized americium from lanthanides by use of pillared metal(IV) phosphate-phosphonate hybrid materials. *Radiochim. Acta* **2012**, *100* (12), 901–906.
- (33) Burns, J. D.; Shehee, T. C.; Clearfield, A.; Hobbs, D. T. Separation of Americium from Curium by oxidation and ion exchange. *Anal. Chem.* **2012**, *84* (16), 6930–6932.
- (34) Mincher, B. J.; Schmitt, N. C.; Schuetz, B. K.; Shehee, T. C.; Hobbs, D. T. Recent advances in f-element separations based on a new method for the production of pentavalent americium in acidic solution. *RSC Adv.* **2015**, *5* (34), 27205–27210.
- (35) Mincher, B. J.; Martin, L. R.; Schmitt, N. C. Diamylamylphosphonate Solvent Extraction of Am(VI) from Nuclear Fuel Raffinate Simulant Solution. *Solvent Extr. Ion Exch.* **2012**, *30* (5), 445–456.
- (36) Mincher, B. J.; Schmitt, N. C.; Case, M. E. A TRUEX-Based Separation of Americium from the Lanthanides. *Solvent Extr. Ion Exch.* **2011**, *29* (2), 247–259.
- (37) Kumada, N.; Kinomura, N.; Sleight, a. W. Neutron powder diffraction refinement of ilmenite-type bismuth oxides: $ABiO_3$ (A = Na, Ag). *Mater. Res. Bull.* **2000**, *35* (14–15), 2397–2402.
- (38) Mehlig, J. P. Spectrophotometric Determination of Manganese in Steel. *Ind. Eng. Chem. Anal. Ed.* **1935**, *7* (1), 27–29.
- (39) Yu, K.; Yang, S.; Liu, C.; Chen, H.; Li, H.; Sun, C.; Boyd, S. A. Degradation of Organic Dyes via Bismuth Silver Oxide Initiated Direct Oxidation Coupled with Sodium Bismuthate Based Visible Light Photocatalysis. *Environ. Sci. Technol.* **2012**, *46* (13), 7318–7326.
- (40) Ding, Y.; Yang, F.; Zhu, L.; Wang, N.; Tang, H. Bi^{3+} self doped $NaBiO_3$ nanosheets: Facile controlled synthesis and enhanced visible light photocatalytic activity. *Applied Catal. B Environ.* **2015**, *164*, 151–158.
- (41) Ding, Y.; Zhou, P.; Tang, H. Visible-light photocatalytic degradation of bisphenol A on $NaBiO_3$ nanosheets in a wide pH range: A synergistic effect between photocatalytic

- oxidation and chemical oxidation. *Chem. Eng. J.* **2016**, *291*, 149–160.
- (42) Liu, J.; Chen, S.; Liu, Q.; Zhu, Y.; Zhang, J. Correlation of crystal structures and electronic structures with visible light photocatalytic properties of NaBiO₃. *Chem. Phys. Lett.* **2013**, *572*, 101–105.
- (43) Takei, T.; Haramoto, R.; Dong, Q.; Kumada, N.; Yonesaki, Y. Photocatalytic activities of various pentavalent bismuthates under visible light irradiation. *J. Solid State Chem.* **2011**, *184* (8), 2017–2022.
- (44) Horwitz, P. E.; McAlister, D. R.; Bond, A. H.; Barrans Jr., R. E. Novel Extraction Chromatographic Resins Based on Tetraalkyldiglycolamides: Characterization and Potential Applications. *Solvent Extr. Ion Exch.* **2005**, *23* (3), 319–344.
- (45) Gingell, T. The Determination of Uranium in Environmental Samples Using Extraction Chromatography. *J. Radioanal. Nucl. Chem.* **1997**, *226* (1–2), 188–189.
- (46) Stock, S. A. Quantitative comparison of sample preparation methods for low-level alpha spectrometry, University of Nevada Las Vegas, 2007.
- (47) Amberchrom CG71 Technical Data Sheet. Rohm and Haas 2007.
- (48) Amberlite XAD-4 Product Data Sheet Form No. 177-02319-0614.
- (49) Amberlite XAD-7 Product Data Sheet Form No. 177-03084-0313.
- (50) Boswell, G. G. J.; Soentono, S. Ruthenium nitrosyl complexes in nitric acid solutions. *J. Inorg. Nucl. Chem.* **1981**, *43* (7), 1625–1632.
- (51) Fletcher, J. M.; Brown, P. G. M.; Gardner, E. R.; Hardy, C. J.; Wain, A. G.; Woodhead, J. L. Nitrosylruthenium nitrato complexes in aqueous nitric acid. *J. Inorg. Nucl. Chem.* **1959**, *12* (1–2), 118–277.
- (52) Siczek, A.; Steindler, M. The chemistry of ruthenium and zirconium in the PUREX solvent extraction process. *At. Energy Rev.* **1978**, *16* (4), 575–618.
- (53) Richards, J. M.; Mincher, B. J. Selective Partitioning of Ruthenium from Nitric Acid Media. *Solvent Extr. Ion Exch.* **2017**, *35* (1), 49–60.
- (54) Garino, T. J.; Nenoff, T. M.; Krumhansl, J. L.; Rademacher, D. X. Low-Temperature Sintering Bi–Si–Zn-Oxide Glasses for Use in Either Glass Composite Materials or Core/Shell 129 I Waste Forms. *J. Am. Ceram. Soc.* **2011**, *94* (8), 2412–2419.
- (55) El Batal, F. H. Gamma ray interaction with bismuth silicate glasses. *Nucl. Instruments Methods Phys. Res.* **2007**, *254* (2), 243–253.
- (56) Kumada, N.; Xu, N.; Miura, A.; Takei, T. Preparation and photocatalytic properties of new calcium and lead bismuthates. *J. Ceram. Soc. Japan* **2014**, *122* (1426), 509–512.

- (57) Kodialam, S.; Korthius, V. C.; Hoffmann, R.; Sleight, A. W. Electrodeposition of potassium bismuthate: KBiO_3 . *Mater. Res. Bull.* **1992**, 27 (12), 1379–1384.
- (58) Firouzabadi, H.; Mohammadpour-Baltork, I. Zinc Bismuthate $\text{Zn}(\text{BiO}_3)_2$: A Useful Oxidizing Agent for the Efficient Oxidation of Organic Compounds. *Bull. Chem. Soc. Jpn.* **1992**, 65 (4), 1131–1134.
- (59) Dulanska, S.; Gardonova, V.; Sebesta, F.; Matel, L. A rapid determination of Ra in water using composite ion. *J. Radioanal. Nucl. Chem.* **2015**, 303 (1), 47–51.

CURRICULUM VITAE

Jason M. Richards

Curriculum Vitae

jason.richards241@gmail.com

- Education** **Ph.D. Candidate**, Radiochemistry Program, University of Nevada Las Vegas
Current GPA 4.00/4.00
Expected graduation: May 2018
- Bachelor of Science in Chemistry**, Utah State University, May 2014
GPA 3.89/4.00, Magna Cum Laude
- ACS Nuclear and Radiochemistry Summer School**, San Jose State University,
Summer 2013
Intensive six-week course on the fundamentals of nuclear science, radiochemistry, and
other related fields. The course included lectures and laboratory experience.
- Fellowships & Scholarships** Integrated University Program Graduate Fellowship – Department of Energy, Office of
Nuclear Energy (2015 – Present)
- R. Gaurth Hansen, Ph. D. Scholarship Award (2013)
- Lillywhite Presidential Scholarship (2012)
- Awards** Innovations in Nuclear Technology R&D Awards – First Place in Nuclear Science and
Engineering for *Selective Partitioning of Ruthenium from Nitric Acid Media* (2017)
- NNSA, Next Generation Safeguards Initiative, Participant in the 4th Nuclear Facilities
Experience – United Kingdom (2017)
- Department of Chemistry and Biochemistry Undergraduate Research Award (2014)
- Undergraduate Research and Creative Opportunities Grant Recipient (2013)
- Research Experience** **University of Nevada Las Vegas**, Radiochemistry Ph.D. Program (July 2014 – Present)
Advisor: Ralf Sudowe
Research focuses on development of a novel method for partitioning of americium from
curium using sodium bismuthate as both an oxidant and a separation medium.
Application of this partitioning method is being expanded to include fission product
elements and to explore applicability of the method to advanced partitioning of used
nuclear fuel. Research involves adsorption studies, chromatographic separations, liquid
scintillation counting, alpha spectrometry, inductively coupled plasma mass spectrometry
and atomic emission spectroscopy.
- Idaho National Laboratory**, Internship, Aqueous Separations and Radiochemistry
Department (June 2016 – August 2016)
Advisor: Bruce J. Mincher

Research focused on selective partitioning of ruthenium from nitric acid media to assist in the development of advanced actinide partitioning technologies that utilize hexavalent americium. A method was developed where ruthenium was oxidized to ruthenium tetroxide and absorbed into polymer beads. Research involved UV-Visible spectroscopy and gamma counting.

Utah State University, Undergraduate Research, Chemistry and Biochemistry Department (May 2013 – May 2014)

Advisor: Lisa M. Berreau

Research focused on synthesizing and characterizing flavonols with red-shifted absorbance spectra for use as photo-induced CO₂-releasing molecules. Research involved organic synthesis, chelation chemistry, inert-atmosphere glovebox use, photochemistry, nuclear magnetic resonance spectrometry and UV-Visible spectroscopy.

Oak Ridge National Laboratory, Internship, Chemical Separations Group, Chemical Sciences Division (June 2012 – August 2012)

Advisor: Bruce A. Moyer

Research focused on selective extraction of sulfate from legacy (cold war-era) nuclear waste. A novel ligand was tested in a solvent extraction system to determine the selectivity of the ligand for the sulfate anion. Research included radiotracer studies with S-35, solvent extraction, and liquid scintillation counting.

Publications **Richards, J. M.**; Mincher, B. J. Selective Partitioning of Ruthenium from Nitric Acid Media. *Solvent Extraction and Ion Exchange*. **2017**.

Faye, S. A.; **Richards, J. M.**; Gallardo, A. M.; Campbell, K. R.; Sudowe, R. Development of a Standardized Sequential Extraction Protocol for Simultaneous Extraction of Multiple Actinide Elements. *Journal of Radioanalytical and Nuclear Chemistry*. **2017**.

Richards, J. M.; Sudowe R. Separation of Americium in High Oxidation States from Curium Utilizing Sodium Bismuthate. *Analytical Chemistry*. **2016**.

Anderson, S. N.; **Richards, J. M.**; Esquer, H. J.; Benninghoff, A. D.; Arif, A. M.; Berreau, L. M. A Structurally-Tunable 3-Hydroxyflavone Motif for Visible Light-Induced Carbon Monoxide-Releasing Molecules (CORMs). *Chemistry Open*. **2015**.

Presentations “Isolation of Americium from PUREX Raffinate utilizing Sodium Bismuthate Chromatography” (Oral Presentation) **Richards J. M.**; Mincher B. J. 5th International Nuclear Chemistry Congress at Chalmers University, Gothenburg, Sweden. August 2017

“Selective Partitioning of Ruthenium from Nitric Acid Media” (Poster) **Richards, J. M.**; Sudowe R. 41st Actinide Separations Conference at Argonne National Laboratory, Argonne, IL. May 2017

“Isolation of Americium from Curium and the Lanthanides utilizing Sodium Bismuthate Chromatography” (Poster) **Richards, J. M.**; Sudowe R. 41st Actinide Separations Conference at Argonne National Laboratory, Argonne, IL. May 2017

“Separation of Americium in High Oxidation States from Curium Utilizing Sodium Bismuthate” (Oral Presentation) **Richards, J. M.**; Sudowe, R. 251st American Chemical Society National Meeting & Exposition in San Diego, CA. March 2016

“Separation of Americium in High Oxidation States from Curium” (Poster) **Richards, J. M.**; Sudowe, R. University & Industry Technical Interchange (UITI) Program & Technical Review Meeting in Ann Arbor, Michigan. June 2015

Skills & Knowledge Chemistry of the lanthanides, actinides and fission product elements (inorganic, trace and environmental chemistry)

Separation and chromatography techniques (liquid-liquid extraction, solid-phase extraction, ion exchange and extraction chromatography)

Charged-particle and gamma-ray detection and radiation counting (α -spec, γ -spec, LSC, gas proportional counting)

Analytical chemistry (AAS, AES, ICP-MS, UV-Vis, IR, ¹H NMR, Fluorescence)

Handling of radioactive materials

Inert-atmosphere glovebox and Schlenk line operation (handling of air/light-sensitive materials)

Conversational fluency in Portuguese

References

Ralf Sudowe (Doctoral Advisor)

Department of Environmental and Radiological Health Sciences

Colorado State University

Phone: (970) 491-0219

Email: ralf.sudowe@colostate.edu

Bruce J. Mincher (Internship Advisor)

Aqueous Separations and Radiochemistry Department

Idaho National Laboratory

Phone: (208) 526-3086

Email: bruce.mincher@inl.gov

Gary Cerefige (Doctoral Committee Member)

National Security Technologies, LLC

Remote Sensing Lab – Nellis

Phone: (702) 295-8034

Email: cerefigs@nv.doe.gov